U.S. DEPARTMENT OF COMMERCE
National Technical Information Service

PB-253 383

A PASSIVE FLOW MEASUREMENT SYSTEM FOR STORM AND COMBINED SEWERS

GRUMMAN AEROSPACE CORPORATION

PREPARED FOR
MUNICIPAL ENVIRONMENTAL RESEARCH LABORATORY

MAY 1976

161012

PB 253 383

EPA-600/2-76-115
May 1976

Environmental Protection Technology Series

A PASSIVE FLOW MEASUREMENT SYSTEM FOR STORM AND COMBINED SEWERS

REPRODUCED BY
NATIONAL TECHNICAL
INFORMATION SERVICE
U. S. DEPARTMENT OF COMMERCE
SPRINGFIELD, VA. 22161

Municipal Environmental Research Laboratory
Office of Research and Development
U.S. Environmental Protection Agency
Cincinnati, Ohio 45268

RESEARCH REPORTING SERIES

Research reports of the Office of Research and Development, U.S. Environmental Protection Agency, have been grouped into five series. These five broad categories were established to facilitate further development and application of environmental technology. Elimination of traditional grouping was consciously planned to foster technology transfer and a maximum interface in related fields. The five series are:

1. Environmental Health Effects Research
2. Environmental Protection Technology
3. Ecological Research
4. Environmental Monitoring
5. Socioeconomic Environmental Studies

This report has been assigned to the ENVIRONMENTAL PROTECTION TECHNOLOGY series. This series describes research performed to develop and demonstrate instrumentation, equipment, and methodology to repair or prevent environmental degradation from point and non-point sources of pollution. This work provides the new or improved technology required for the control and treatment of pollution sources to meet environmental quality standards.

This document is available to the public through the National Technical Information Service, Springfield, Virginia 22161.

TECHNICAL REPORT DATA

(Please read Instructions on the reverse before completing)

1. REPORT NO.
EPA-600/2-76-115

2.

3. RECIPIENT'S ACCESSION NO.
PB-253 383

4. TITLE AND SUBTITLE
A Passive Flow Measurement System for Storm and Combined Sewers

5. REPORT DATE
May 1976 (Issuing Date)

6. PERFORMING ORGANIZATION CODE

7. AUTHOR(S)
K. M. Foreman*

8. PERFORMING ORGANIZATION REPORT NO.

9. PERFORMING ORGANIZATION NAME AND ADDRESS
Grumman Ecosystems Corporation, Bethpage, N.Y. 11714
Through subcontract with:
*Research Dept., Grumman Aerospace Corporation
Bethpage, N.Y. 11714

10. PROGRAM ELEMENT NO.
1BC611

11. CONTRACT/GRANT NO.
EPA Contract 68-03-2121

12. SPONSORING AGENCY NAME AND ADDRESS
Municipal Environmental Research Laboratory
Office of Research and Development
U.S. Environmental Protection Agency
Cincinnati, Ohio 45268

13. TYPE OF REPORT AND PERIOD COVERED
Final Report 6/'74 to 8/'75

14. SPONSORING AGENCY CODE
EPA-ORD

15. SUPPLEMENTARY NOTES
PO: Hugh Masters

16. ABSTRACT

This investigation concerns a new, nonintrusive, low cost, passive flow measurement method to meet the urgent needs for good management of storm and combined sewer systems. Operation of the system is based on sensing the near field sound emitted by the disturbed flow at a channel discontinuity. These local pressure pulses are called pseudosound and radiate as dipole sound sources orthogonal to the flow direction. The output signal of passive transducers, such as accelerometers, attached to the outer wall of the channel indicates flow rate after processing by a Fourier Analyzer. Feasibility has been demonstrated by laboratory tests using full scale sewer pipe elements, and by a brief series of field tests measuring sanitary sewage flow. Recommendations are made for further field site testing using an instrumented sewer line.

17. KEY WORDS AND DOCUMENT ANALYSIS

a. DESCRIPTORS	b. IDENTIFIERS/OPEN ENDED TERMS	c. COSATI Field/Group
Flow, Acoustics, Sewers, Flowmeters, Experimental Design, Acoustic Signatures, Sound Level Meters, Electronic Computers, Electroacoustic transducers	Acoustic Emission Flowmeter	20C, 20A 13B 14B 17A 9A, 9B

PRICES SUBJECT TO CHANGE

18. DISTRIBUTION STATEMENT
Release Unlimited

19. SECURITY CLASS (This Report)
unclassified

20. SECURITY CLASS (This page)
unclassified

21. NO. OF PAGES
137

22. PRICE
$6.00

☆ U. S. GOVERNMENT PRINTING OFFICE: 1976-657-695/5422 Region No. 5-11

EPA-600/2-76-115
May 1976

A PASSIVE FLOW MEASUREMENT SYSTEM
FOR STORM AND COMBINED SEWERS

by

K. M. Foreman
Research Department
Grumman Aerospace Corporation
Bethpage, New York 11714

Contract No. 68-03-2121

Project Officer

Hugh Masters
Storm and Combined Sewer Section
Wastewater Research Division
Municipal Environmental Research Laboratory (Cincinnati)
Edison, New Jersey 08817

U.S. ENVIRONMENTAL PROTECTION AGENCY
OFFICE OF RESEARCH AND DEVELOPMENT
MUNICIPAL ENVIRONMENTAL RESEARCH LABORATORY
CINCINNATI, OHIO 45268

DISCLAIMER

This report has been reviewed by the Municipal Environmental Research Laboratory, U.S. Environmental Protection Agency, and approved for publication. Approval does not signify that the contents necessarily reflect the views and policies of the U. S. Environmental Protection Agency, nor does mention of trade names or commercial products constitute endorsement or recommendation for use.

FOREWORD

The Environmental Protection Agency was created because of increasing public and government concern about the dangers of pollution to the health and welfare of the American people. Noxious air, foul water, and spoiled land are tragic testimony to the deterioration of our natural environment. The complexity of the environment and the interplay between its components require a concentrated and integrated attack on the problem.

Research and development is that necessary first step in problem solution and it involves defining the problem, measuring its impact, and searching for solutions. The Municipal Environmental Research Laboratory develops new and improved technology and systems for the prevention, treatment, and management of wastewater and solid and hazardous waste pollutant discharges from municipal and community sources, for the preservation and treatment of public drinking water supplies, and to minimize the adverse economic, social, health, and aesthetic effects of pollution. This publication is one of the products of that research; a most vital communications link between the researcher and the user community.

The need exists to develop innovative, passive, nonintrusive, and low cost solutions to the problems of continuous measurement and recording of flows in storm and combined sewers. This experimental investigation is of one such technique that monitors the pseudosound produced by flow past a channel discontinuity. The results of laboratory and field tests demonstrate the feasibility of this method of flow measurement using an accelerometer transducer attached to the outside surface of a flow channel.

Francis T. Mayo, Director
Municipal Environmental Research
Laboratory

ABSTRACT

This investigation concerns a new, nonintrusive, low cost, passive flow measurement method to meet the urgent needs for good management of storm and combined sewer systems. Operation of the system is based on sensing the near field sound emitted by the disturbed flow at a channel discontinuity. These local pressure pulses are called pseudosound and radiate as dipole sound sources orthogonal to the flow direction. The output signal of passive transducers, such as accelerometers, attached to the outer wall of the channel indicates flow rate after processing by a Fourier Analyzer. Feasibility has been demonstrated by laboratory tests using full scale sewer pipe elements, and by a brief series of field tests measuring sanitary sewage flow. Recommendations are made for further field site testing using an instrumented sewer line.

This report was submitted in fulfillment of EPA Contract 68-03-2121 by Grumman Aerospace Corporation under the sponsorship of the Environmental Protection Agency. Work was completed as of August 22, 1975.

CONTENTS

		Page
Foreword		iii
Abstract		iv
Figures		vi
Acknowledgments		xiii
I	Conclusions	1
II	Recommendations	5
III	Technical Study	7
IV	References	119
V	Glossary	120

FIGURES

No.		Page
1	Ringing Frequency, fr, for Various Diameter Pipes and Pipe Materials	14
2	Limiting Transmission Loss of Sound Across Cylindrical Steel Pipe Walls at Less than the Ringing Frequency, fr	15
3	Theoretical Sound Transmission Loss, R, for Mass Controlled Panels	17
4	Grumman Research Water Supply Facility	19
5	240 Gallon Facility Water Storage Tank	20
6	Air Pressurization and Water Supply Pipes to Storage Tank	20
7	20 Foot Length of 3-in. Diameter Pipe of Facility Water Supply System	21
8	View of Facility Test Section Showing Diversion Trough, Water Collection Drums, and Weighing Scale. 8-in. Diameter Aluminum Pipe on Test in Concentric Configuration	21
9	View of Water Flowing from 8-in. Diameter Test Pipe into Diversion Trough	23
10	Overall Side View of Facility Test Section Showing Diversion Trough, Water Collection Drums, and Weighing Scale. 4-in. Diameter Transite Pipe on Test............................	23
11	Sensor Locations and Channel Discontinuities Tested in Research Laboratory	24
12	Schematic of Testing Instrumentation	27
13	Side View of Box for Containing Sand Used to Simulate Buried Pipe Installation	29

No. Page

14 Top View of Box Used to Simulate Buried Pipes. 6-in. Diameter Transite Pipe is Shown on Test with Sand Removed. Flow Direction is from Left to Right 29

15 End View of 8-in. Diameter Pipe Showing Initial Condition of Heavy (1-in.) Bed Load of Stone Chips 30

16 Heavy Bed Load After Being Disturbed by Water Flow at Rates up to 3 Pounds Per Second 30

17 Equipment Used to Feed Sand Grit into Upstream Water Supply 31

18 Closeup of Speed Controlled Motor and Supply Hopper Used to Feed Sand Grit into Water Supply .. 31

19 Screen Tray Added to Water Collection System to Separate Grit from Collected Water. 6-in. Diameter Transite Pipe is Shown on Test. Tray is Just Below Pipe Exit 34

20 Exterior View of Valve Vault (Foreground at Grumman Waste Treatment Plant "A". This is First Site of Field Test Preview Experiments 34

21 Interior View of Valve Vault Showing 8-in. Plug Valve and 8 x 10-in. Reducer Section with Accelerometer Attached to Outer Wall for Acoustic Emission Monitoring of Flow 35

22 Exterior View of Aeration Tank at Grumman Waste Treatment Plant "A". 10-in. Diameter Pipe Emerges from Underground Installation at Left Center of Photo. This is Site of Second Series of Field Test Preview Experiments 35

23 Closeup of 10-in. Diameter Pipe Where Second Field Test Preview Series Was Conducted. Sensor is Shown Attached to Top Center of Horizontal Pipe. Tape Recorder and Amplifier Used is Shown in Foreground 37

No. Page

24 Data Processing Equipment Used to Obtain Spectral Distribution from Flow Acoustic Emission Recordings. HP-5465A Fourier Analyzer Computer is in Center of Picture 37

25 Schematic of Acoustic Emission Data Processing System 38

26 Closeup of Data Processing Equipment Showing (L to R) HP-5465A Fourier Analyzer Computer, Penco Continuous Loop Recorder and Playback, and Nagra Tape Recorder Used for Laboratory and Field 38

27 Typical Fourier Processed Spectral Distributions of Laboratory Sound Recordings (10 Hz Bandwidth) . 40

28 Acoustic Signal Variation with Flow Rate in a 3-in. (7.62 cm) Diameter Steel Pipe 46

29 Typical Spectral Distributions of Laboratory Sound Recordings. Distributions Obtained by Fourier Analyzer (10 Hz Bandwidth) 47

30 Hydraulic Radius of Test Channel For Different Water Level Heights 49

31 Calibration of Research Facility Water Supply (A = Flow Area, Q = Volumetric Flow Rate) 51

32 Variation of Normalized Acoustic Signal with Flow (Cylindrical Pipe Exiting to a Trapezoidal Open Channel) 53

33 Acoustic Signal Variation with Flow Rate (Cylindrical Pipe Discharging to Trapezoidal Open Channel) 54

34 Variation of Normalized Acoustic Signal with Flow Rate - Different Sensor Locations (Cylindrical to Trapezoidal Channal Transition) 55

No. Page

35 Variation of Normalized Acoustic Signal with Flow Rate - Effect of Sensor Location (Eccentric Cylindrical Pipe Elements and Extended Inlet) 57

36 Effect of Sensor on Variation of Normalized Acoustic Signal with Flow Rate (Eccentric (Cylindrical Pipe Elements and Extended Inlet) .. 58

37 Effect of Extended Inlet on Acoustic Signal Variation with Flow Rate (Eccentric Cylindrical Pipe Elements) 60

38 Effect of Sensor Position and Sound Frequency on Acoustic Emission of Water Flow (Eccentric Cylindrical Pipe Elements and Flush Inlet) 61

39 Effect of Exit Weir Height on Normalized Acoustic Signal of Water Flow (Eccentric Cylindrical Pipe Elements and Flush Inlet) 62

40 Effect of Exit Weir Height on Normalized Acoustic Signal of Water Flow Eccentric Cylindrical Pipe Elements and Flush Inlet) 63

41 Variation of Signal with Flow at Different Sensor Locations; (Eccentric Cylindrical Pipe Elements and Flush Inlet)(with 4.24-in. Weir at Exit Unless Noted Otherwise) 65

42 Variation of Normalized Acoustic Signal with Flow Rate for Different Frequencies and Test Conditions (Eccentric Cylindrical Pipe Elements and Flush Inlet) 67

43 Variation of Normalized Acoustic Signal with Flow Rate for Different Test Conditions (Flush Inlet, Eccentric Cylindrical Pipe Step) 68

44 Variation of Acoustic Signal with Flow for 3 Sensor Locations and Various Test Conditions 70

45 Closeup of Concentric Discontinuity Plane Assembly of 3-in. Steel Water Supply Pipe to 8-in. Diameter Aluminum Test Pipe 70

No. Page

46 Internal Relation of 3-in. Supply Pipe to 8-in. Test Pipe with Heavy Bed Load of Stone Chips. View Taken Before Flow Established 72

47 View of Upset Bed Load After Water Flow Rate of 5 Pounds Per Second 72

48 Variation of Normalized Acoustic Signal wtih Flow Rate at Various Sensor Locations and Characteristic Frequency (Concentric Cylindrical Pipe Array with Extended Inlet) 74

49 Variation of Normalized Acoustic Signal with Flow Rate for Different Frequencies (Concentric Cylindrical Pipe Array with Extended Inlet) 75

50 Effect of Sensor Circumferential and Axial Location on Useful Signal (Concentric Cylindrical Pipe Array with Flush Inlet) 77

51 Varation of Acoustic Signal with Flow at Two Sensor Locations for Different Test Conditions (Flush Inlet, Concentric Cylindrical Pipes) 78

52 Variation of Acoustic Signal with Flow at Three Sensor Locations and for Two Frequencies - with 4.24" Weir at Pipe Exit Plane - (Concentric Cylindrical Pipe Elements) 79

53 Variation of Acoustic Signal with Flow at Three Sensor Locations and Three Frequency Bands - with 4.24-in. Weir at Pipe Exit Plane - (Concentric Cylindrical Pipe Elements). See Fig. 52 for Sensor Position Location on Pipe 80

54 Variation of Acoustic Signal with Flow at Two Sensor Locations and Two Frequency Bands (Concentric Cylindrical Pipe Elements) - with 4.24" Weir at Pipe Exit and 8" Deep Sand Overburden, Except Where Noted 82

55 Varation of Acoustic Signal with Flow at Five Frequency Bands and One Sensor Location (Concentric Cylindrical Pipe Elements) - with 4.24" Weir at Pipe Exit and 8" Deep Sand Overburden, Except Where Noted 83

No. Page

56 Effect of Heavy Bed Load of Stones (1" Deep) in 8" Diameter Pipe on Acoustic Signal Variation with Flow - Sand Covered Array 84

57 Effect of Two Bed Loads of Stones in 8-in. Diameter Pipe on Acoustic Signal Variation with Flow - Sand Covered Array with 4.24-in. Weir 85

58 Sketches of Heavy Bed Load Movement at Different Stages of Water Flow Test Conditions 86

59 Variation of Acoustic Signal with Flow at Four Frequencies and Two Sensor Positions (8" Sand Cover and Monolayer of Stone Chips Within 8" Diameter Pipe. 4.24" Weir at Exit of Pipe) 88

60 Closeup of Eccentric Connection of 3-in. Water Supply Pipe to 4-in. Diameter Transite Test Pipe . 91

61 Closeup of Special Assembly Collar Used for Eccentric Connection of 3-in. Pipe to 6-in. Diameter Transite Test Pipe. Flow is from Right to Left. Two Sensor Mounting Studs are Shown Cemented at Top Centerline Surface of Transite Pipe 91

62 Variation of Acoustic Signal with Flow (Eccentric Cylindrical Pipe Array) - Transite and Steel Pipe Elements without Sand Overburden Except Where Noted 93

63 Variation of Acoustic Signal with Flow (Eccentric Cylindrical Pipe Array) - Transite and Steel Pipe Elements Buried Under 8-in. (20.3 cm) of Sand, Except Where Noted 95

64 Variation of Acoustic Signal with Flow (Eccentric Cylindrical Pipe Array) - Transite and Steel Pipe Elements Without Sand Overburden, Except Where Noted 95

65 Effect of Grit Addition to Water Flow on the Acoustic Signal Variation with Flow - Transite and Steel Pipe Elements, Without Sand Overburden, in Eccentric Assembly 96

No. Page

66 Variation of Acoustic Signal with Flow at Grumman Waste Treatment Plant "A" Valve Vault for Different Sensor Positions - First Test Series 98

67 Variation of Signal with Flow at Grumman Waste Treatment Plant "A" Aeroation Pond for Different Frequencies and Sensor Positions - Second Test Series 100

68 Typical Variation of Acoustic Signal with Flow for Two Conduit Configurations (Cylindrical to Trapezoidal Cross-Sectional Discontinuity) 103

69 Effect of Extended Inlet on Acoustic Signal Variation with Flow Rate (Concentric Cylindrical Pipe Elements) 106

70 Effect of Pipe Configuration on Normalized Acoustic Signal Variation with Flow Rate (Cylindrical Pipe Elements) with 4.24-in. Weir, 8-in. Sand Overburden, and Flush Inlet 110

71 Effect of Pipe Material on Normalized Acoustic Signal Variation with Flow Rate (Eccentric Cylindrical Pipe Elements and Flush Inlet) - 8-in. Sand Overburden 113

ACKNOWLEDGMENTS

This work was performed for Grumman Ecosystems Corporation, Bethpage, New York, who are the prime contractors to the U.S. Environmental Protection Agency (EPA) under Contract 68-03-2121.

We acknowledge the assistance of Mr. James Rogers of Grumman Aerospace Corporation (GAC) for programming and otherwise assisting in the computer processing of our recorded sound data. Thanks are also directed to Mr. Chris Clamser and Mr. Norman Peele of GAC for making possible the many facility and testing changes, on a timely basis, during the course of this program.

Finally we are indebted to Mr. Hugh Masters and Mr. Richard Field of EPA who provided helpful guidance during the program, and enlightenment regarding simulation of sewage solids.

SECTION I

CONCLUSIONS

The results of this program demonstrate the feasibility of Grumman's acoustic emission flowmeter concept[*] for channels where a discontinuity exists because of a conduit cross-sectional increase. Since these geometric cross section changes are common in sewer systems, this passive, nonintrusive, flow measurement technique is directly applicable to storm and combined sewers.

On a scale that is without precedent regarding physical size and variety of laboratory test conditions, the acoustic emission monitored by an accelerometer has been found to produce unambiguous signals that increase in magnitude as the fluid flow rate increases. The source of the acoustic emission is the pseudosound created by the interaction of fluid with a solid surface in the near field of a conduit discontinuity. Pseudosound does not propagate with the flow, but radiates as a dipole, orthogonal to the flow direction. Data has been obtained for open channel, full flow, and pressurized flow conditions involving full scale metallic and Transite pipe sections used to conduct fluid waste.

During these laboratory tests, steady, unsteady, uniform, and nonuniform flows were established. In addition to tests of freely suspended pipes flowing clean water, corroborative data has been obtained from tests with simulated buried installations of the pipes and with water containing suspended and settleable solids characteristic of sewage. Tests with cylindrical as well as trapezoidal conduits cross sections have confirmed general similarity of results for these geometries.

---

[*] Patent pending.

A field test preview, in which the acoustic emission flowmeter technique was used to monitor sanitary sewage from large industrial buildings, demonstrated good correlations with test trends obtained in the laboratory, and with theoretical predictions.

Data of value to future engineering design of prototype systems have been obtained. This experience indicates that low cost accelerometers having a wide range of voltage sensitivities, between 10 and 100 mv/g, are well suited to the acoustic monitoring function. These sensors are easily emplaced or removed by screwing on to inexpensive, dedicated mounting plates which may be cemented or magnetically attached to the outer surface of the flow channel. Epoxy cement with high metallic content has proven very satisfactory for this purpose. For discontinuities involving sudden enlargements of conduit cross section, the sensor location yielding the strongest signal for the greatest range of flows is at the bottom-most circumferential position and two to three (upstream) pipe diameters downstream of the discontinuity plane. Transmission of flow acoustic emission through most sewer conduit walls is of a sufficiently high percentage so that adequate signal quality is available to the sensors. Sound transmission circumferentially in solid conduit walls is of such high magnitude that useful sensor signals can be obtained at nearly any circumferential position, at a given axial position. These results hold for metallic as well as inhomogeneous material (e.g., cement and Transite) used in pipe constructions and for conventional wall thickness to pipe diameter ratios of sewers.

In the early phases of this project, no special measures were taken to simulate real sewer installation features in our laboratory experiments. This initial oversimplification of the test setups was intended to expedite acquisition of test data and to avoid special equipment costs if unneeded. As a result, however, some of the acoustic emission data appeared to conflict with the expected trends of pseudosound production. To overcome this equipment inadequacy, we developed inexpensive but effective techniques to simulate properly sewer installations. The acoustic emission signals obtained under these changed test conditions were completely unambiguous, and in general agreement with dipole theory predictions.

The most reliable unambiguous signal for flow rate measurement is the acoustic emission component at a characteristic frequency, f_c, which is inversely proportional to the maximum geometric step at the discontinuity, δ, and directly proportional to the bulk sound speed, c, of the fluid, or $f_c \propto c/\delta$. Because of secondary flow interaction processes, minor transient changes in c, instrumentation sensitivity, and acoustic energy conversion process, the useful signal actually exists in a frequency band of up to 200 Hz width, centered about f_c. For most practical sewer applications the characteristic frequency will be in the midaudible range of the sound spectrum. Random background noise is of the order of 10^{-3} to 10^{-4} (i.e., -30 to -40 dB) the intensity of flow acoustic emission. Response of sewer pipes to this noise follows a general mass distribution law where amplitude varies inversely with frequency. In contrast, the spectra of flow acoustic emission have high amplitude content at frequency bands associated with flow-related sources. In this regard, a bed load that does not adhere to the conduit wall in the near field of the discontinuity will not alter the basic character of the flow acoustic emission. However, some conversion of the acoustic emission energy to sound propagating downstream with the flow can take place if the bed load consists of sharp edged material that induces much turbulence. In the laboratory, at low flows, the acoustic signal at characteristic frequency increases with flow at a rapid rate, approximating the ideal ($\sim \dot{w}^4$)[†] dipole theoretical prediction of 12 dB per doubling of flow rate. However, while this trend is moderated at higher flow rates, it increases without ambiguity and assumes a direct proportionality to flow ($\sim \dot{w}$)[†] at the highest rates tested in the laboratory. In the limited field test preview, the trend of high flow rate data taken at an underground pipe installation follows dipole theoretical predictions reasonably well.

In addition to its flow measurement capability, acoustic emission monitoring can be an operational tool for determining maintenance needs of the sewer. To the experienced human monitor at a central location, qualitative evaluation of total sound content from various and diverse remote sites can provide a mental image of local sewer conditions that almost rivals in situ observations by a mobile crew, but with greater convenience and lower cost.

The contractual limitations of this project did not permit an exhaustive investigation to reveal the full potential of Grumman's passive measurement technique for all pipe geometries. However, there are sufficient reasons, by virtue of the data obtained, to justify extreme optimism on the future prospects for this new, low cost approach to flow measurement.

[†] $\dot{w}$ = rate of change of weight flow = $\Delta w/\Delta t$

SECTION II

RECOMMENDATIONS

Feasibility of the passive acoustic emission flowmeter has been demonstrated in the laboratory with a breadboard, research type, instrumentation system. The features of this technique should be appealing to management of municipal and regional sewer districts. Therefore, to expedite the implementation of this method we recommend the following action:

1. Extend field testing conditions to a well instrumented sewer site, using the laboratory breadboard system. Testing should be conducted for a long enough duration (i.e., months) to experience at least a realistic variation of runoff and flushing conditions.

2. Based on the laboratory and extended field testing results, design and build a prototype flow measurement system, and test it at the well instrumented sewer site previously used. Laboratory calibration of the system should precede the field testing. After initial shakedown and possible system design modifications at the field site, continue evaluation over a twelve to twenty four month period for system reliability, maintainability, and operational performance data. These data should be compared to ultimate system objectives defined by EPA.

3. Depending on the experience of step 2 above, either design and construct an advanced prototype or build several initial production systems for more widespread field tests throughout the nation.

Although it may be premature to be unduly concerned about operational aspects of this passive measurement technique, it is clear that its utility would be enhanced if field site calibration could be eliminated. One expeditious and economical way of doing this is to calibrate the transducer in a flow facility where small scale models simulate the relevant local features of the actual sewer installation. To use these calibrations with confidence requires that scaling laws be developed so that model data can be correctly applied directly to the field site geometry. Accordingly, we recommend that theoretical studies be conducted to determine appropriate scaling laws for the acoustic emission process. These similarity laws then should be verified using data from field tests (such as recommended above) and laboratory work reported here as well as from future supplementary laboratory tests.

In order to explore more fully the growth potential of this measurement technique, we recommend further laboratory research with several pipe discontinuity configurations other than sudden enlargements. Among these are contractions, turns, tees, Y-sections, valve bodies, and sumps. Investigations should include independent internal flow diagnostic instrumentation as well as passive acoustic sensing. At least one study should concern identifying and quantifying flow infiltration into sewer lines; simulation methods should be established for the infiltration. Other studies should investigate reverse flow identification and correlations of field measurement performance with laboratory calibrations under simulated field conditions.

SECTION III

TECHNICAL STUDY

A. INTRODUCTION

The project investigations reported here are the first phase of a program to develop a passive flow measurement system for storm and combined sewers. It was performed by Grumman Aerospace Corporation under subcontract to Grumman Ecosystems Corporation in conformance with U.S. Environmental Protection Agency (EPA) Contract 68-03-2121, dated June 28, 1974.

The purpose of this project is to determine, by experiment and analysis, the feasibility of Grumman's innovative acoustic emission flowmeter concept.* Tests have been conducted in the controlled environment of Grumman Research's water flow laboratory under a variety of flow and simulated sewer pipe installations. A brief field test also was conducted to preview the type of data that could be expected from a full field test program. Secondary objectives are to obtain engineering data to guide future flowmeter designs and installations, and to explore the growth potential of the concept to meet ultimate design goals for a sewer flowmeter.

The acoustic emission flowmeter concept uses passive sensors to monitor the sound emitted by fluid flow, and in this way determines flow rate. This sound signal results from the pressure disturbances when flow passes a channel discontinuity. The discontinuity can be any change in conduit cross section or shape, or where flow direction is significantly altered. In the vicinity of the discontinuity, the pressure disturbances depend on the mean velocity of the flow and can be monitored by appropriate sensors at the boundary of the flow. However, because this near field sound does not propagate throughout the flow with the sound speed of the fluid it is termed pseudosound.[1,2] This differentiates it from the more conventional acoustic processes that become coupled to the fluid's far field radiation. Pseudosound has radiation characteristics like a dipole source,[1,3] so it emits acoustic energy orthogonal to the fluid flow direction. For usual sewer pipe construction, a passive sensor, such as an accelerometer, mounted to the outer surface of the sewer wall can listen to pseudosound. The sensor's output signal can be transmitted to nearby or remote devices that use the relationship of pseudosound to local mean velocity to determine flow rate. The features of this simple, passive, nonintrusive flow measurement system are ideally suited to the operational conditions and environment found in storm and combined sewers.

---

*Patent pending.

Background

The EPA need to characterize and assess storm-generated water pollution, and to develop, demonstrate, and evaluate water treatment and control systems, establishes a requirement for real-time data from fast response and remote sensors. Severe flow conditions in combined sewers obviate use of conventional flowmeters. Problems of cost, accuracy, reliability, operational simplicity, and maintenance have limited the application of other advanced active measurement techniques developed in recent years.

A reliable flowmeter that is nonintrusive and passive has attractive prospects for sewer applications because it can be used on new as well as old sewer lines, does not have to be physically subjected to the variable quality of sewer flow, and can have low power requirements.

Pursuing its own independent studies for advanced flow measurement techniques, Grumman Research invented a way by which the relatively little known theory of pseudosound could be used to determine fluid flow rate. This method is inherently passive because it is activated by the sound energy emitted by the flow.

About two years prior to the inception of this contract, Grumman had demonstrated that the variation of pseudosound intensity with flow rate could be measured and that it followed theoretical predictions. The test configuration involved a 0.875-in. (2.22 cm) diameter aluminum pipe discharging to an open rectangular aluminum channel 1.0-in. (2.54 cm) wide by 1.5-in. (3.81 cm) high. Measurements were made at water flow rates to 0.66 lb/sec (0.3 Kg/sec) and used a single transducer type (B&K model 4332) attached to the underside of the open channel by double adhesive faced tape.

However, because of the very limited conduit size and configuration, water flow rate range, and transducer type and installation in these earlier demonstration tests, reservations remained about the applicability of the concept for more representative conditions of storm and combined sewers.

To demonstrate feasibility, tests were necessary for greatly extended conditions of:

- a) Flow rate
    - 1) partial flow
    - 2) full flow
    - 3) pressurized flow
- b) Conduit configurations
    - 1) size
    - 2) construction materials
    - 3) geometry
- c) Transducer
    - 1) type
    - 2) sensitivity
    - 3) method of attachment
    - 4) location relative to discontinuity plane

In addition, examination of such operational factors as buried pipe installations and the addition of solids to water flow were required.

Test Phasing

The test program discussed in this report was designed to examine these questions in a phased sequence, giving systematically increased knowledge and preparation for progressively more complex situations. First, we scaled up the supply conduit flow area by a factor of 10, and roughly duplicated the circular to open rectangular conduit transition cross section geometry used in the original demonstration. Next, we examined the characteristics of various candidate transducers and selected the best for our purposes. Methods of sensor attachment were considered and tested for acoustic coupling, ease of installation, and operational reliability.

Supply flow rates were established in the water flow research laboratory that were ten times the maximum previously used in concept demonstration; later, flow rates twenty times greater than initial demonstrations were used.

Following demonstration of reproducibility of results of the prior demonstration tests, with cylindrical-to-rectangular elements, we proceeded to test conduit arrays embodying only cylindrical metal elements. After validating the acoustic emission concept in completely cylindrical conduit geometry, we returned to more detailed studies of the original conduit test sections. The next test series was a detailed examination of metallic cylindrical pipe configurations, and included extending the flow rates to the maximum capable of being accurately measured. We then proceeded to test nonmetallic (Transite) cylindrical pipe elements. After confirming the similarity of flow acoustic emission measurements for Transite and metallic pipes, we examined simulated buried installations of cylindrical pipe discontinuities. The simulated overburden was found to be helpful in reducing airborne noise and did not adversely affect the flow acoustic emission signal. Several succeeding tests with simulated buried conduits involved metallic and Transite cylindrical pipe elements. These data revealed detailed flow characteristics for different sensors and sensor locations relative to the pipe discontinuity. Toward the end of this series, exploratory tests were made of the effect of solids in the water. Screened grit was added to the upstream water supply in one set of runs, and coarse stone chips were pre-placed as a pipe bed in other tests. Finally a preview of field test acoustic emission measurements was made at various locations of the sanitary sewer line to Grumman's main sewage treatment plant.

The test apparatus used in this program is described in Section IIIB. The results of tests for each phase of this project are described in Section IIIC, and discussed in Section IIID.

Theoretical Approach

Fluid flow in pipes or conduits produces sound that may be caused by over-all or locally induced unsteadiness of embedded turbulence. The local pressure disturbances induced by channel discontinuities and not propagated downstream is pseudosound. The sound pressure of pseudosound, p_p, is of the order of ρu^2 where ρ is the average fluid density and u is the fluid velocity.[1] The radiation field of pseudosound is like a dipole source so the total sound power, P_T, in a free field is

$$P_T \simeq \frac{p_p^2}{\rho c} \ell^2$$

where

p_p = pressure disturbance

ℓ = characteristic dimension of the local flow conduit

ρc = characteristic acoustic impedance of fluid

c = fluid sonic speed ($\sim 15 \times 10^4$ cm/sec for water)

However, since $p_p \simeq \rho u^2$, the theoretical sound power is

$$P_T \simeq \frac{\rho \ell^2 u^4}{c}$$

This equation is the theoretical basis for the fourth power relation of flow rate and sound emission. Note that the volumetric flow rate, $\dot{Q}$, is proportional to velocity, U, in a given conduit geometry, so $P_T \simeq \dot{Q}^4$.

The characteristic frequency, f_c, of the dipole sound produced at the conduit discontinuity is inversely proportional to the characterizing dimension of the discontinuity, δ. From the fundamental relation $f = c/\lambda$, where λ is sound wavelength in the fluid, $f_c \simeq c/\delta$ or $\delta \simeq \lambda$. (Empirically, we have determined that the proportionality factor for λ/δ is 4, or $4\delta = \lambda$.)

When the sound is "shadowed" by the shape of the discontinuity, from being radiated locally downstream, the net radiated power within the conduit is (ϵP_t). There is a sound power loss through the walls of the conduit by the transmission coefficient, τ, so that at the outer surface of the pipe the radiated sound power is

$$P_r \simeq P_T \, \epsilon\tau$$

For bends and branch points in a conduit, ϵ tends to unity; valves and metering sections have values of ϵ less than one. The ratio of transmitted to incident acoustic power equals τ. It is approximately proportional to the pipe diameter to wall thickness ratio, D/t, for excitation wavelengths larger than the circumference of the cylindrical conduit,[2] $\pi D = \lambda_r$. The ringing frequency, f_r, equals c/λ_r (see Fig. 1).

The "limiting transmission loss"[4] in dB, for steel cylindrical pipe is given by Fig. 2. The minor correction for actual frequency relative to f_r is shown.

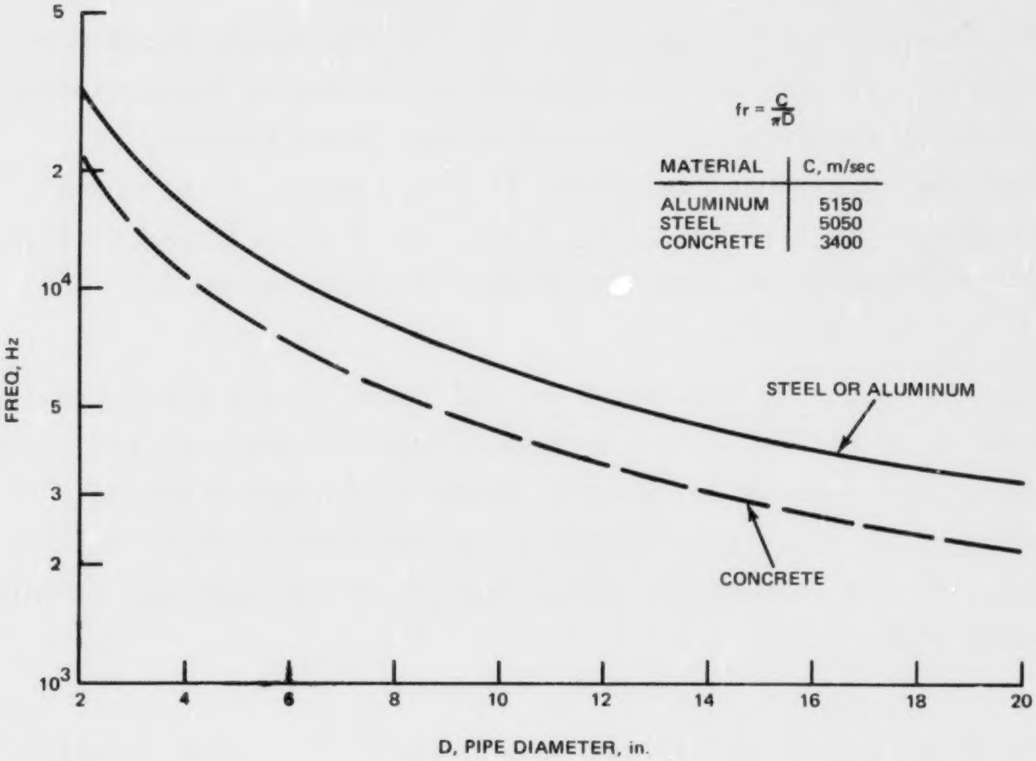

Fig. 1 Ringing frequency, fr, for various diameter pipes and pipe materials

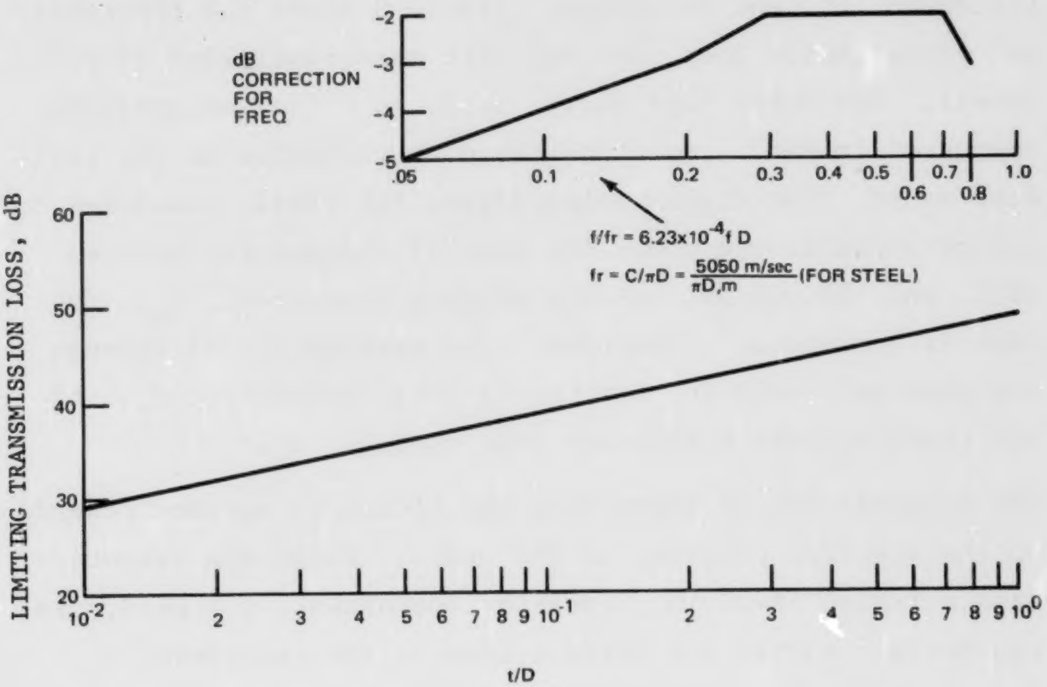

Fig. 2 Limiting transmission loss of sound across cylindrical steel pipe walls at less than the ringing frequency, fr

For smaller wavelengths than λ_r the loss corresponds to that of a flat panel of equal material and thickness to the conduit.[4] Here, the controlling factor is the product of the surface mass (equal to the mass density divided by the thickness) and the frequency. Figure 3 shows the theoretical transmission loss, in dB, for mass-controlled flat panels. The three loss curves apply to different criteria, discussed in Ref. 4, used for the directionality of the incident sound. The transmission losses for steel, aluminum, and concrete panels are shown for several frequencies between 1000 and 20,000 Hz. At the ringing frequency, f_r, the loss is a minimum.[4] Therefore, the maximum signal through the pipe wall will be obtained at this frequency, f_r, if the sound sources within the pipe contain f_r.

The transmission of sound from one medium to another depends on the acoustic coupling of the media. Using the transmission relation involving acoustic impedances, $r = \rho c/S$, in two media,[3] where S = surface area at the interface:

$$P_{12} = \frac{4r_1r_2}{(r_1 + r_2)^2}$$

The sound transmission from water to iron or concrete is about 15% and 53%, respectively. The poor acoustic coupling to air is indicated by values of P_{12}, of about 10^{-3}%, 10^{-4}%, and 10^{-5}% for water to air, concrete to air and iron to air interfaces, respectively.

B. EXPERIMENTAL FACILITIES

Most of the investigations made under this contract were conducted in the Grumman Research water flow facility. As shown

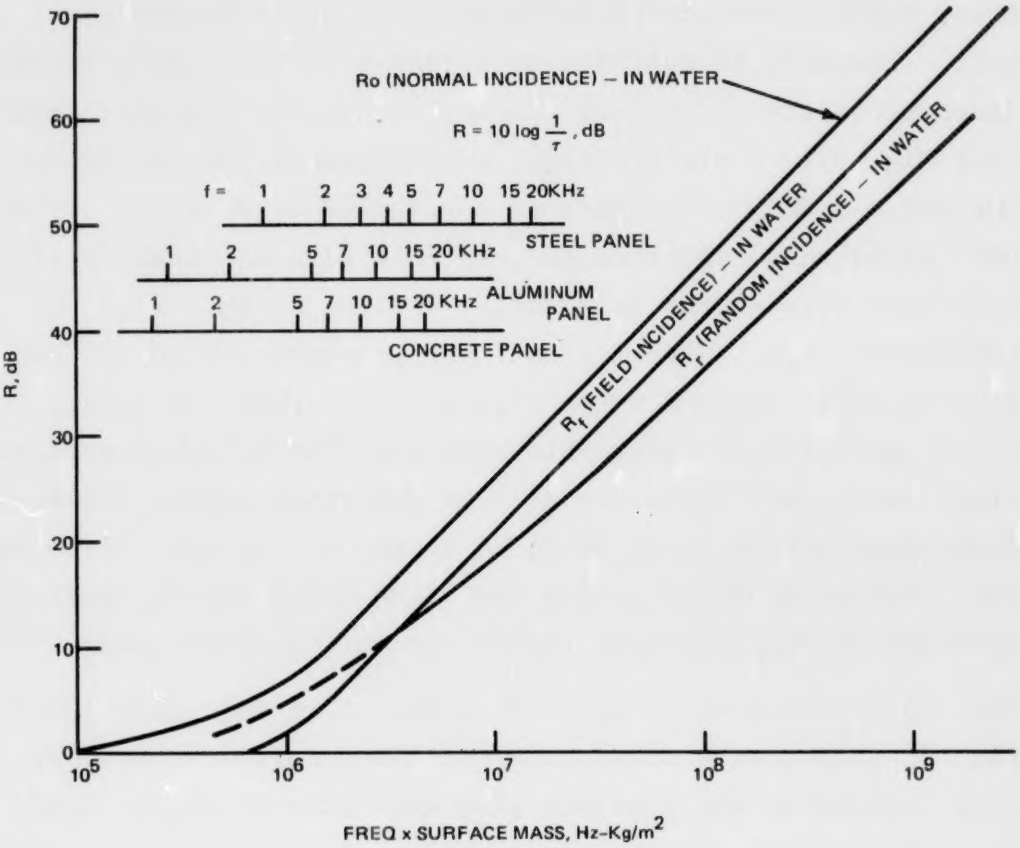

Fig. 3 Theoretical sound transmission loss, R, for mass controlled panels

in Fig. 4, this facility uses a 240 gallon (908 liter) cylindrical tank (see Fig. 5) as the primary water supply to feed a 3-in. (7.6 cm) diameter steel pipe. Water is fed into the tank by means of a hose connection from the plant water supply, and stored under pressure until needed for test. Pressure is supplied by a regulated air supply introduced above the water level in the vertically oriented tank (see Fig. 6). A plastic sight tube provides indications of the water level. Flow rate is controlled by a 3-in. (7.6 cm) globe valve inserted in the 6 ft (1.8 m) high vertical riser between the tank outlet and the 3-in. (7.6 cm) horizontal pipe. With initial tank pressures up to 30 psi (2.1 kg/cm^2) maximum water flow rates of over 15 lb/sec (6.82 kg/sec) are manageable with the flow measurement technique used; this technique will be described later. Constant flow rates during tests of up to about 2.5 lb/sec (1.10 kg/sec) are possible by having the plant water supply feeding directly through the tank to the 3-in. (7.6 cm) pipe.

The 20 ft (6.1 m) length of 3-in. (7.6 cm) pipe (see Fig. 7) effectively eliminates the flow profile irregularities induced by the flexible line and three 90 degree bands between the tank and the pipe. At the downstream end of the 3-in. (7.6 cm) pipe the conduit discontinuity is introduced by means of a test pipe section. Duration of tests usually are between 30 seconds and one minute, and for flows above about 3.5 lb/sec (1.4 kg/sec) the flow rate slowly decreases during the latter part of the run. The outflow drops into a wooden trough (Figs. 8 and 9) where it can be diverted by a flapper valve into a drain, or into a collection drum. The 55 gallon (208 liter) drum is connected by hose (see

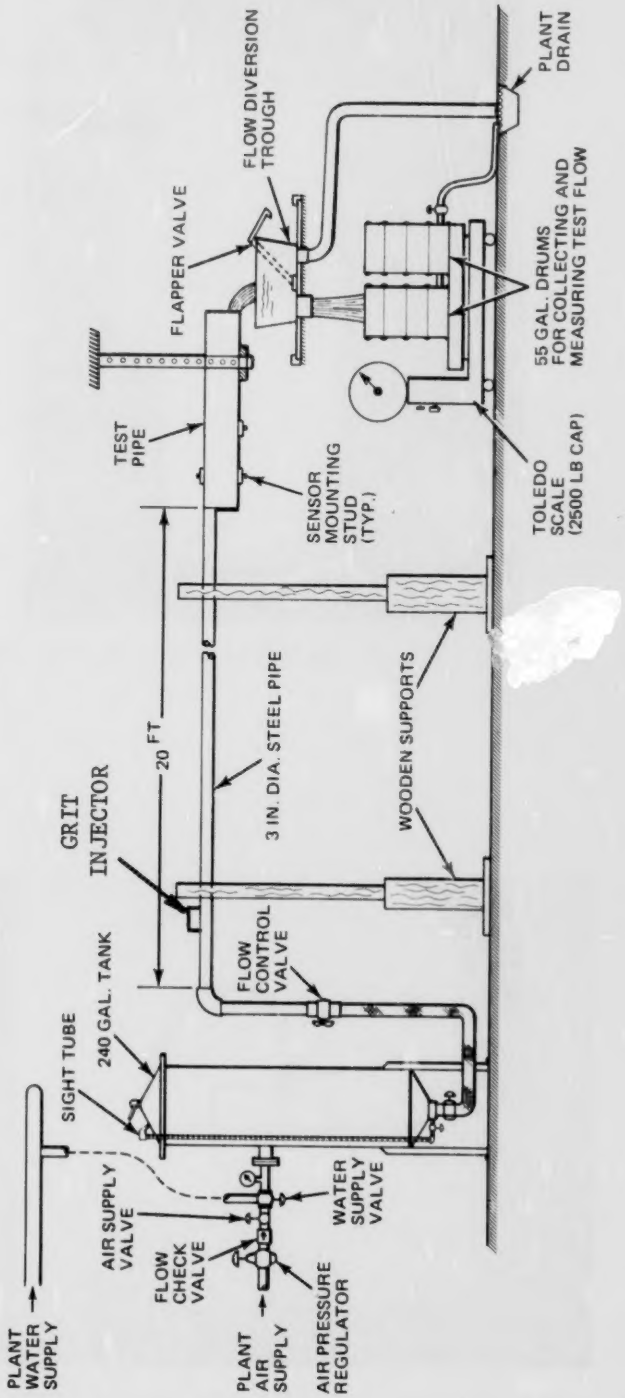
PLANT WATER SUPPLY
PLANT AIR SUPPLY
AIR PRESSURE REGULATOR
FLOW CHECK VALVE
AIR SUPPLY VALVE
WATER SUPPLY VALVE
SIGHT TUBE
240 GAL. TANK
FLOW CONTROL VALVE
GRIT INJECTOR
20 FT
3 IN. DIA. STEEL PIPE
WOODEN SUPPORTS
TEST PIPE
SENSOR MOUNTING STUD (TYP.)
TOLEDO SCALE (2500 LB CAP)
FLAPPER VALVE
55 GAL. DRUMS FOR COLLECTING AND MEASURING TEST FLOW
FLOW DIVERSION TROUGH
PLANT DRAIN

Fig. 4 Grumman Research water supply facility

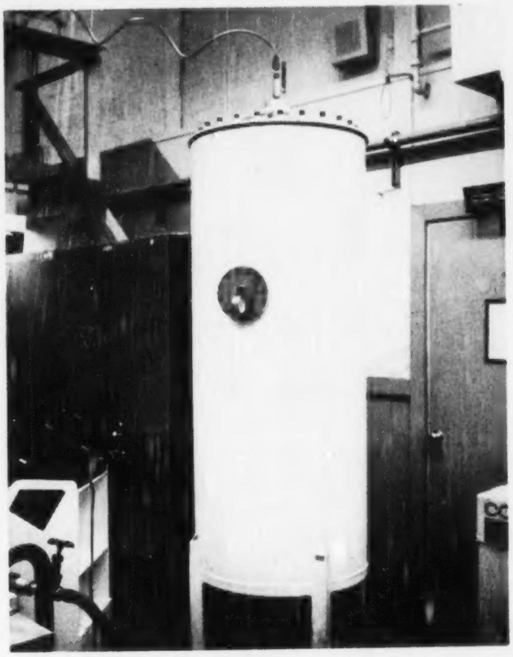

Fig. 5 240 gallon facility water storage tank

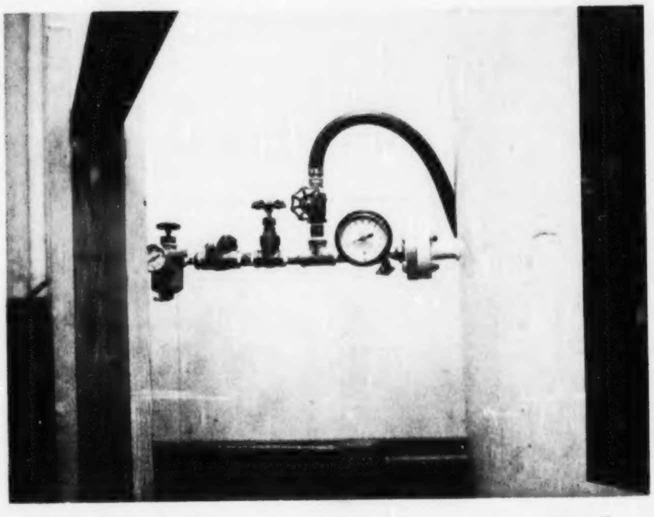

Fig. 6 Air pressurization and water supply pipes to storage tank

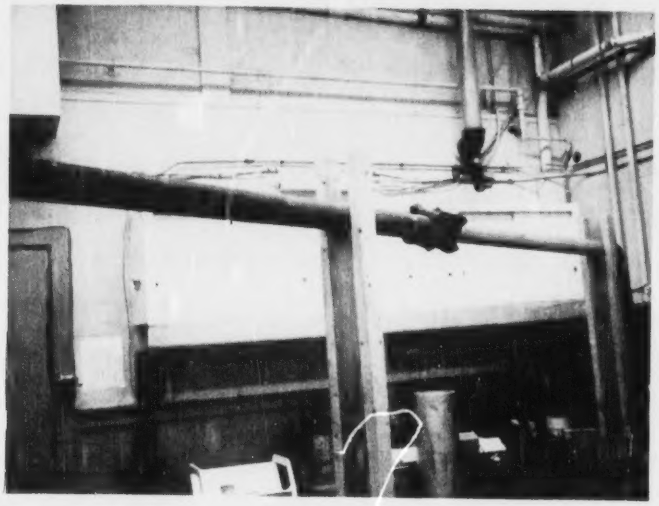

Fig. 7 20 foot length of 3-in. diameter pipe of facility water supply system

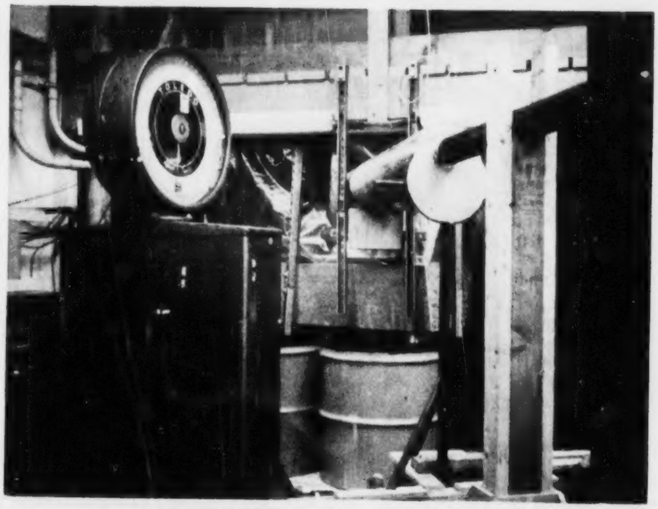

Fig. 8 View of facility test section showing diversion trough, water collection drums, and weighing scale. 8-in. diameter aluminum pipe on test in concentric configuration

Figs. 10 and 8) to another one to double the total collection capacity and both drums rest on the weighing platform of a Toledo scale. This scale has a 2500 lb (1136 kg) weighing capacity and has been calibrated to 1/8th lb (0.06 gm) accuracy. Prior to each test run, a tare weight reading is taken. When flow conditions are stabilized, the flapper valve is opened allowing water to be diverted into the drums, and a stop watch is activated. At the conclusion of the test period, the watch is stopped as the flapper valve is closed and a final weight is read off the scale dial. The average rate of flow during this time is determined from these data. By reducing the collection time to, for example, 10 seconds, a fairly constant flow rate is obtained for all but the highest rates. After each run, a new tare reading is taken or the drums are drained, depending on the anticipated magnitude of flow rate for the next run.

For this program, the test sections of conduit were:

- ~ 2-in. (5.1 cm) high by ~ 5-in. (12.7 cm) wide open aluminum channel
- 8-in. (20.3 cm) diameter aluminum pipe
- 4-in. (10.2 cm) diameter transite sewer pipe
- 6-in. (15.3 cm) diameter transite sewer pipe

and they were attached either concentrically or eccentrically. The resulting discontinuity geometries and distances are depicted by Fig. 11.

The transducer types used to monitor the pseudosound at the discontinuity are accelerometers. We selected accelerometers in preference to several other transducer types that appeared

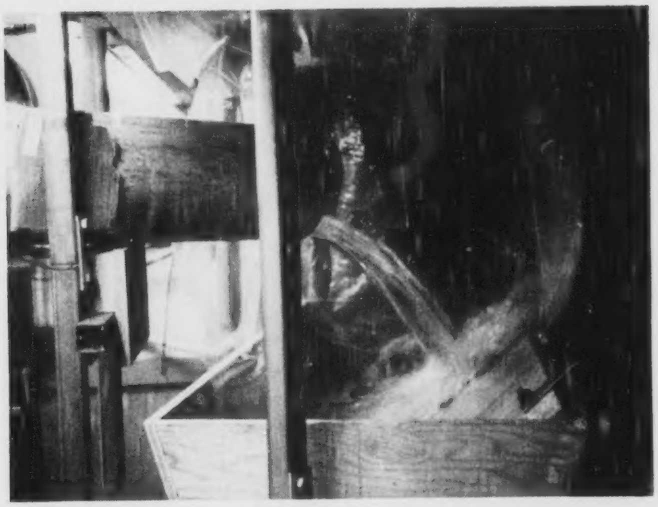

Fig. 9 View of water flowing from 8-inch diameter test pipe into diversion trough

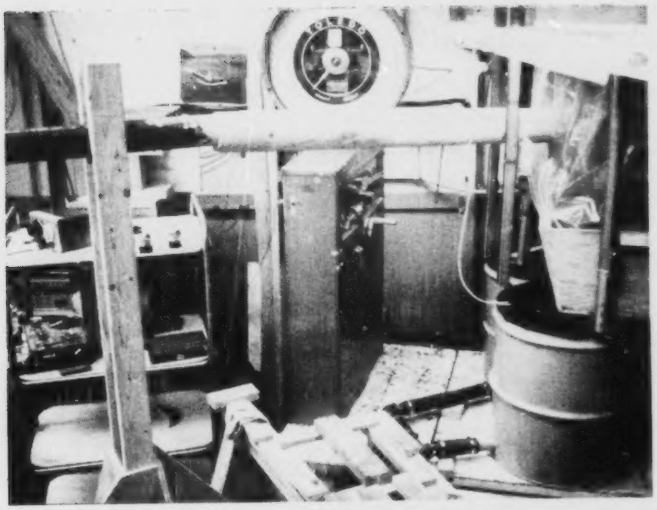

Fig. 10 Overall side view of facility test section showing diversion trough, water collection drums, and weighing scale. 4-inch diameter transite pipe on test

1. CLOSED CYLINDRICAL TO OPEN TRAPEZOIDAL

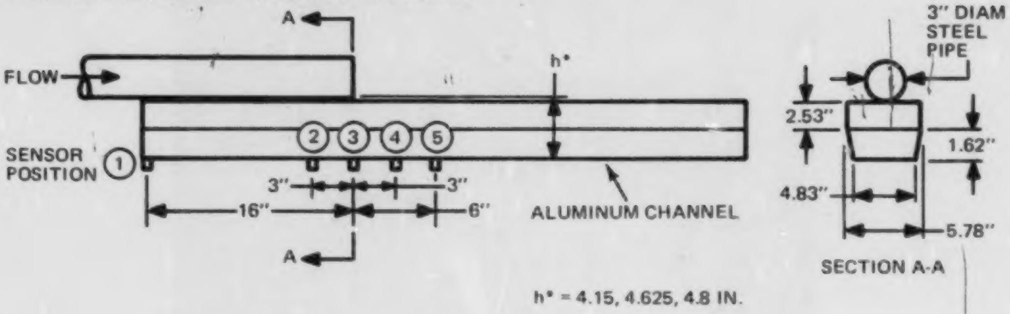
A
FLOW
h*
SENSOR POSITION
① ② ③ ④ ⑤
3"
3"
16"
6"
ALUMINUM CHANNEL
A
3" DIAM STEEL PIPE
2.53"
1.62"
4.83"
5.78"
SECTION A-A
h* = 4.15, 4.625, 4.8 IN.

2. 3-IN. DIAM STEEL PIPE TO 3-IN. DIAM STEEL PIPE

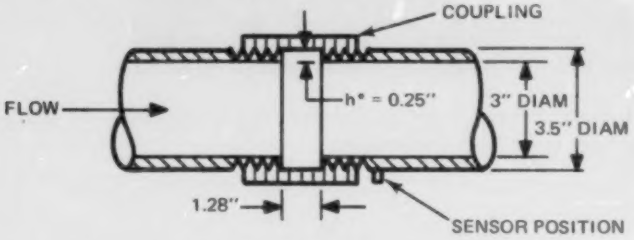
COUPLING
FLOW
h* = 0.25"
3" DIAM
3.5" DIAM
1.28"
SENSOR POSITION

3. 3-IN. DIAM STEEL PIPE TO 8-IN. DIAM ALUMINUM PIPE
a) CLOSED ECCENTRIC CYLINDRICAL CONFIGURATION
1) WITH EXTENDED INLET

NOTE: 1 IN. = 2.54 cm

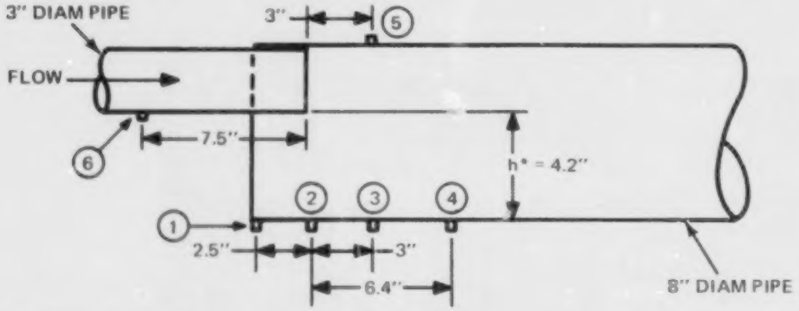
3" DIAM PIPE
3"
⑤
FLOW
⑥
7.5"
h* = 4.2"
② ③ ④
①
2.5"
3"
6.4"
8" DIAM PIPE

2) WITH FLUSH INLET

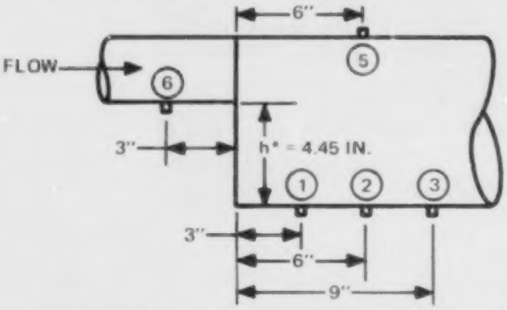
6"
FLOW
⑥
⑤
3"
h* = 4.45 IN.
① ② ③
3"
6"
9"

(NUMBER IN CIRCLE DENOTES SENSOR POSITION REFERENCE)

Fig. 11 Sensor locations and channel discontinuities tested in research laboratory, sheet 1 of 2

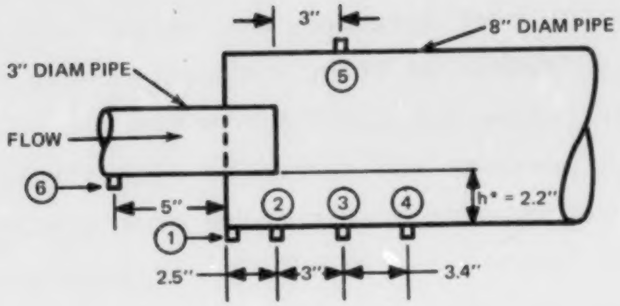
3"
8" DIAM PIPE
3" DIAM PIPE
FLOW
⑤
⑥
5"
h* = 2.2"
①
②
③
④
2.5"
3"
3.4"

3. b) CLOSED CONCENTRIC CYLINDRICAL CONFIGURATION
1) WITH EXTENDED INLET

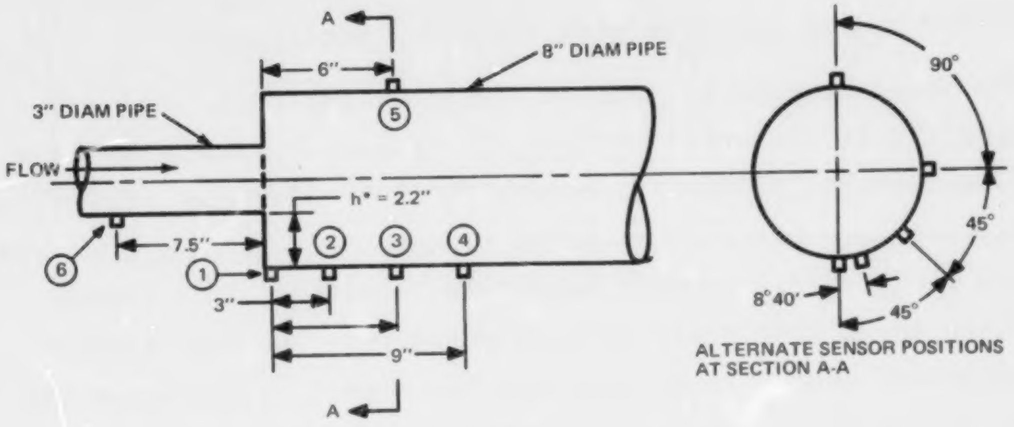
A
6"
8" DIAM PIPE
3" DIAM PIPE
FLOW
⑤
h* = 2.2"
7.5"
⑥
①
②
③
④
3"
9"
A
90°
45°
8°40'
45°
ALTERNATE SENSOR POSITIONS
AT SECTION A-A

2) WITH FLUSH INLET

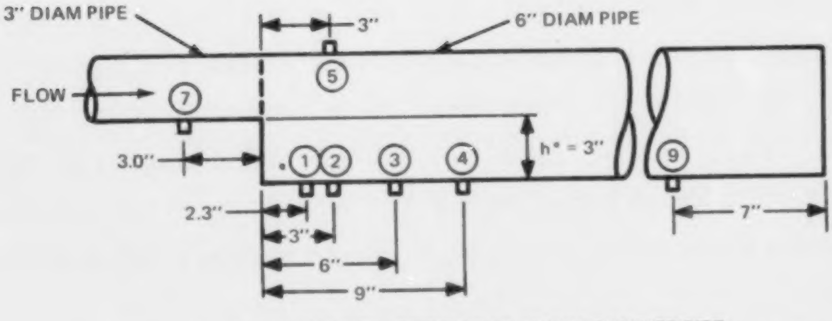
3" DIAM PIPE
3"
6" DIAM PIPE
FLOW
⑦
⑤
h* = 3"
3.0"
①
②
③
④
⑨
2.3"
3"
6"
9"
7"

4. 3-IN. DIAM STEEL PIPE TO 6-IN. DIAM TRANSITE PIPE
CLOSED ECCENTRIC CYLINDRICAL CONFIGURATION WITH FLUSH INLET

Fig. 11 Sensor locations and channel discontinuities tested in research laboratory, sheet 2 of 2

potentially useful because these devices are inexpensive (~ $250), have the best frequency and sensitivity characteristics, and are capable of being environmentally sealed without difficulty. Condenser microphones require an opening to equalize static pressure and cannot be effectively sealed. Piezoelectric microphones also require pressure equalization and usually are limited to 10,000 Hz frequency. Hydrophone type microphones are very expensive, and piezoresistive microphones have low output sensitivity. Magnetic variable reluctance transducers are affected by ambient magnetic fields and do not have high frequency sensitivity.

The accelerometer is screwed onto mounting studs that are cemented to the outer surface of the test conduit. We have found Devcon "F" epoxy cement with 80% aluminum content to provide good acoustic coupling between the mounting stud and the various test conduit materials. However, this cement takes about four hours to cure properly. The many sensor locations needed to be examined for signal optimization can be accommodated best by attaching many mounting studs at judiciously selected locations prior to test. Several accelerometer models were used during the program. They vary in sensitivity, size, weight, and one model has an integral preamplifier to match impedance with external recording circuits. All acoustic data have been recorded on $\frac{1}{4}$-in. by 600 ft (6.3 mm by 180 m) Scotch brand magnetic instrumentation tape using a Nagra III model tape recorder. The typical instrumentation equipment used is shown schematically in Fig. 12.

About midway in the program, a wooden container, 22.4-in (57 cm) wide by 48-in. (122 cm) long was constructed to

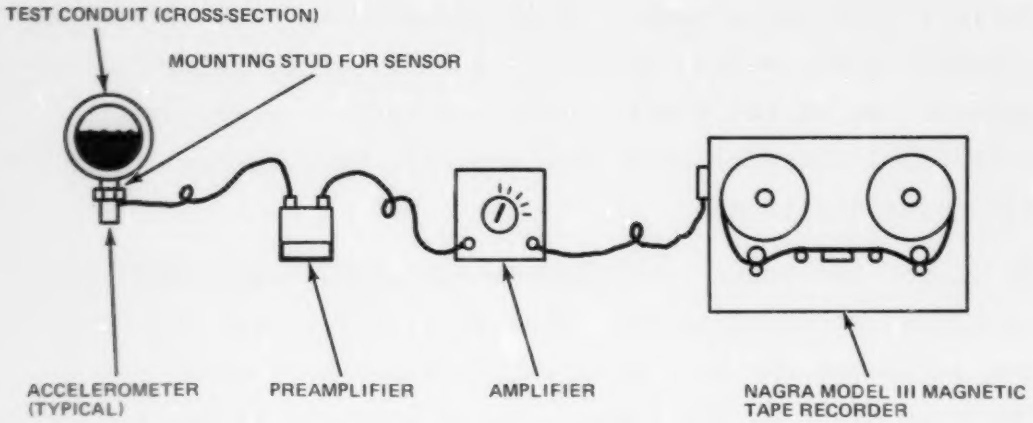
TEST CONDUIT (CROSS-SECTION)
MOUNTING STUD FOR SENSOR
ACCELEROMETER (TYPICAL)
PREAMPLIFIER
AMPLIFIER
NAGRA MODEL III MAGNETIC TAPE RECORDER

Fig. 12 Schematic of testing instrumentation

hold sand or soil (see Fig. 13). This equipment simulates buried installations of the pipeline especially in the vicinity of the conduit discontinuity (see Fig. 14). A maximum buried depth of 8-in. (20.3 cm) can be accommodated with a uniform layer of sand circumferentially around the largest test pipes used. It is possible to test with either completely uncovered, partially buried, or fully buried installations of the pipes. This simulation closely meets ASTM C-361 specifications for two pipe bedding techniques in field installations.

In one of the tests conducted to simulate a heavy bed load of coarse grit relatively large stone chips were placed at the bottom of the test pipe and retained by a metal dam at the exit plane of the pipe. Figure 15 shows an extra heavy bed loading before water flow. Figure 16 shows the partial washout of the uniform bed after being subjected to flow rates above 2-3 lb/sec (0.9-1.4 kg/sec).

In another study, medium-to-coarse sand grit (sieve sizes between 8 and 20 and a specific gravity of 2.62) was injected into the flow. This required an additional piece of equipment at the upstream end of the 3-in. (7.6 cm) pipe. This grit feed device uses a dc servo motor-generator (Motomatic Model E6500 Series 125) and a motor speed controller (see Figs. 17 and 18). The motor shaft is attached to a 5/8-in. (1.6 cm) diameter feed screw that traverses the bottom of a grit storage hopper. The flow rate of the grit depends on the rotational speed of the motor which is set by a 1000 division vernier rheostat on the controller box. For a given rheostat setting, the motor speed is maintained constant by the servo circuit.

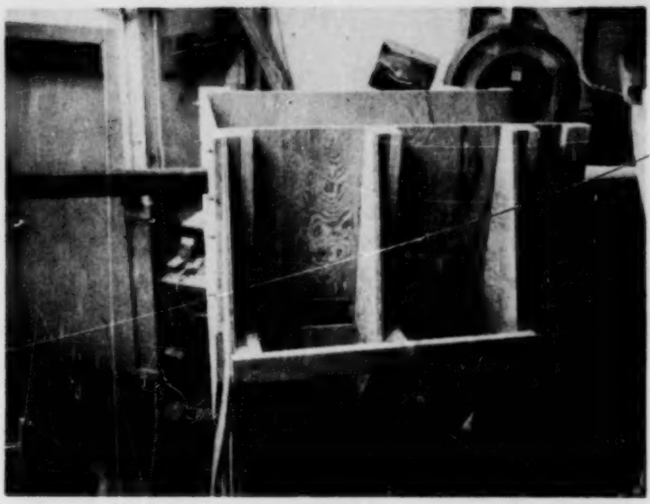

Fig. 13 Side view of box for containing sand used to simulate buried pipe installation

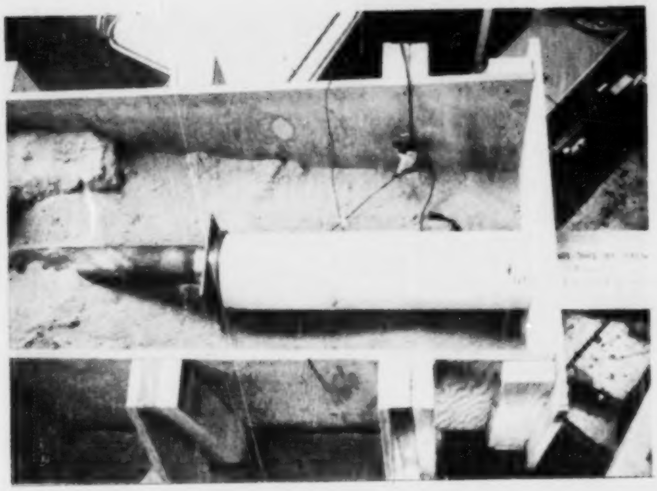

Fig. 14 Top view of box used to simulate buried pipes. 6-inch diameter transite pipe is shown on test with sand removed. Flow direction is from left to right

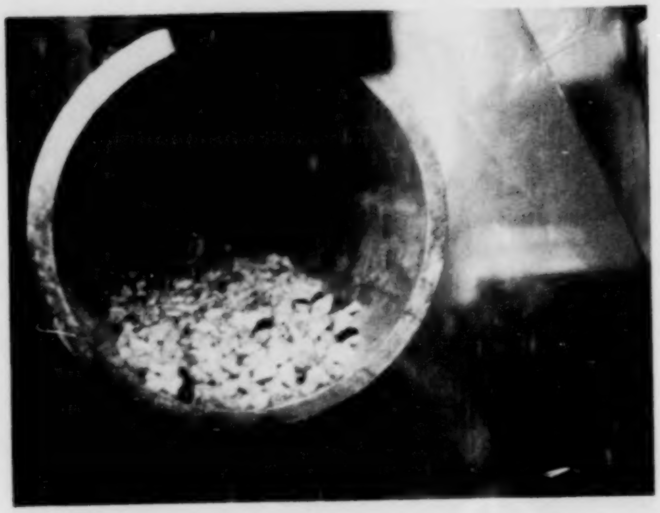

Fig. 15 End view of 8-inch diameter pipe showing initial condition of heavy (1-inch) bed load of stone chips

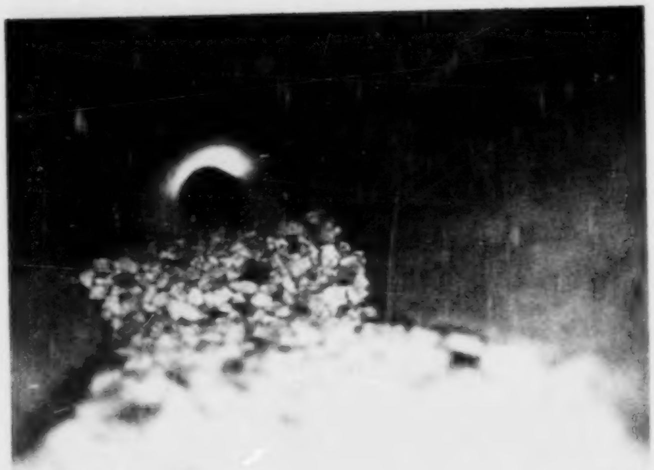

Fig. 16 Heavy bed load after being disturbed by water flow at rates up to 3 pounds per second

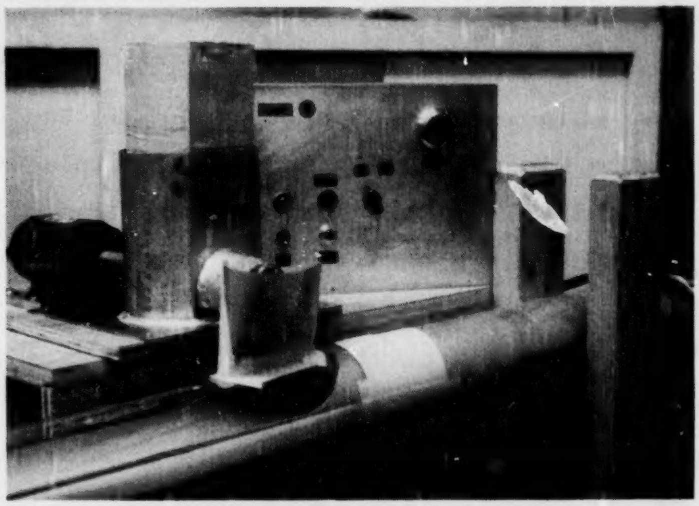

Fig. 17 Equipment used to feed sand grit into upstream water supply

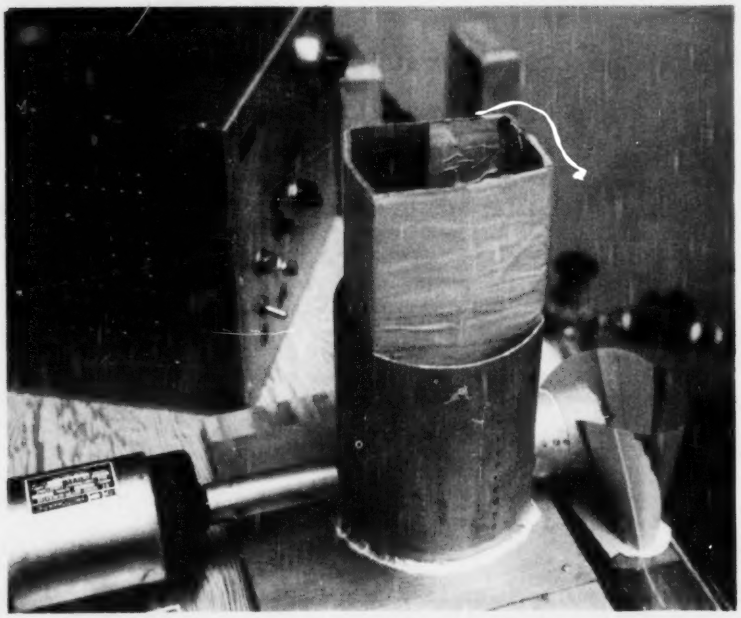

Fig. 18 Closeup of speed controlled motor and supply hopper used to feed sand grit into water supply

Dry loose sand is dropped into the water flow through a $\frac{1}{4}$-in. (0.64 cm) wide slit near the upstream end of the 3-in. (7.6 cm) pipe. As seen by the photos, the upper portion of this pipe was partially removed and replaced by a curved plastic shield. In this way the movement of the sand particles downstream of the slit can be tracked visually. However, because of the opening in the pipe it is not possible to introduce sand and exceed a water flow rate of somewhat more than 6 lb/sec (2.73 kg/sec). This flow rate corresponds to a completely filled pipe. To eliminate clogging of the drains and prevent serious error in measuring water flow with the collection barrels, the grit is separated from the water at the outflow of the test pipe. This is done by a screening tray, mounted on rails, just under the test pipe exit (see Fig. 19); the separated sand is removed for drying and reused. Baffle plates prevent the outflow from splashing out of the tray. The concentration of grit in the test water flow is determined from a grab sample taken about midway through a test run. The sample is contained in a 250 ml glass beaker that has been manually inserted into the outflow. The grit is filtered from the water sample and measurements are made of the captured water volume and the grit weight in order to determine mg/liter concentration value. It is assumed that the grab sample is representative of the entire flow composition while the acoustic recordings are made. For the test made, the sand concentrations were between 86 and 1682 mg/liter. These values simulate very closely the recommended sewage characteristics for grit (20-360 mg/liter) and settleable solids (200-1150 mg/liter).[5]

In order to provide a preview of the type of results that could be obtained in a field test phase, a limited amount of field testing was made during this project. Several flow measurements were made using pipelines feeding Grumman's main sanitary sewage treatment plant. Figure 20 shows where some of these data were obtained. This location is an underground concrete vault, at the SE corner of the treatment plant, where valves are installed to control the diversion of sewage to two aerating tanks on either side of the building at the rear of the picture. Figure 21 shows the 8-in. (20.3 cm) plug valve and the 8 by 10-in. (20.3 x 25.4 cm) expansion section which adapts the valve to the 10-in. (25.4 cm) diameter cast iron sewer pipe. The accelerometer sensor is seen about two-thirds of the section length downstream from the valve flange. To expedite versatility in field measurements, a magnetic mounting stud was used to couple acoustically the sensor to the pipe. A more intimate coupling would have resulted if we used the epoxy-based adhesive for the mounting stud, but the time necessary to cure the epoxy would have delayed the test program. With the magnetic attachment, we are able to shift rapidly sensor locations upstream and downstream of the valve body. Another field location used to make acoustic measurements is shown in Fig. 22. This is at the north aeration tank of the treatment plant. The 10-in. diameter sewer pipe rises from its buried installation to enter a comminuter as shown in Fig. 23. The sewer pipe changes from a cylindrical steel channel to an open concrete conduit before entering the comminuter. A smaller, 4-in. diameter (10.2 cm) pipe can be seen in Fig. 23 as also rising from underneath the surface

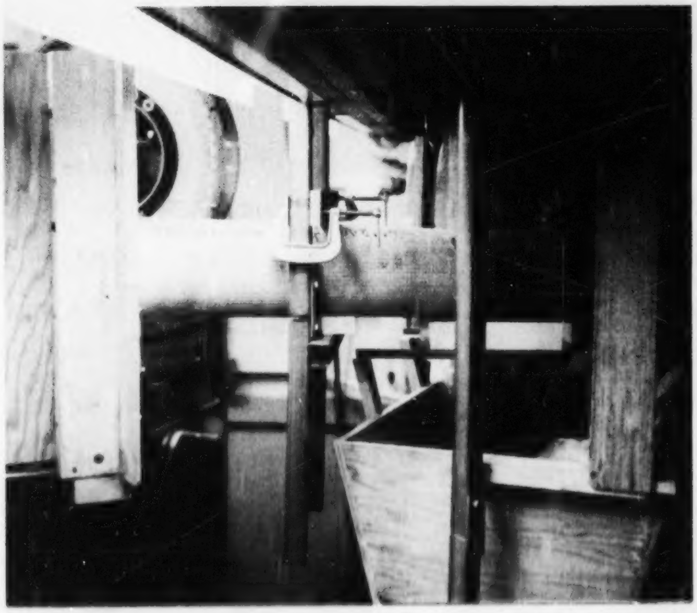

Fig. 19 Screen tray added to water collection system to separate grit from collected water. 6-inch diameter transite pipe is shown on test. Tray is just below pipe exit

Fig. 20 Exterior view of valve vault (foreground) at Grumman waste treatment plant "A". This is first site of field test preview experiments

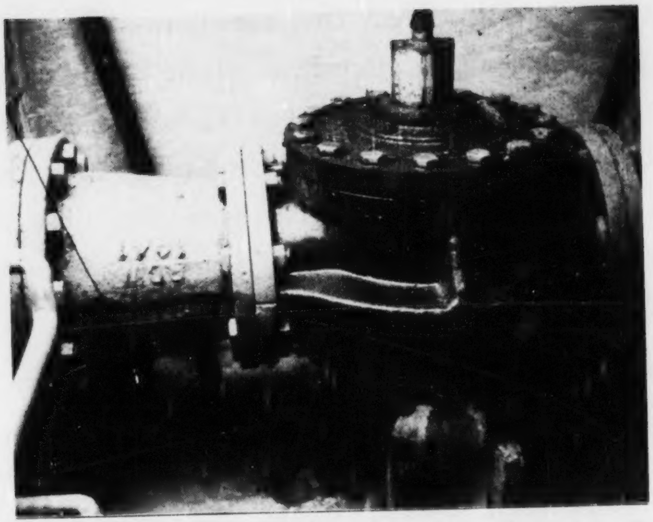

Fig. 21 Interior view of valve vault showing 8-inch plug valve and 8 x 10-inch reducer section with accelerometer attached to outer wall for acoustic emission monitoring of flow

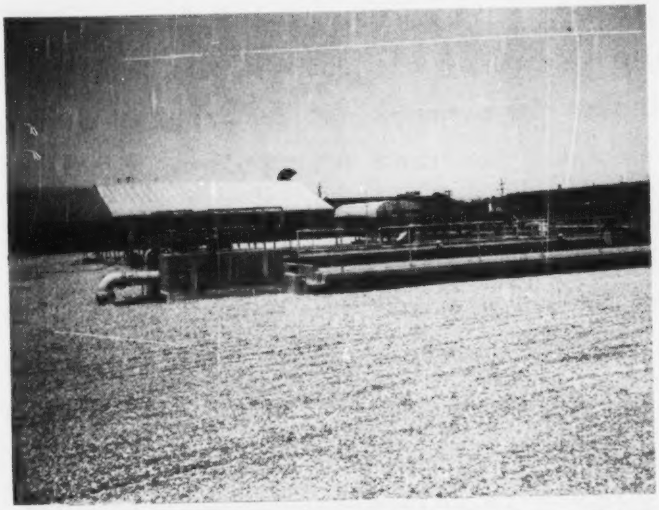

Fig. 22 Exterior view of aeration tank at Grumman waste treatment plant "A". 10-inch diameter pipe emerges from underground installation at left center of photo. This is site of second series of field test preview experiments

and conducting its flow over the concrete wall. This pipe brings sewage from another Grumman plant and discharges it into the comminuter channel vertically above the exit plane of the 10-in. (25.4 cm) pipe. Several pipe locations were acoustically examined at this site for flow of just the 10-in. (25.4 cm) pipe as well as combined flow with the 4-in. (10.2 cm) pipe.

Processing of the tape recorded data is made with Grumman's Fourier analyzer computer facilities shown in Fig. 24. The block schematic of electronic and display equipment is shown in Fig. 25. A closeup of the Nagra data recorder, Pemco continuous loop transfer recorder and HP-5465A, HP-5460A, and HP-2114B Fourier Analyzer system is shown from right to left in Fig. 26.

Total sound data, in the 40 to 22,000 Hz frequency band, is transferred from the Nagra recorder to the Pemco continuous loop recorder. The amount of original data transferred depends on the length of the loop on the Pemco recorder; usually at least 10 seconds of continuous recording was used in our program for each test point. Sixty random samplings of the loop, representing about one-fifth to one-tenth of the total original recorded information, are processed by the HP-5465A computer. Each sampling is broken down by this digital computer into 1028 frequency components and associated amplitudes using Fourier transforms of the time-varying sensor signals, and then the spectra are co-added (this process is called ensemble averaging). This technique extracts the useful signal from the recordings and practically cancels extraneous random noise. The rms average data

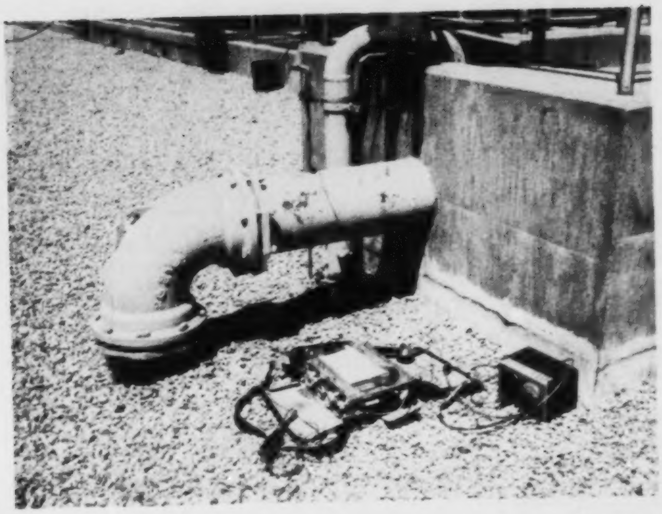

Fig. 23 Closeup of 10-inch diameter pipe where second field test preview series was conducted. Sensor is shown attached to top center of horizontal pipe. Tape recorder and amplifier used is shown in foreground

Fig. 24 Data processing equipment used to obtain spectral distribution from flow acoustic emission recordings. HP-5465A Fourier analyzer computer is in center of picture

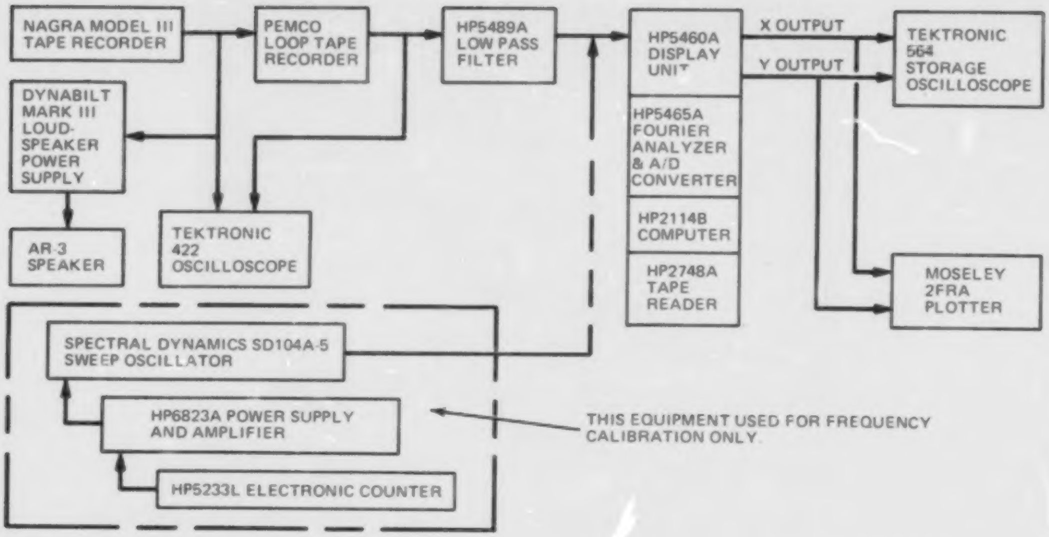
NAGRA MODEL III TAPE RECORDER
PEMCO LOOP TAPE RECORDER
HP5489A LOW PASS FILTER
HP5460A DISPLAY UNIT
X OUTPUT
Y OUTPUT
TEKTRONIC 564 STORAGE OSCILLOSCOPE
DYNABILT MARK III LOUD-SPEAKER POWER SUPPLY
HP5465A FOURIER ANALYZER & A/D CONVERTER
HP2114B COMPUTER
HP2748A TAPE READER
AR-3 SPEAKER
TEKTRONIC 422 OSCILLOSCOPE
MOSELEY 2FRA PLOTTER
SPECTRAL DYNAMICS SD104A-5 SWEEP OSCILLATOR
HP6823A POWER SUPPLY AND AMPLIFIER
HP5233L ELECTRONIC COUNTER
THIS EQUIPMENT USED FOR FREQUENCY CALIBRATION ONLY.

Fig. 25 Schematic of acoustic emission data processing system

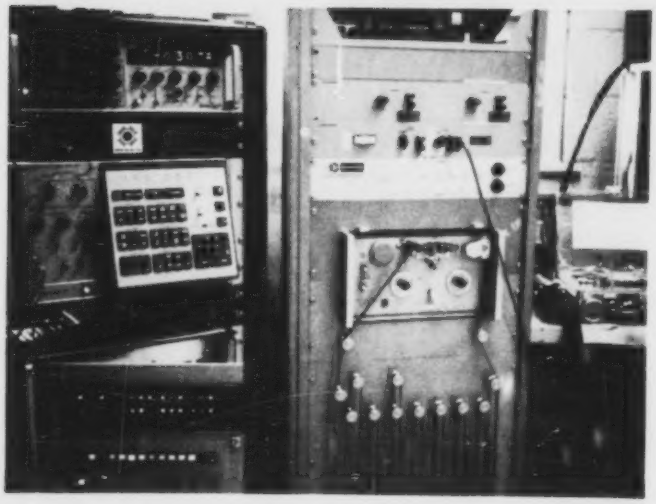

Fig. 26 Closeup of data processing equipment showing (L to R) HP-5465A Fourier analyzer computer, Pemco continuous loop recorder and playback, and Nagra tape recorder used for laboratory and field

value of the signal[†] is displayed digitally on the HP-5460A unit and a spectral distribution of amplitude is plotted on semilog paper (dB versus frequency) by the Moseley 2FRA plotter. Typical spectral distributions for the April 28 test series (see Section IIIC-7) are shown in Fig. 27 (a) and (b). The upper curve (a) for the no flow condition shows the mass distribution law fall-off of amplitude with frequency for random, broadband noise.[3] By contrast, the spectra at a relatively high flow (~ 13 lb/sec = 5.9 kg/sec) given by curve (b) shows specifically strong content in various frequency bands that are produced by the flow across the conduit discontinuity as well as from other nonrandom sources (e.g., bubbles, turbulence, valve noises, etc.). In addition, the rms signal[†] (i.e., integrated over-all frequencies between 40 and 22,000 Hz) is 32 db greater for the flow case [curve (b)] than the ambient noise level [curve (a)].

A few select studies during the course of this program indicated that biasing the transferred acoustic data to a particular portion of the original recording can result in a ± 2 db change in the rms signal value, for given test flow conditions. This bias can be minimized but at considerable inconvenience by transferring and connecting small pieces of the original recording taken over its entire duration for a test point. The limited magnitude of this bias effect, and the extent of reproducibility of results, considering the number of components integrated into all laboratory systems, did not warrant the delay that would be incurred in processing with greater care the thousands of data points.

[†] Referenced to 1 volt.

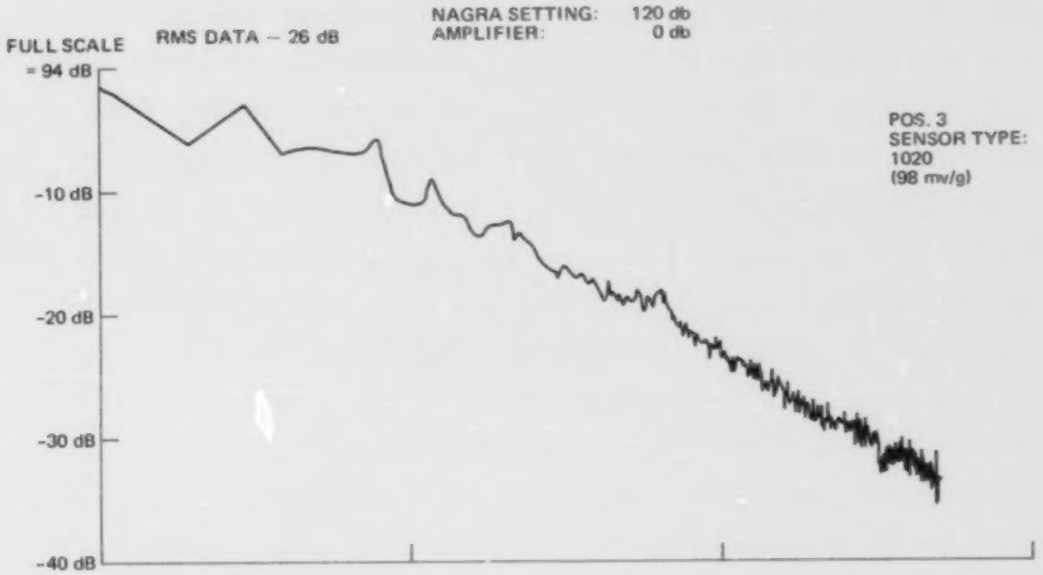

a) AMBIENT – NO FLOW

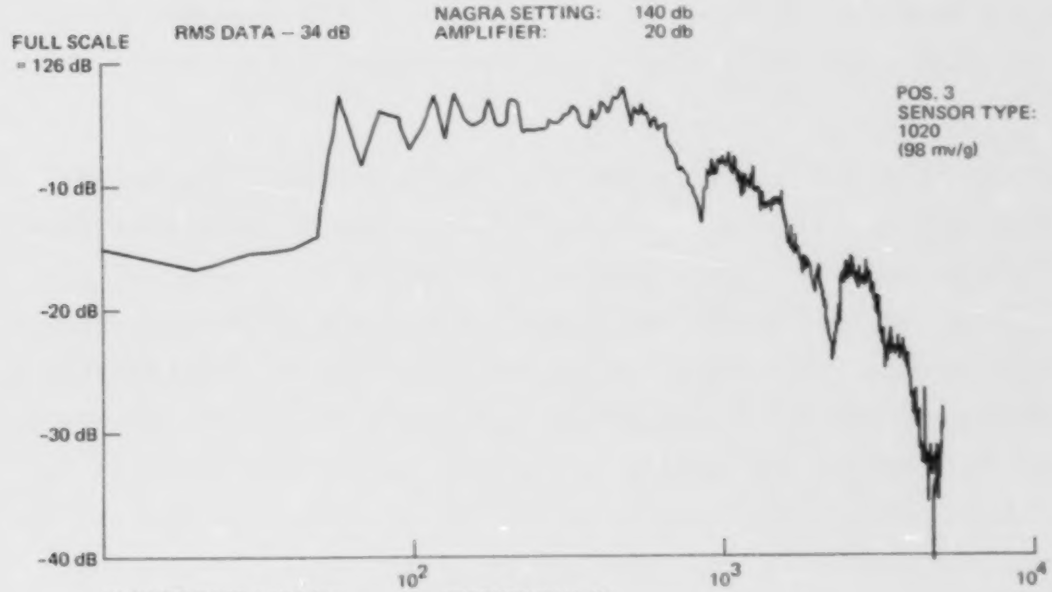

b) FLOW RATE = 13 lb/sec

Fig. 27 Typical Fourier processed spectral distributions of laboratory sound recordings (10 Hz bandwidth)

Another study to improve processing accuracy involved doubling the quantity of samples randomly selected by the Fourier analyzer. The processing time is doubled, but the results obtained for several exploratory cases are not sufficiently better than with 60 samples to justify the extra processing time. Apparently, our standard sampling number produces statistically good results.

C. EXPERIMENTAL PHASE

The experimental investigations of this program were mainly concerned with clean water flow in Grumman's hydraulics research laboratory. However, a brief field test preview was conducted after the laboratory tests were concluded. Descriptions of these facilities have been presented in the previous section.

The test program was conducted from August 14, 1974 to July 1, 1975 and used various size pipes as well as an open channel. Salient features of the conduits, transducers, flow parameters, and experimental setup conditions of each test series are summarized in chronological order in the table. In reviewing these tests here, each group of closely related experiments is described separately with minimal comment. Full discussion of the results is covered in Section IIID.

It is to be noted that approximately the initial half of the test program has been run with no special attempt to simulate real underground installations of sewers (see item number 8 of Table T-1). This measure simplified the test setups and

TABLE T-1. SUMMARY OF TESTING FEATURES (SHEET 1 OF 2)

		1974																	
	Date of Test	8/14	8/22	8/23	9/9	9/12	10/28	10/29	10/29	10/30	11/8	11/11	11/11	11/11	1/16	1/17	1/22	1/23	1/29
No.	Feature																		
1	Channel size																		
	a. 3" diam steel (stl)	•																	
	b. 3" diam steel to 2" x 5" trapezoidal		•	•		•					•	•	•						
	c. 3" diam steel to 8" diam aluminum				•		•	•	•	•				•	•	•	•	•	•
	d. 3" diam steel to 4" diam transite																		
	e. 3" diam steel to 6" diam transite																		
2	Channel type																		
	a. Concentric cylindrical, closed	•							•	•				•	•	•	•	•	
	b. Eccentric cylind., closed				•		•	•											•
	c. Closed cylind. to open trapezoidal		•	•		•					•	•	•						
3	Max. discontinuity dimension (in.)	0.25	3.8	3.8	4.25	4.625	4.2	4.2	2.2	2.2	4.15	4.8	4.15	2.2 →	→	→	→	→	4.45
4	Characteristic frequency (kHz)	~60.	3.91	3.91	3.50	3.21	3.54	3.54	6.76	6.76	3.58	3.10	3.58	6.76 →	→	→	→	→	3.32
5	Sensor type																		
	a. B&K model (no.)	4332	4332	4333	4333 4332	4332 4333	4332	4333	→	→	→	→	→	→	4333 (2)	4333 4339	4333 (2)	→	4333 (2)
	b. Vibrametrics model (no.)																		
6	Sensor sensitivity, (mv/g)	62	62.	19.5	19.5 62	19.5 62	62	19.5	→	→	→	→	→	→	19.5 21.5	19.5 10.	19.5 21.5	→	19.5 21.5
7	Sensor installations																		
	a. No. of axial positions	1	1	1	2	2	3	3	3	2	3	4	3	1	2	→	→	→	→
	b. No. of circumferential posit.	1	→	→	→	→	→	→	→	→	→	→	→	→	→	2	1	→	→
8	Pipe installation features																		
	a. Freely suspended in air	•	•	•	•	•	•	•	•	•	•	•	•	•	•	•	•	•	•
	b. Simulated underground																		
	c. In sim. box but not buried																		
9	Max. flow rate (lb/sec)	8.4	NA	NA	7.6	5.5	7.0	7.0	8.0	7.0	7.0	7.5	7.25	7.5	8	8	10	15	11
10	Pipe exit condition																		
	a. Open exit	•	•	•	•	•	•	•	•	•	•	•	•	•	•	•			
	b. Exit weir installed																•	•	•
11	Supply pipe inlet condition																		
	a. Extended inlet (overlap dist., in.)		•(3)	•(3)	•(3)	•(3)	•(2.5)	•(2.5)	•(2.5)	•(2.5)	•(16)	•(16)	•(16)	•(2.5)					
	b. Flush inlet	•													•	•	•	•	•
12	Solids in flow?																		
	a. None (except rust)	•	•	•	•	•	•	•	•	•	•	•	•	•	•	•	•	•	•
	b. Heavy bed load of stone chips																		
	c. Light bed load of stone chips																		
	d. Upstream dispersed grit																		
13	Remarks	Prelim. data	Exploratory acoustical data																

TABLE T-1. SUMMARY OF TESTING FEATURES (SHEET 2 OF 2)

		1975																	
	Date of Test	2/26	2/27	2/28	3/6	3/12	3/21	3/27	3/31	3/31	4/9	4/23	4/24	4/24	4/28	5/8	5/8	6/26	7/1
No.	Feature																		
1	Channel size																		10" Diam cast iron
	a. 3" diam steel (stl)																		
	b. 3" diam steel to 2" x 5" trapezoidal																		
	c. 3" diam steel to 8" diam aluminum				•	•	•	•	•	•	•								
	d. 3" diam steel to 4" diam transite	•	•	•															
	e. 3" diam steel to 6" diam transite											•	•	•	•	•	•	•	
2	Channel type																		
	a. Concentric cylindrical, closed						•	•	•	•	•								•
	b. Eccentric cylind., closed	•	•	•	•	•						•	•	•	•	•	•	•	
	c. Closed cylind. to open trapezoidal																		
3	Max. discontinuity dimension (in.)	0.69	→	→	4.45	4.25	2.2	→	→	→	→	3.0	→	→	→	→	→	→	NA
4	Characteristic frequency (kHz)	21.5	→	→	3.32	3.50	6.76	→	→	→	→	5.57	→	→	→	→	→	→	NA
5	Sensor type																		
	a. B&K model (no.)	4333 (2)	→	→	4333 (2)	→	→	→	4333 (2)	→	4333 (2)	→	→	→	4333	4333 (2)	→	4333	4332
	b. Vibrametrics model (no.)				1020	→	→	→			1020	→			1020			1020	
6	Sensor sensitivity. (mv/g)	19.5 21.5	→	→	19.5, 21.5, 98	→	→	→	19.5 21.5	→	19.5, 21.5 98	→	19.5, 21.5	→	19.5 98	19.5 21.5	→	19.5 98	62
7	Sensor installations																		
	a. No. of axial positions	1	→	→	2	2	3	3	2	2	3	4	2	2	3	1	2	1	6
	b. No. of circumferential posit.	3	2	2	1	→	→	→	→	→	→	→	→	→	→	→	→	→	6
8	Pipe installation features																		a) In buried vault, b) Emerging from underground
	a. Freely suspended in air	•																	
	b. Simulated underground			•		•		•	•	•	•			•	•	•			
	c. In sim. box but not buried		•		•		•					•	•				•	•	
9	Max. flow rate (lb/sec)	10	10	8	12.5	13.25	12	12	11.5	8.25	11.0	11.0	14.2	11.6	14.0	2	15.4	5	125.0
10	Pipe exit condition																		
	a. Open exit	•	•	•					•			•	•	•	•	•	•	•	•
	b. Exit weir installed				•	•	•	•		•	•								
11	Supply pipe inlet condition																		
	a. Extended inlet (overlap dist., in.)																		
	b. Flush inlet	•	•	•	•	•	•	•	•	•	•	•	•	•	•	•	•	•	•
12	Solids in flow?																		
	a. None (except rust)	•	•	•	•	•	•	•	•			•	•	•	•	•	•		
	b. Heavy bed load of stone chips									•									
	c. Light bed load of stone chips										•								
	d. Upstream dispersed grit																	•	Sanitary Sewage •
13	Remarks																	8-20 Sieve Size S.G.= 2.62	Field Test Preview •

was designed originally to expedite test schedules as well as to avoid constructing test equipment that might prove superfluous. Some of the data obtained with this initial simple test setup, particularly for cylindrical pipe elements, appear in conflict with dipole theory trend predictions. In the interest of completeness several plots of these discrepant data are included in the material of this section. The reader is cautioned not to interpret these data as evidence of a basic defect in our flow measurement concept. As will be explained later in Section IIID, Discussion, these discrepant test data are solely the result of shortcomings in our initial laboratory simulation technique. This situation was rectified in the latter half of the experimental program with relatively simple, yet effective, measures developed to simulate underground sewer installations.

1. Steel Supply Pipe (Tests of August 14, 1974)

Measurements were made for a 5 ft (1.52 m) length of 3-in. (7.6 cm) diameter steel pipe coupled to the 20 ft (6.1 m) long, 3-in. (7.6 cm) steel water supply pipe of the test facility. Because of the threaded coupling geometry [3.25-in. (8.3 cm) long] and pipe wall thickness [0.216-in. (0.55 cm)] a 0.25-in. (0.64 cm) annular step existed for a distance of 1.28-in. (3.25 cm) between the two pipe sections (see Fig. 11).

The objective of this test was to record the inherent noise of the facility supply line for a case where just a minor perturbation discontinuity was introduced into the pipeline. A B&K 4332 accelerometer was attached to a steel mounting stud that had been cemented to the outer surface of the pipe at a position abutting the downstream end of the coupling and on the bottom centerline. Devcon "F" epoxy cement with 80% aluminum content, was the adhesive. Initial supply pressure for the water was 15 $\mathrm{lb/in.}^2$ ($1.05\ \mathrm{kg/cm}^2$) and 20 seconds collection time was employed to obtain average flow rates for several control value settings. Between flows of 0 to 8.4 lb/sec (0 to 3.8 kg/sec), the overall signal between frequencies 40 and 22,000 Hz varied as shown by Fig. 28. These data are duplicated by data obtained during the October 28-30 test series (see Section IIIC-3) in which the sensor was located 2.5 pipe diameters upstream of a significant conduit discontinuity (see Fig. 28). Both sets of acoustic data appear to follow a lower rate of change with flow than predicted by dipole theory. Data for two frequencies exhibiting repeated peak amplitudes in the spectral distribution also are plotted on Fig. 28. The ambient sound (zero flow) recorded in the laboratory displays two major peak amplitudes in its spectral distribution, at 80 and 2160 Hz, and a general trend of decreasing signal with increasing frequency (see Fig. 29); this is characteristic of a mass-law distribution of broadband acoustic energy.[3] Spectral distributions for several flow rates exhibit less of the

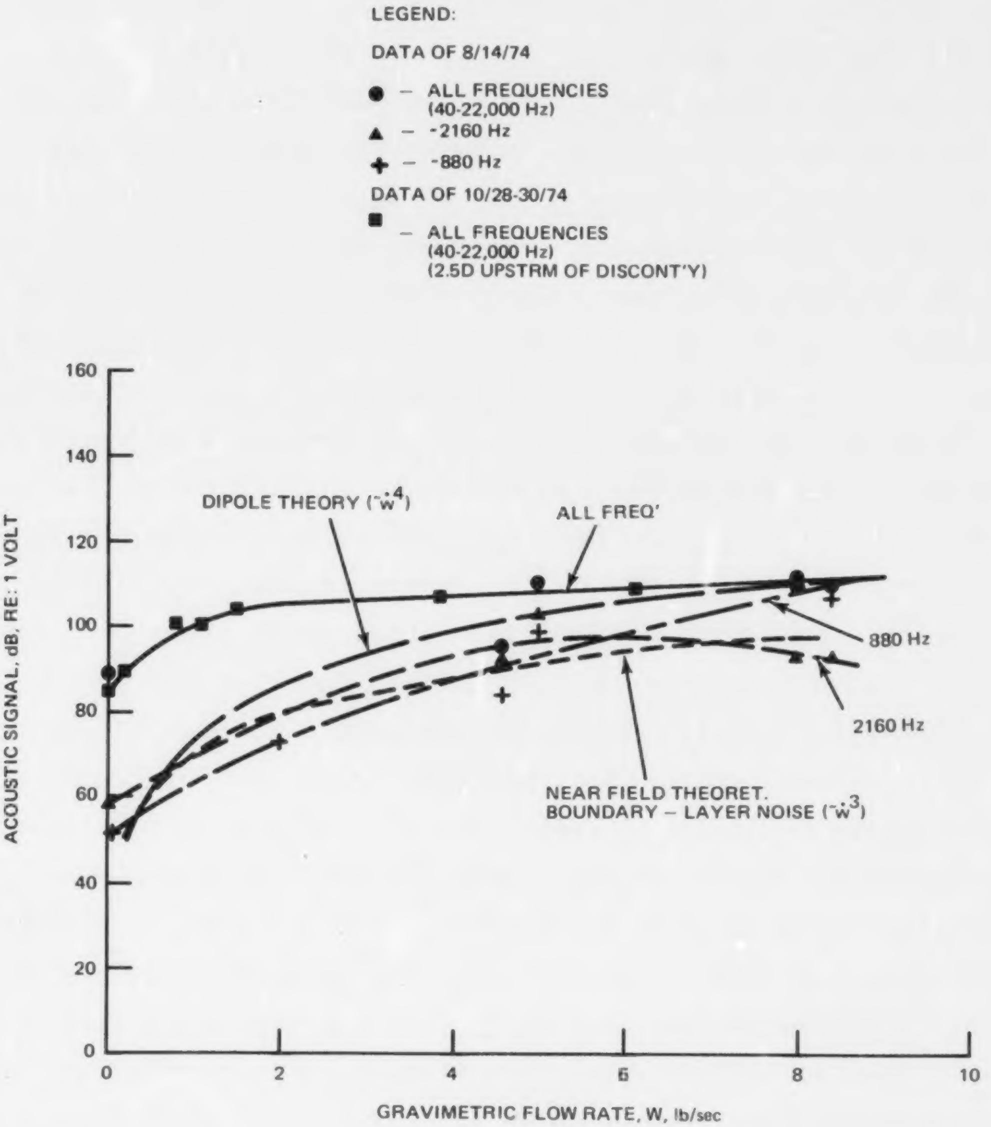

Fig. 28 Acoustic signal variation with flow rate in a 3-inch (7.62 cm) diameter steel pipe

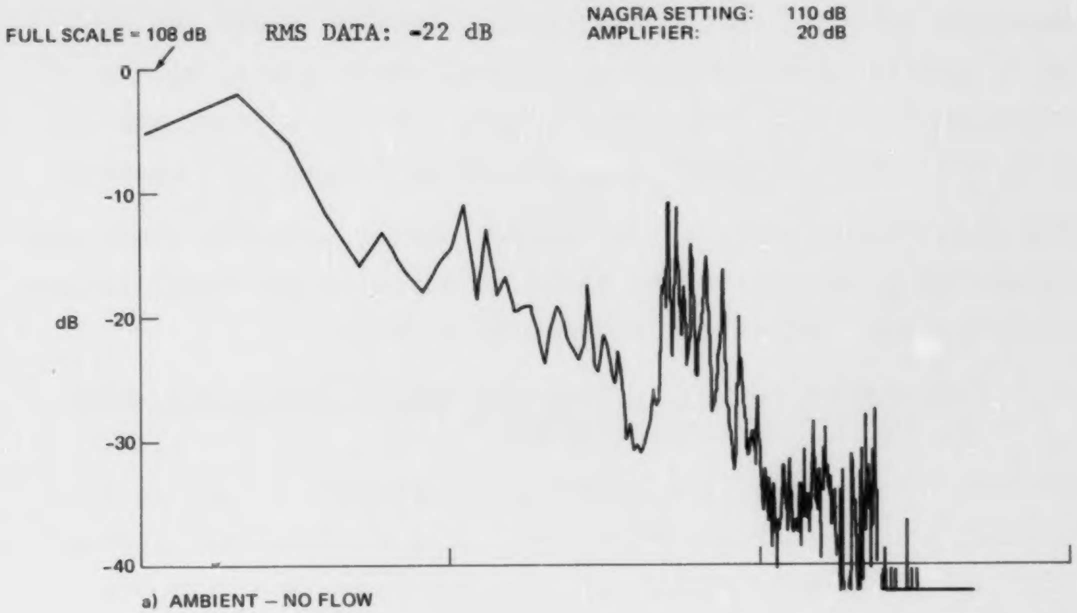

a) AMBIENT – NO FLOW

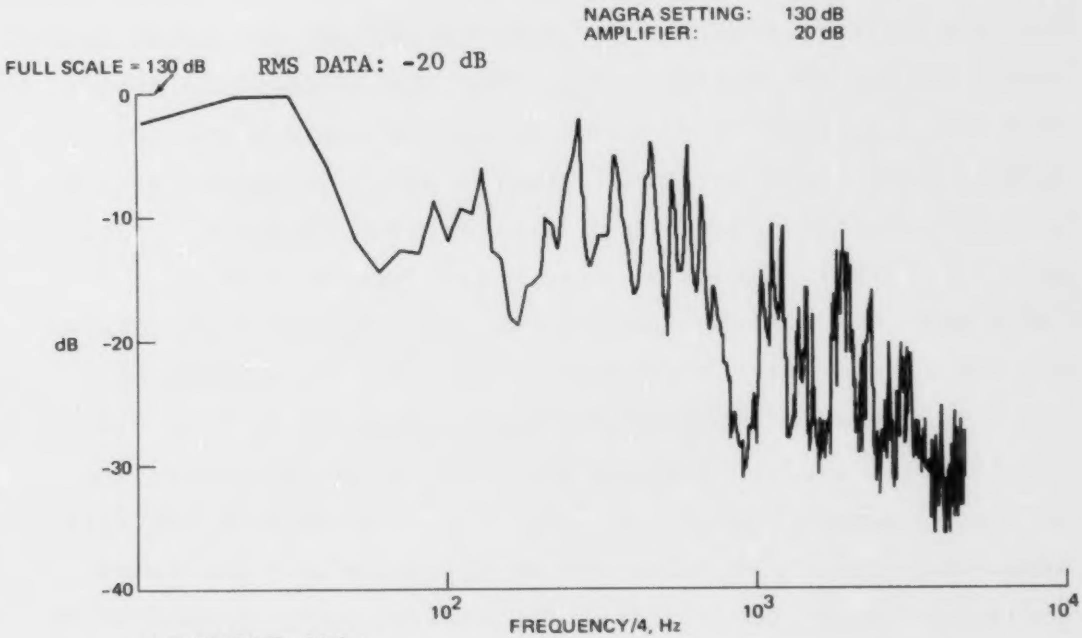

b) FLOW RATE = 5 lb/sec

Fig. 29 Typical spectral distributions of laboratory sound recordings. Distributions obtained by Fourier analyzer (10 Hz bandwidth)

mass-law fall off that characterizes ambient noise and more of a profile distinguished by several minor peaks, with a major band at about 880 Hz. Figure 29b for a flow rate of 5 lb/sec (2.27 kg/sec) typifies these latter type spectra.

The epoxy-based adhesive for accelerometer mounting studs was judged satisfactory on the basis of adhesion and sound transmission, and used in all subsequent tests.

2. Open Channel Conduit (Tests of August 22-23, September 12, and November 8-11, 1974)

In this test series, the supply pipe discharged into an open channel having a trapezoidal flow cross section with a (see Fig. 11) 4.82-in. (12.2 cm) minimum width and 1.66-in. (4.2 cm) height. The maximum cross-sectional width of this 6 ft (1.8 m) long aluminum channel is 5.78-in. (14.7 cm). The hydraulic radius of this open channel for different water levels varies according to Fig. 30. The cylindrical supply pipe was supported at a minus 40 minute slope above and independent of the trapezoidal channel so as to permit various waterfall heights equal to or greater than 4.15-in. (10.5 cm). The supply pipe exit also overlapped by 16-in. (40.6 cm) the upstream end of the open channel. The channel was mounted with a downward slope of 25 minutes of arc. Two types of transducers were installed at four different axial locations along the outside bottom centerline of the aluminum channel (see Fig. 11). In outward physical appearance this test setup was an approximately ten times scale version of the original exploratory tests conducted by Grumman Research in August 1972.

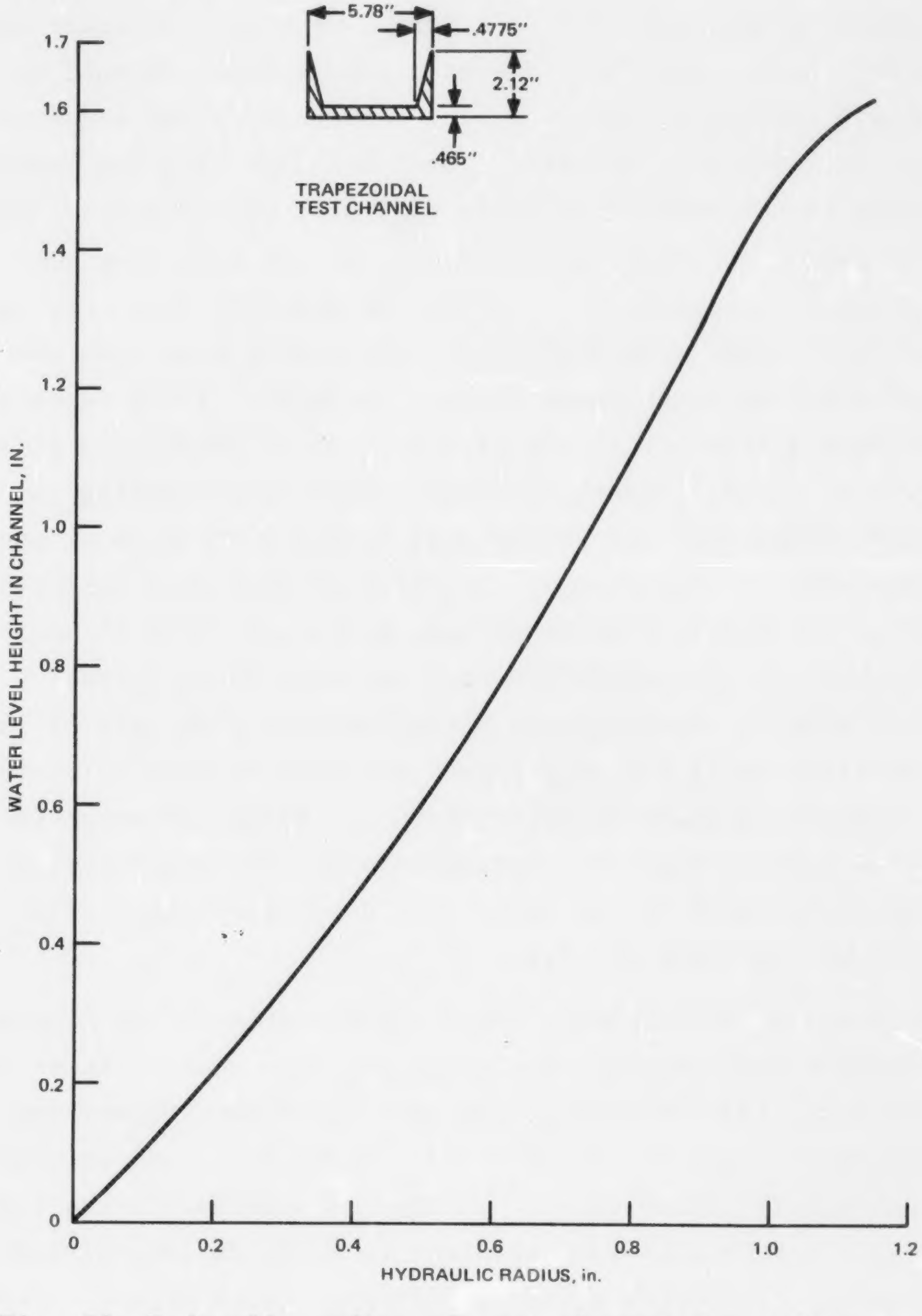

Fig. 30 Hydraulic radius of test channel for different water level heights

The open channel downstream of the discontinuity made it convenient to determine the relation of flow rate to water level in the 3-in. (7.6 cm) diameter supply pipe, as well as the outfall trajectory parameters. These results are shown in Fig. 31. The data for water level and flow rate are experimental in the upper half of this figure; the area and volume flow ratios are from tables in Ref. 5, and full flow area is 7.07-in.^{2} (45.6 cm^2). Using the measured flow rate and the flow ratios from this figure the supply pipe will run full for flow rates above about 7.0 lb/sec (3.18 kg/sec) and have a velocity at the pipe exit of at least 2.3 ft/sec (0.70 m. /sec). Higher exit velocities corresponding to higher flow rates can be obtained by pressurization of the water supply. For example, the highest flow rate measured during the entire laboratory test phase was 15.4 lb/sec (7.0 kg/sec) for which the exit velocity is 5 ft/sec (1.52 m/sec). The measured variation with flow rate of the normalized axial offset distance for the waterfall's center of contact upon the receiver channel, Xc/h, is shown in the bottom half of Fig. 31. Extrapolated to the maximum flow rate experienced in our tests, the normalized axial offset would be a maximum of 2.2.

The acoustic measurements taken concurrent with the flow measurements employed two accelerometers with sensitivities of 62.7 mv/g and 19.5 mv/g and with corresponding working frequency ranges of 26,000 and 35,000 Hz, respectively (1 g equals 980.6 cm/sec^2). The 3:1 ratio for the transducer sensitivities is equivalent to a 10 dB signal difference. Flow rates up to 7.6 lb/sec (3.45 kg/sec) were

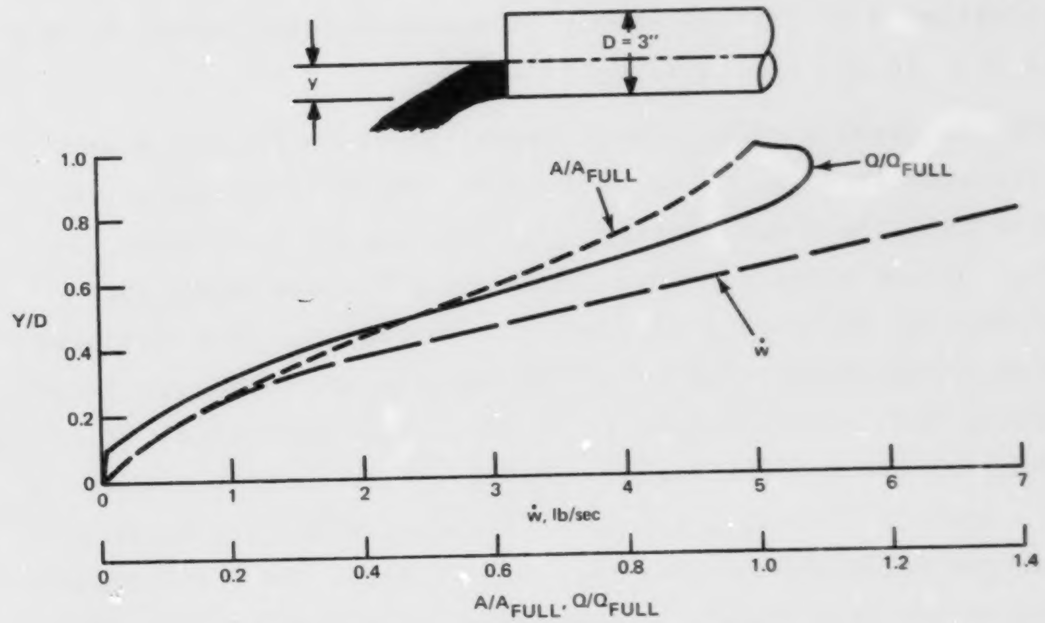

a) HEIGHT OF PARTIALLY FILLED PIPE FLOW VS WATER FLOW RATE

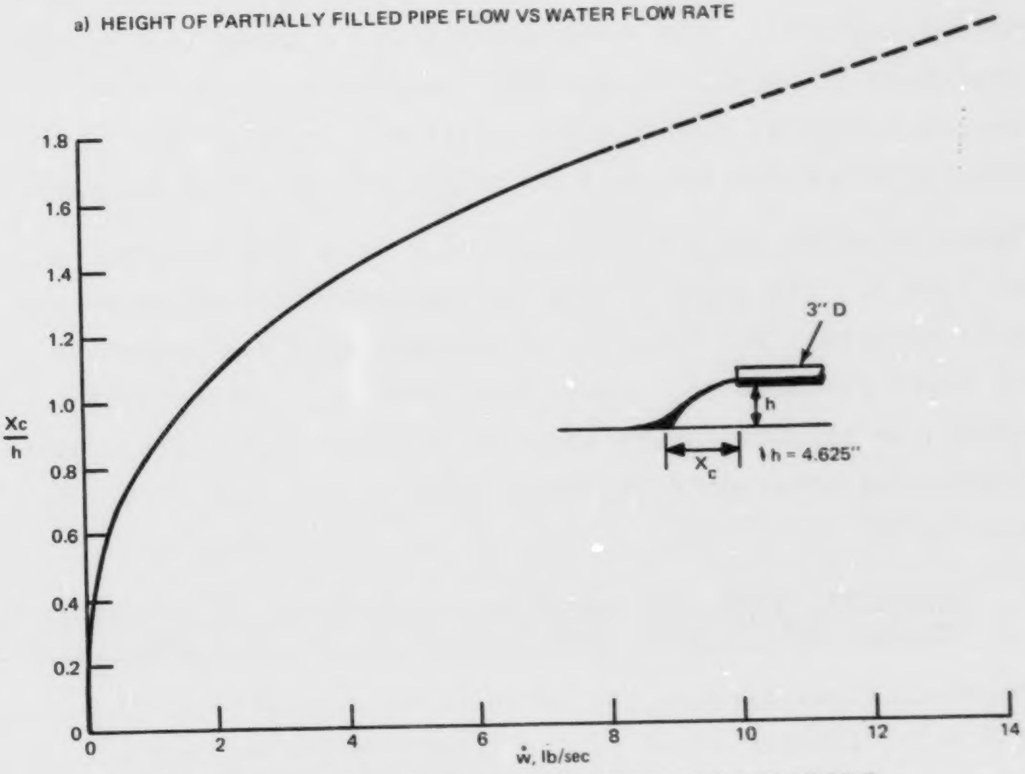

b) NORMALIZED DISTANCE TO WATERFALL CENTER OF CONTACT VS FLOW RATE

Fig. 31 Calibration of research facility water supply (A = flow area, Q = volumetric flow rate)

established at initial supply pressures between about 8 and 18 psi (0.56 and 1.27 kg/cm^2).

Typical results of processed signal level to flow rate are presented in Figs. 32 to 34 for two waterfall heights, two accelerometer sensitivities, and four sensor locations. In Fig. 32 the signals at two frequency bands are shown normalized to the zero flow (ambient) condition. This has been done to compensate for the difference in accelerometer sensitivity that would produce a 10 dB level difference, if shown on an absolute scale. In Fig. 33 the signal components at 3600 Hz (i.e., $f/4 \simeq 900$) are considered characteristic for the waterfall height, h, of 4.15-in. (10.5 cm) according to our empirical rule that $h = \lambda/4$ where $\lambda = c/f$. The other frequencies ($f/4 = 800$ and 710 Hz), shown in Fig. 32, correspond to $h = \lambda/4.5$ and $\lambda/5$, respectively, and have been presented because peak signal amplitudes are observed in the computer processed spectral distributions at these frequencies.

Figure 34 shows typical results for a waterfall height, h, of 4.8-in. (12.2 cm). This configuration has a characteristic frequency of 3125 Hz. Processed data are presented for other frequencies, 2040 and 2460 Hz, which exhibit peaking amplitudes in the spectral distribution. These other frequencies correspond to approximately $\lambda/6$ and $\lambda/5$, respectively.

3. Eccentric Steel and Aluminum Pipes (Tests of September 9, October 28-29, 1974, and January 29, March 6 and 12, 1975)

The conduit arrangement for these tests consisted of the 3-in. (7.6 cm) diameter steel pipe discharging into a nominal 8-in. (20.3 cm) diameter, 4 ft (1.22 m) long, aluminum

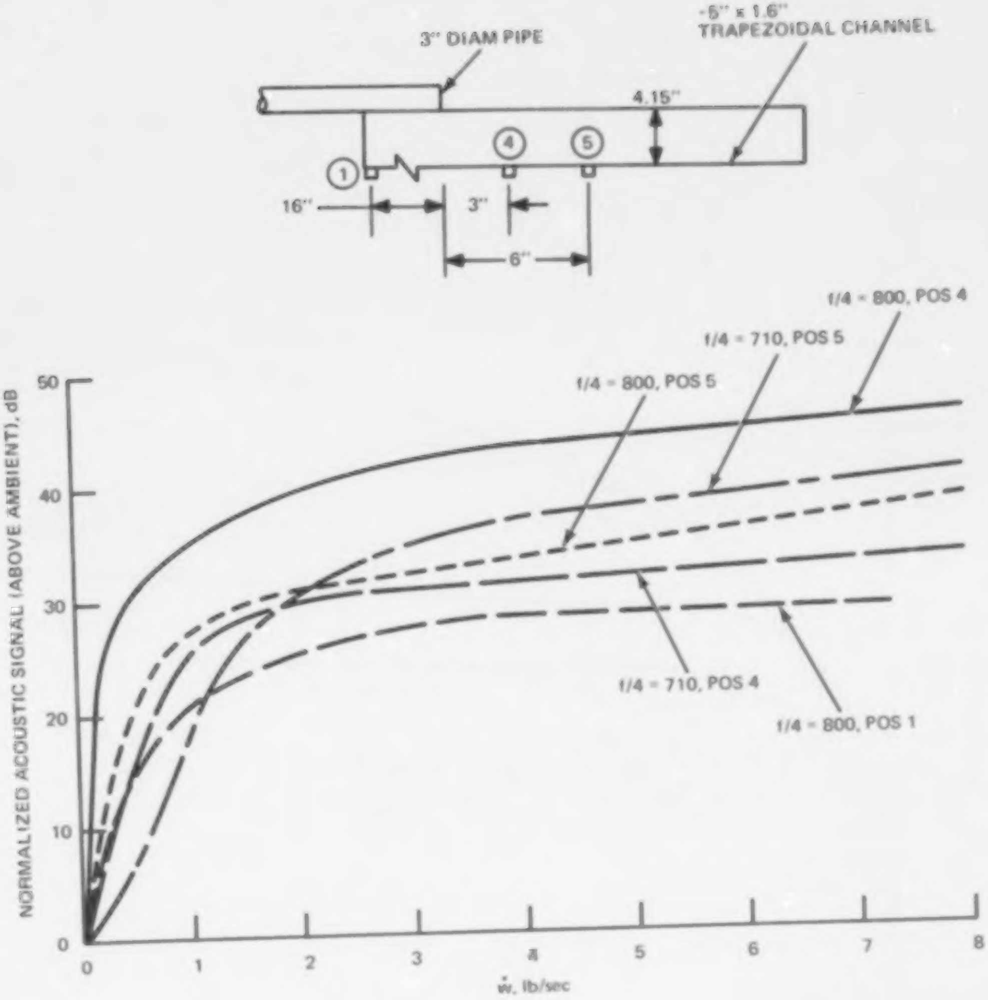

Fig. 32 Variation of normalized acoustic signal with flow (cylindrical pipe exiting to a trapezoidal open channel)

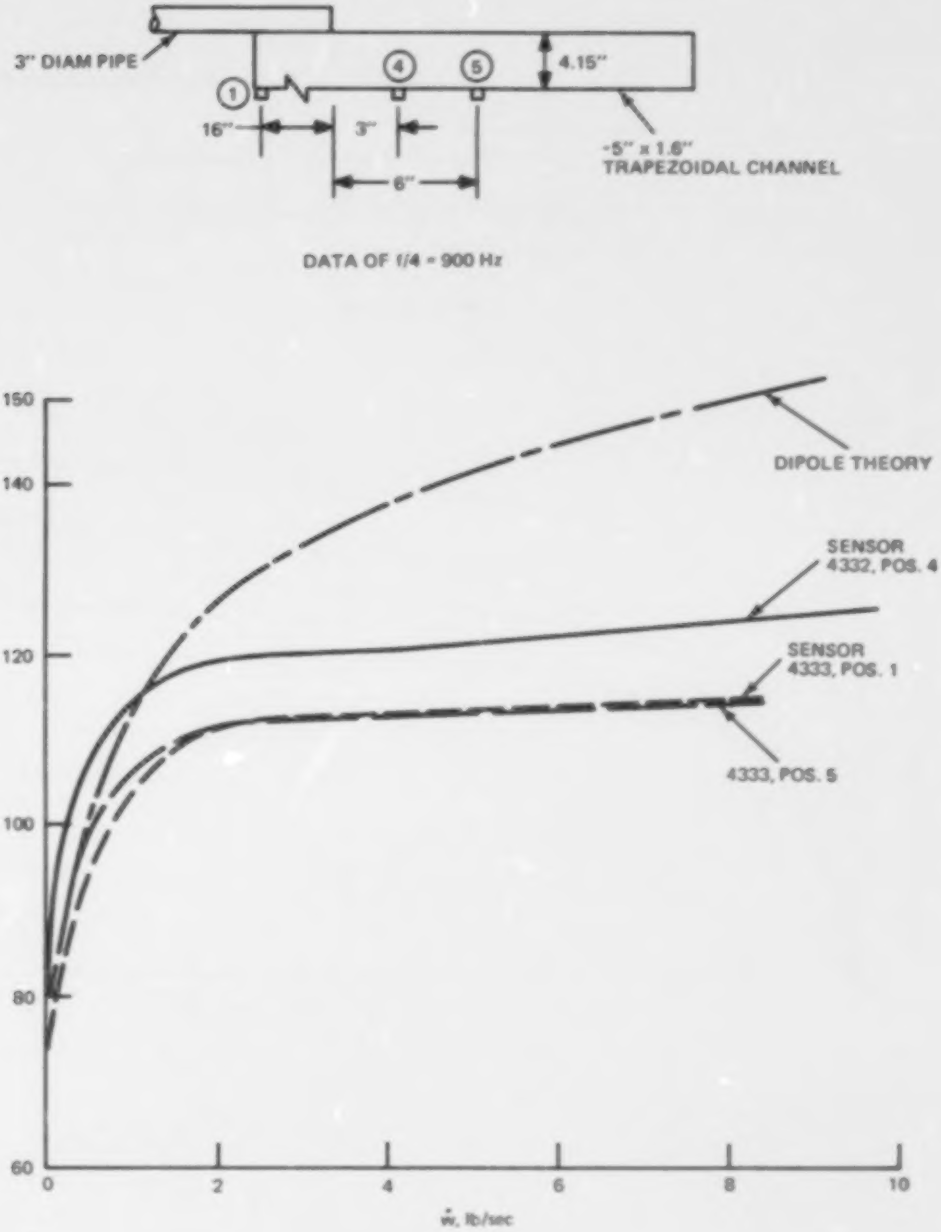

Fig. 33 Acoustic signal variation with flow rate (cylindrical pipe discharging to trapezoidal open channel)

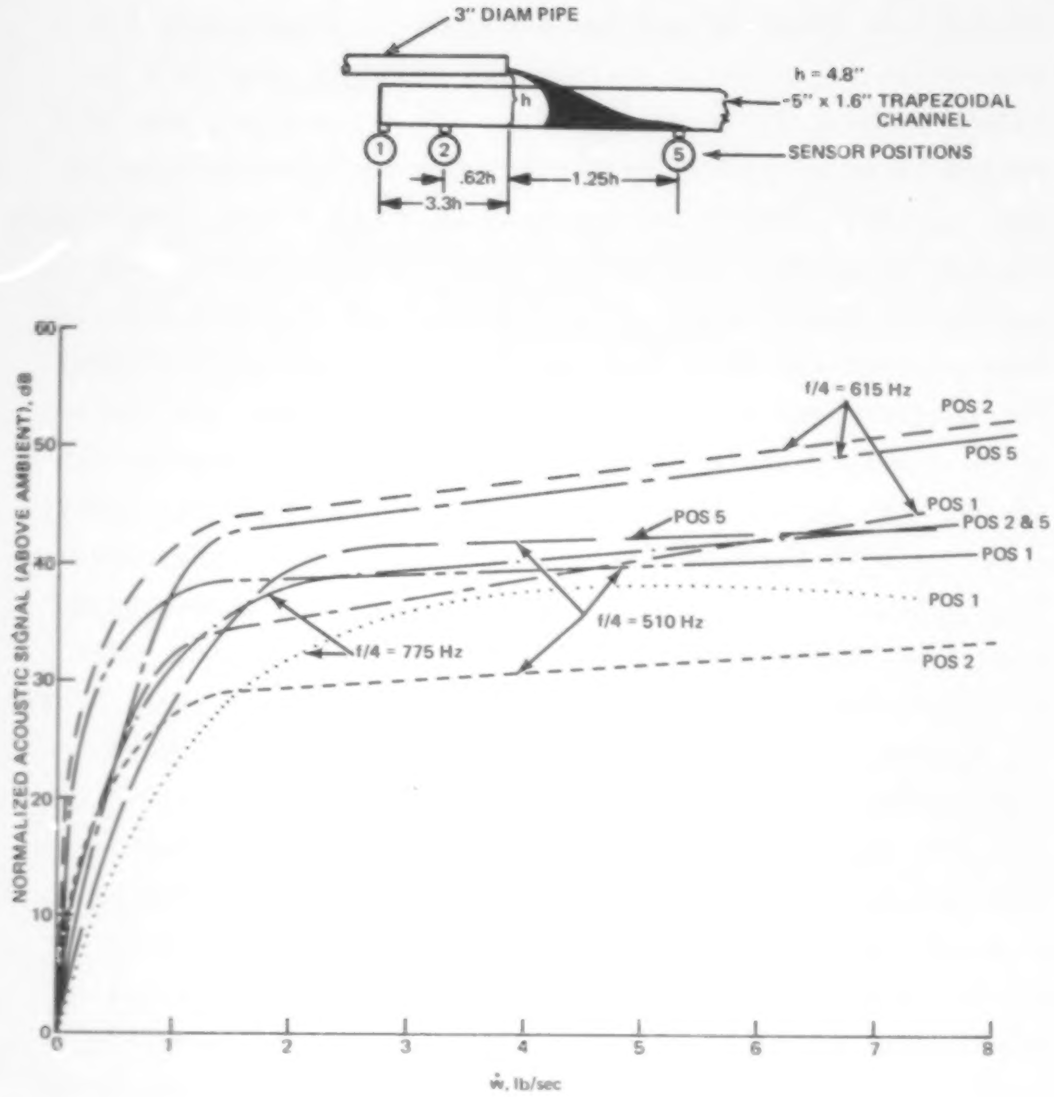

Fig. 34 Variation of normalized acoustic signal with flow rate - different sensor locations (cylindrical to trapezoidal channel transition)

pipe. This setup was the first one involving completely cylindrical elements and was designed to demonstrate the production of acoustic emission in channels that were not always completely open (see Fig. 11). The pipes were attached in an eccentric manner so that the waterfall height was 4.2-in. (10.67 cm) or 4.45-in. (11.3 cm). The height depends on whether the smaller pipe has an extended inlet within the larger one, or is assembled as a sudden enlargement so that the roof line for the joined pipes is tangent. The upstream end of the 8-in. (20.3 cm) pipe was closed by an aluminum plate having an eccentric hole large enough to fit the 3-in. (7.6 cm) pipe (see Fig. 8). All joints were sealed watertight with 1-in. (2.54 cm) wide adhesive faced lead tape. The slope of both pipes was minus 0.3%. Flow rates up to more than 13 lb/sec (5.9 kg/sec) were established at water supply pressures between 8 and 27 psi (0.56 and 1.90 kg/cm^2). Three different accelerometer models were attached to mounting studs at four axial locations on the 8-in. (20.3 cm) diameter pipe and one location on the 3-in. (7.6 cm) pipe. In addition, during several tests two circumferential locations were monitored, at 45 and 180 degrees counterclockwise from the bottom centerline viewed looking upstream, at an axial position 6-in. (15.2 cm) from the upstream end of the larger pipe.

After a series of tests in which the smaller pipe extended 2.5-in. (6.4 cm) into the 8-in. (20.3 cm) pipe, tape recorded acoustic data were processed and typical results are shown in Figs. 35 and 36. The sensor acoustic signals at different positions are shown varying with flow rate in Fig. 35; these trends are for the characteristic frequency

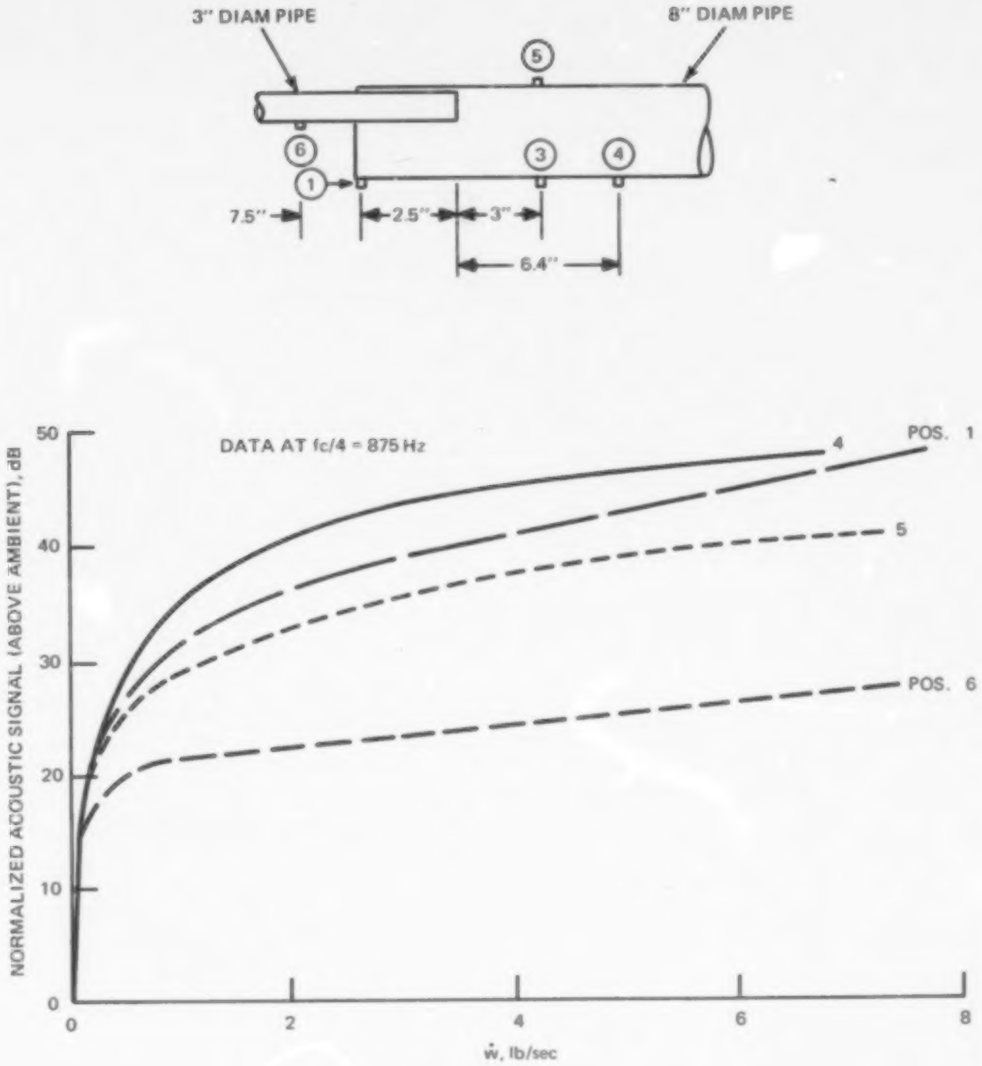

Fig. 35 Variation of normalized acoustic signal with flow rate - effect of sensor location (eccentric cylindrical pipe elements and extended inlet)

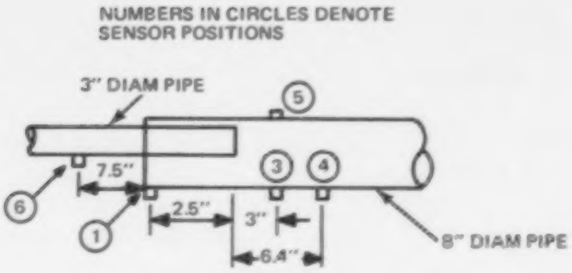
NUMBERS IN CIRCLES DENOTE SENSOR POSITIONS
3" DIAM PIPE
⑤
③
④
⑥
①
7.5"
2.5"
3"
6.4"
8" DIAM PIPE

SYMBOL	SENSOR TYPE	POSITION	SENSITIVITY, mv/g
ơ ○ σ	4332	3	62.7
○	4333	6	19.5
●	4333	4	19.5
✦	4332	4	62.7
▲ ⧗	4333	3	19.5
□	4333	1	19.5
●	4333	5	19.5
ø	4332	5	62.7

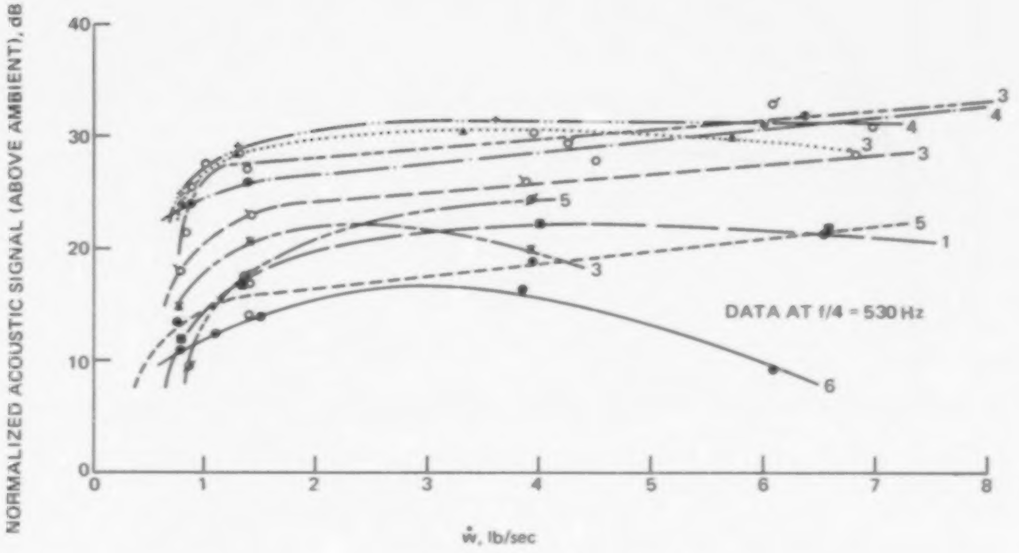

Fig. 36 Effect of sensor on variation of normalized acoustic signal with flow rate (eccentric cylindrical pipe elements and extended inlet)

of 3540 Hz. Figure 36 shows similar data to Fig. 35 but for an additional sensor and at another sensor location. Data points allow results of different test setups to be distinguished from one another.

In another test, the smaller diameter pipe was mounted so that its exit plane and the entrance plane of the larger pipe were flush. The purpose of this geometric array is to examine the influence of the air space behind the waterfall, as a resonance chamber driven by waterfall instabilities, to modulate the flow acoustic emission signal strength. Test data given in Fig. 37 show that for comparable sensor locations (relative to the discontinuity plane) the setup with the maximum air volume behind the waterfall produces the largest signal amplitude. These data are for the signal component at the characteristic frequency and for flow rates up to 11 lb/sec (5.0 kg/sec).

Visual observation of nonuniform or high flow rates reveal various types of mild hydraulic jump conditions in the downstream channel. To investigate the effect that such rapid changes in water level might have on flow sound emission, we made three weirs to be attached to the exit plane of the 8-in. (20.3 cm) diameter pipe. The weirs have heights of 2.24, 3.24, and 4.24-in. (5.7, 8.2, and 10.8 cm). Because of the slope and length of the test pipe section, the shortest weir retains just a film of water directly below the discontinuity, and the highest weir retains a 2-in. (5.1 cm) deep water pool there, which almost halves the free fall of water from the 3-in. (7.6 cm) pipe.

Typical trends of the processed acoustic data to a flow rate of 11 lb/sec (5.0 kg/sec) are shown in Figs. 38-40. In

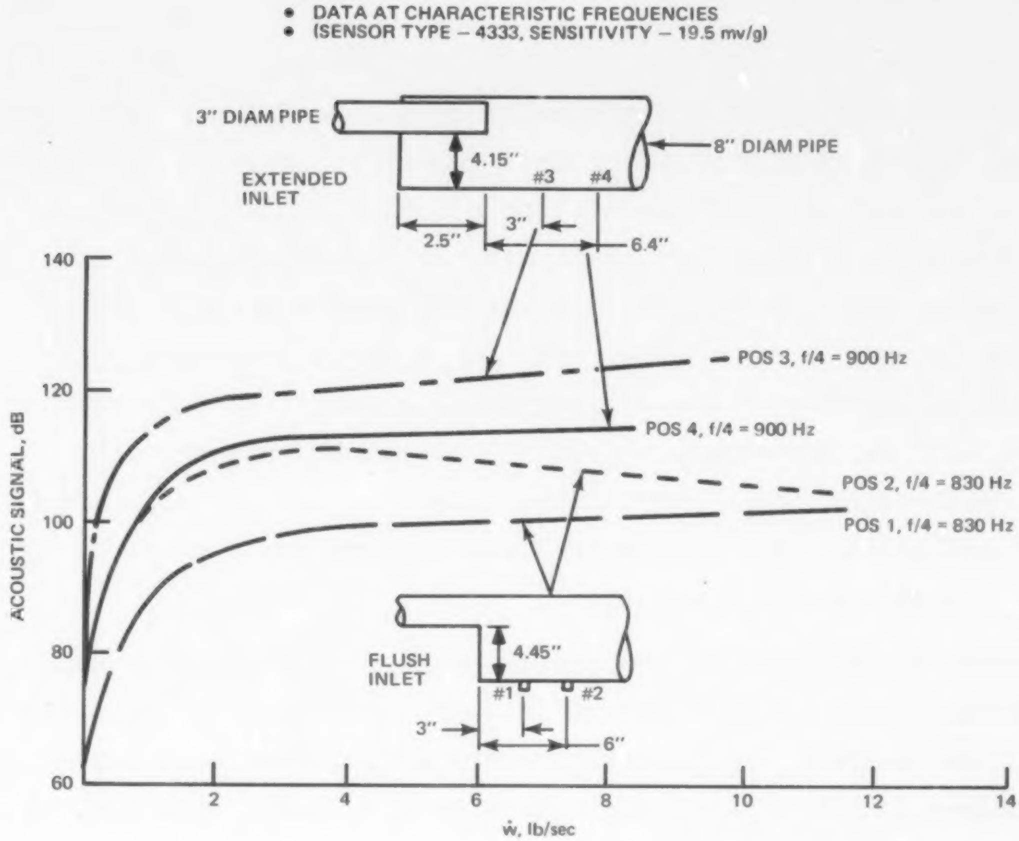

- DATA AT CHARACTERISTIC FREQUENCIES
- (SENSOR TYPE – 4333, SENSITIVITY – 19.5 mv/g)

Fig. 37 Effect of extended inlet on acoustic signal variation with flow rate (eccentric cylindrical pipe elements)

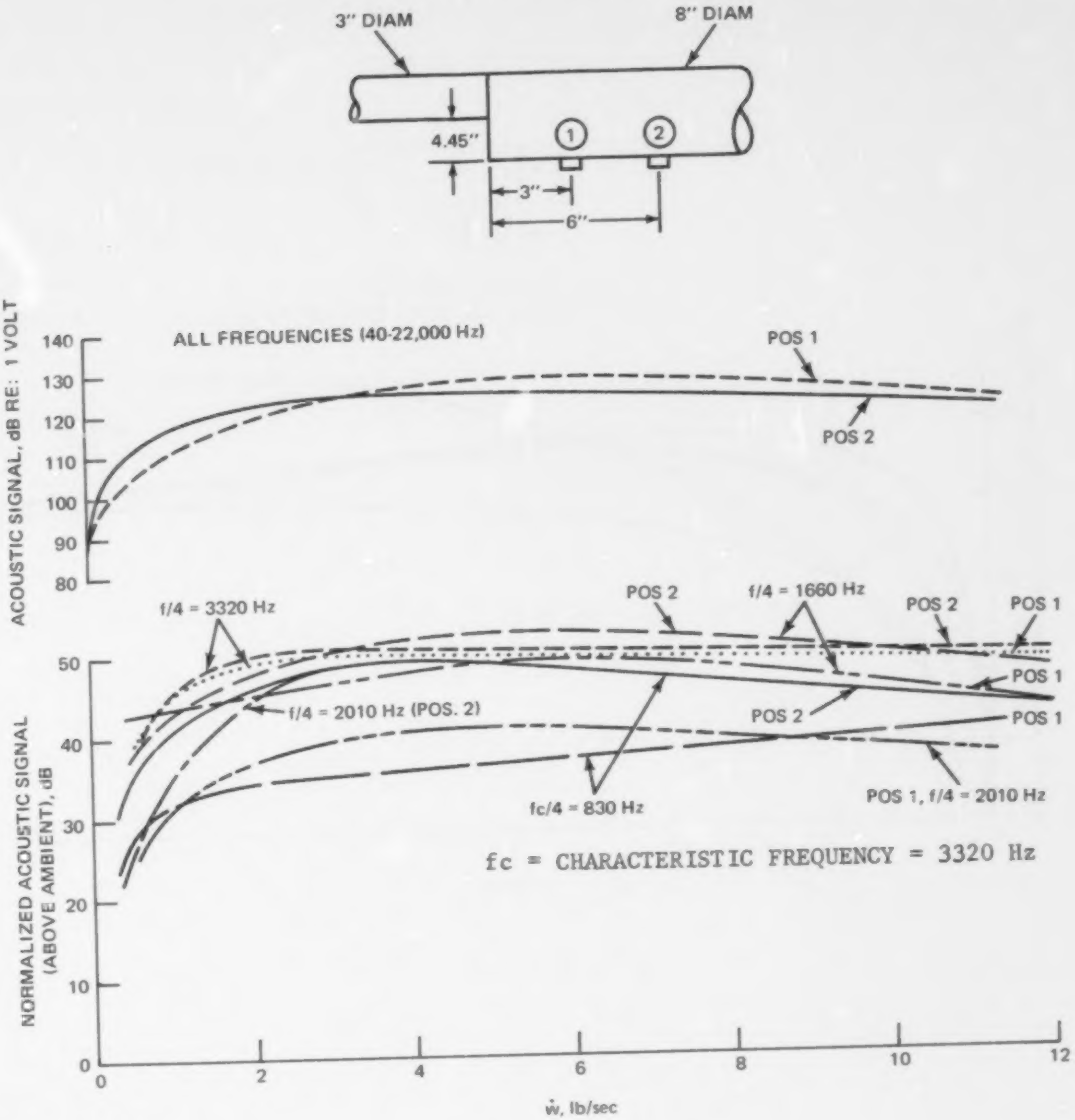

Fig. 38 Effect of sensor position and sound frequency on acoustic emission of water flow (eccentric cylindrical pipe elements and flush inlet)

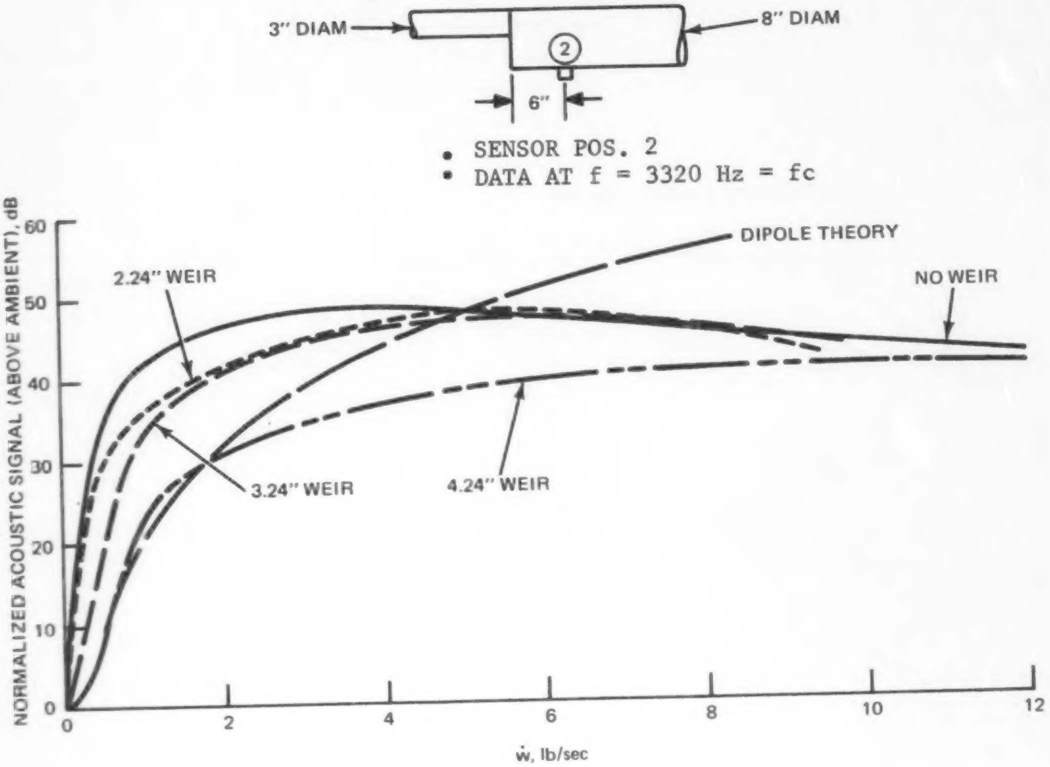

- SENSOR POS. 2
- DATA AT f = 3320 Hz = fc

Fig. 39 Effect of exit weir height on normalized acoustic signal of water flow (eccentric cylindrical pipe elements and flush inlet)

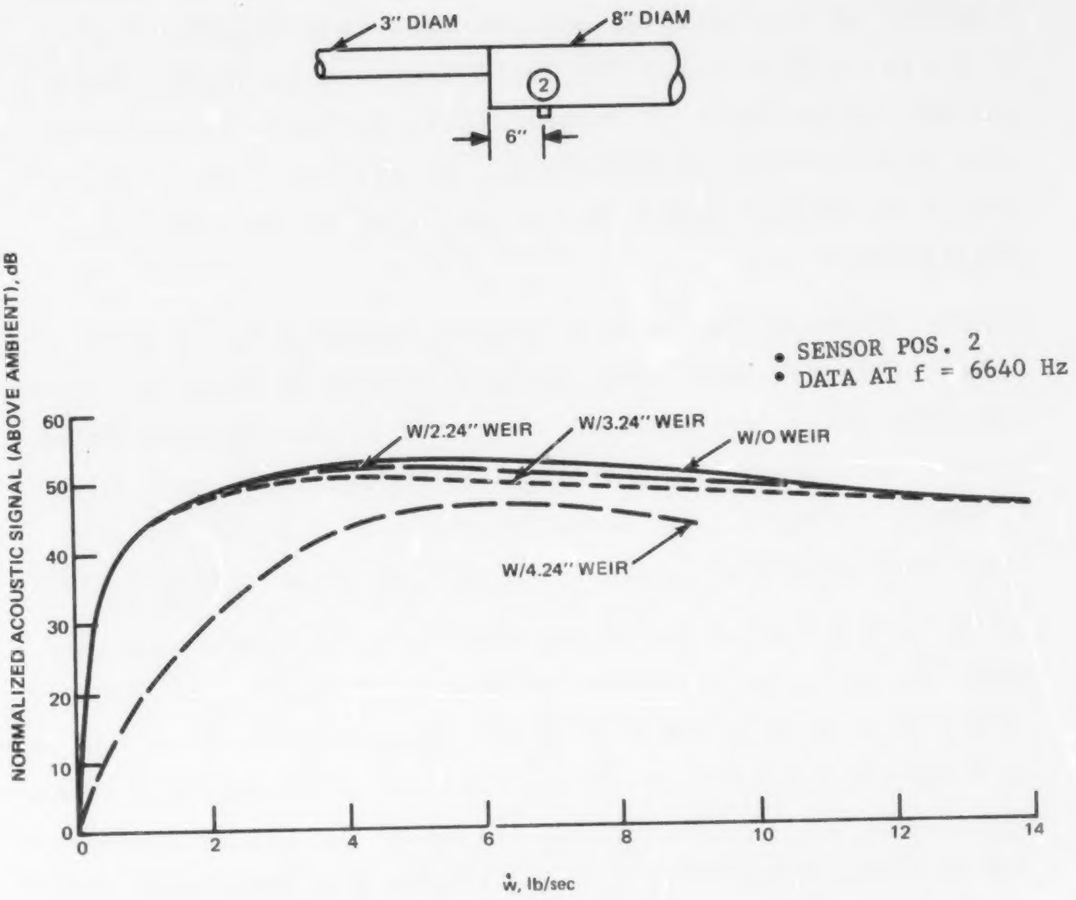

Fig. 40 Effect of exit weir height on normalized acoustic signal of water flow (eccentric cylindrical pipe elements and flush inlet)

the first of these figures the data for two sensor positions and no weir displays the signal for the entire acoustic spectrum and the minimum characteristic frequency (3320 Hz), computed on the basis of maximum waterfall height (4.45-in. = 11.3 cm). The rapid increase in signal above ambient up to about 2 lb/sec (0.91 kg/sec) flow agrees with dipole theory predictions. At greater flows, the increase in useful signal is not as large as theoretically predicted.

Figure 39 shows that when a greater depth of water pool exists (highest weir) the acoustic signal is reduced, at the low flow rates, compared to shallower or nonexistent water pools. At flow rates greater than about 12 lb/sec (5.45 kg/sec), however, the acoustic emission signals for all four pool conditions appear to converge into a single trend.

If the water backed up by the weir were to behave exactly like the solid wall of the conduit in producing pseudosound, then the data at a characteristic frequency based on the free fall distance to the water pool should yield improved acoustic signal data. This is not indicated by the data comparison of Fig. 40 with Fig. 39, where the characteristic frequency of Fig. 40 is computed to correspond to the shortened drop to the 2-in. (5.1 cm) deep water pool. The trends of these two figures are very similar and probably differ only by the differences in background (ambient) noise level at the two frequencies compared.

Figure 41 depicts the variation of normalized acoustic signal with flow at four locations of accelerometer installation. At position 1, closest to the discontinuity plane, the

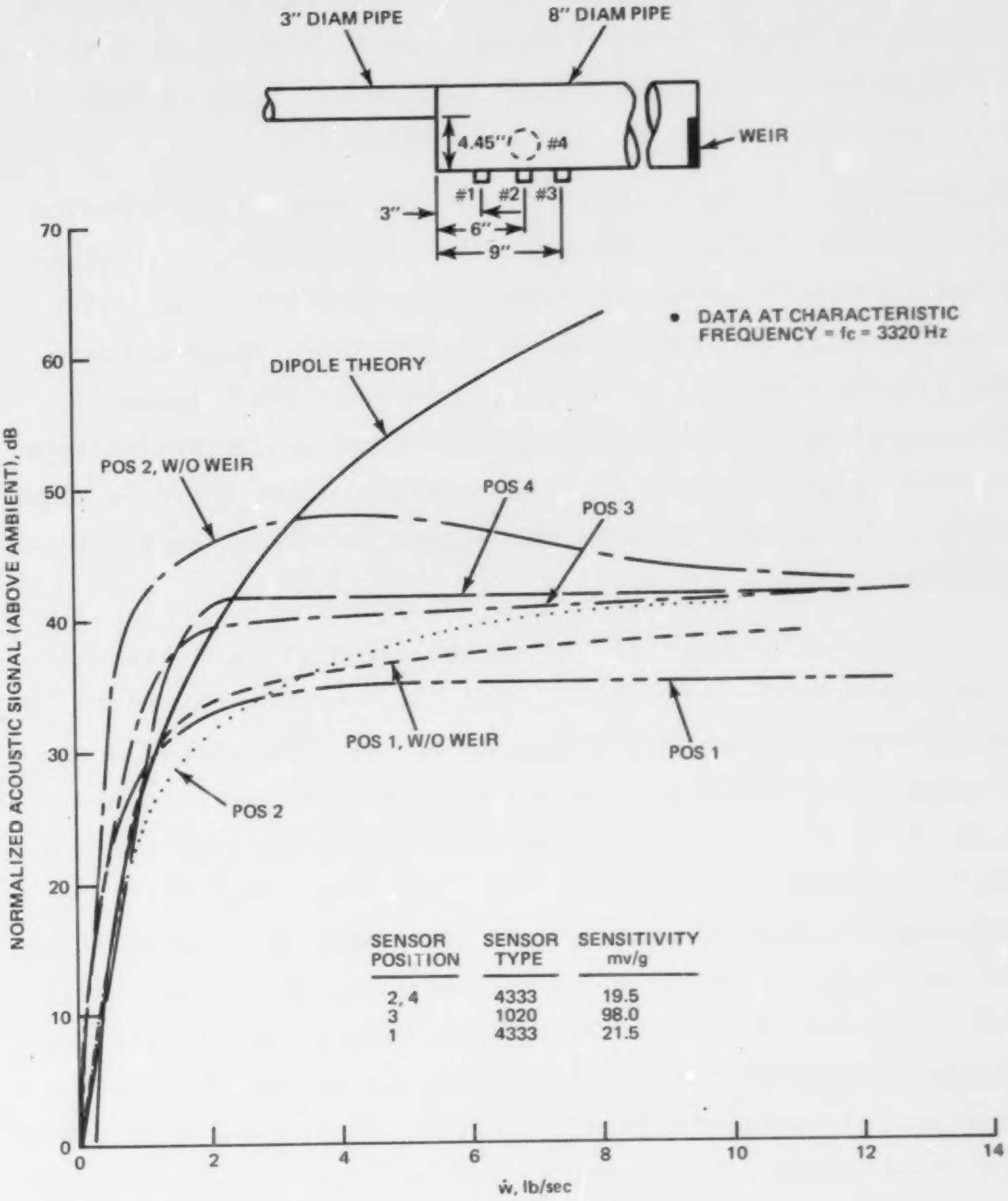

SENSOR POSITION	SENSOR TYPE	SENSITIVITY mv/g
2, 4	4333	19.5
3	1020	98.0
1	4333	21.5

Fig. 41 Variation of signal with flow at different sensor locations; (eccentric cylindrical pipe elements and flush inlet) (with 4.24-inch weir at exit unless noted otherwise)

normalized acoustic signals for the weir equipped pipe are similar to the open-ended conduit, up to a flow of 3 lb/sec (1.36 kg/sec). At higher flows the latter pipe configuration gives 3 to 4 dB greater signal.

At positions 2 and 4, which are at the same axial position but circumferentially separated by 45 degrees, the signal trends for both locations are almost identical and follow dipole theory to flow rates of 1.5 lb/sec (0.68 kg/sec). For greater flows up to about 10 lb/sec (45.5 kg/sec), the signal at position 4 is greater than at the bottom centerline (position 2). At still greater flows there is negligible difference between the signal levels at each sensor location.

Most practical sewers are in buried installations where the overburden depth is at least equal to one pipe diameter. We have simulated such installations in our laboratory by enclosing the section of test pipe, in the vicinity of the discontinuity plane, within a special wooden box (see Section IIIB) and Figs. 13 and 14). The four feet (1.2 m) long box contains coarse sand that we have used to simulate typical backfill. A maximum overburden depth of 8-in. (20.3 cm) is possible as well as partial burials and freely suspended pipe installations. The sand is tamped down before a test series to eliminate air pockets. Typical data obtained for these conditions are presented in Figs. 42-44. In the first figure of this series, the normalized acoustic signal trends are shown for flows up to 13.25 lb/sec (6.02 kg/sec). These curves are at a characteristic frequency, f_c of 3320 Hz, and at twice f_c. They indicate a signal

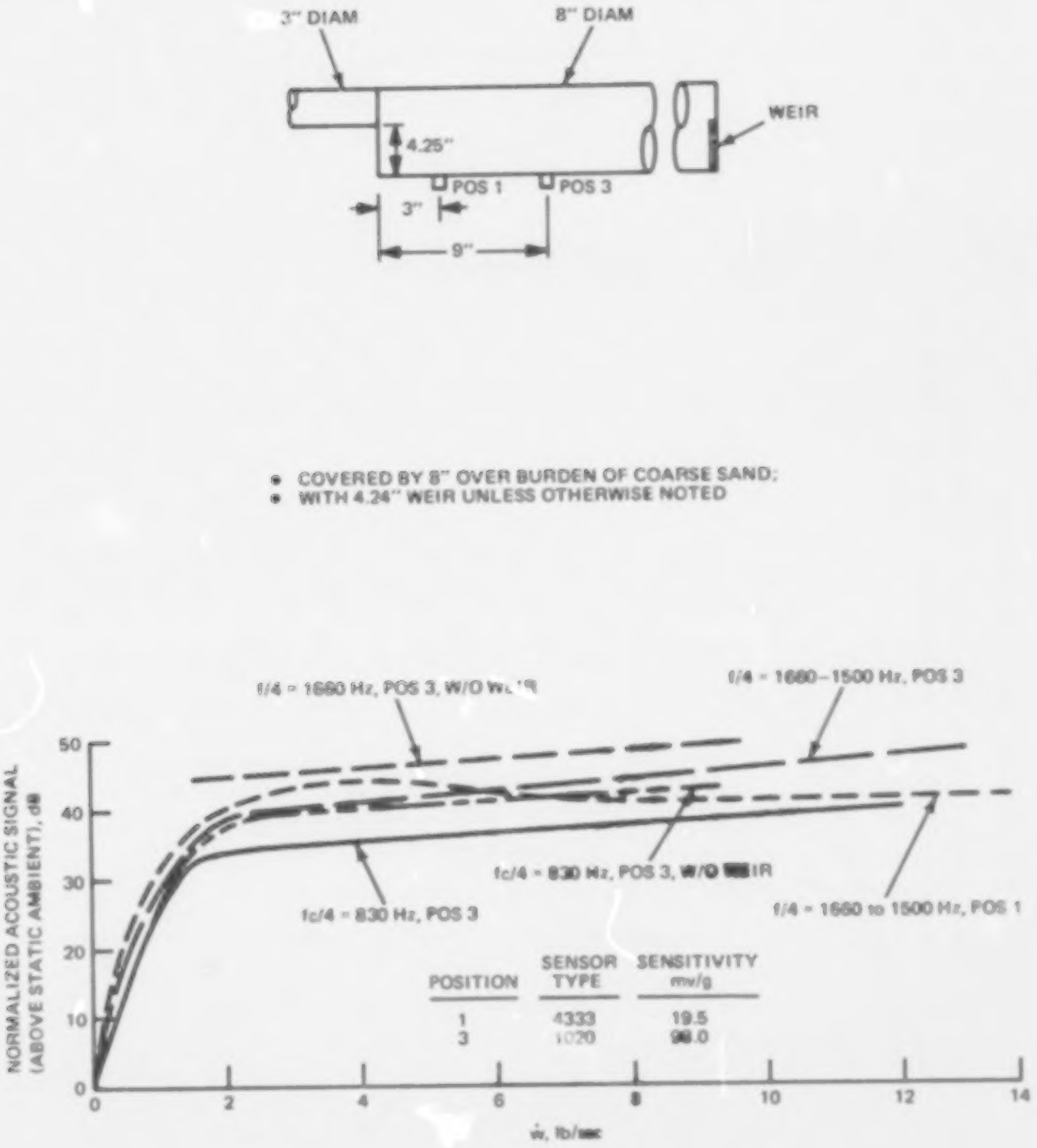

Fig. 42 Variation of normalized acoustic signal with flow rate for different frequencies and test conditions (eccentric cylindrical pipe elements and flush inlet)

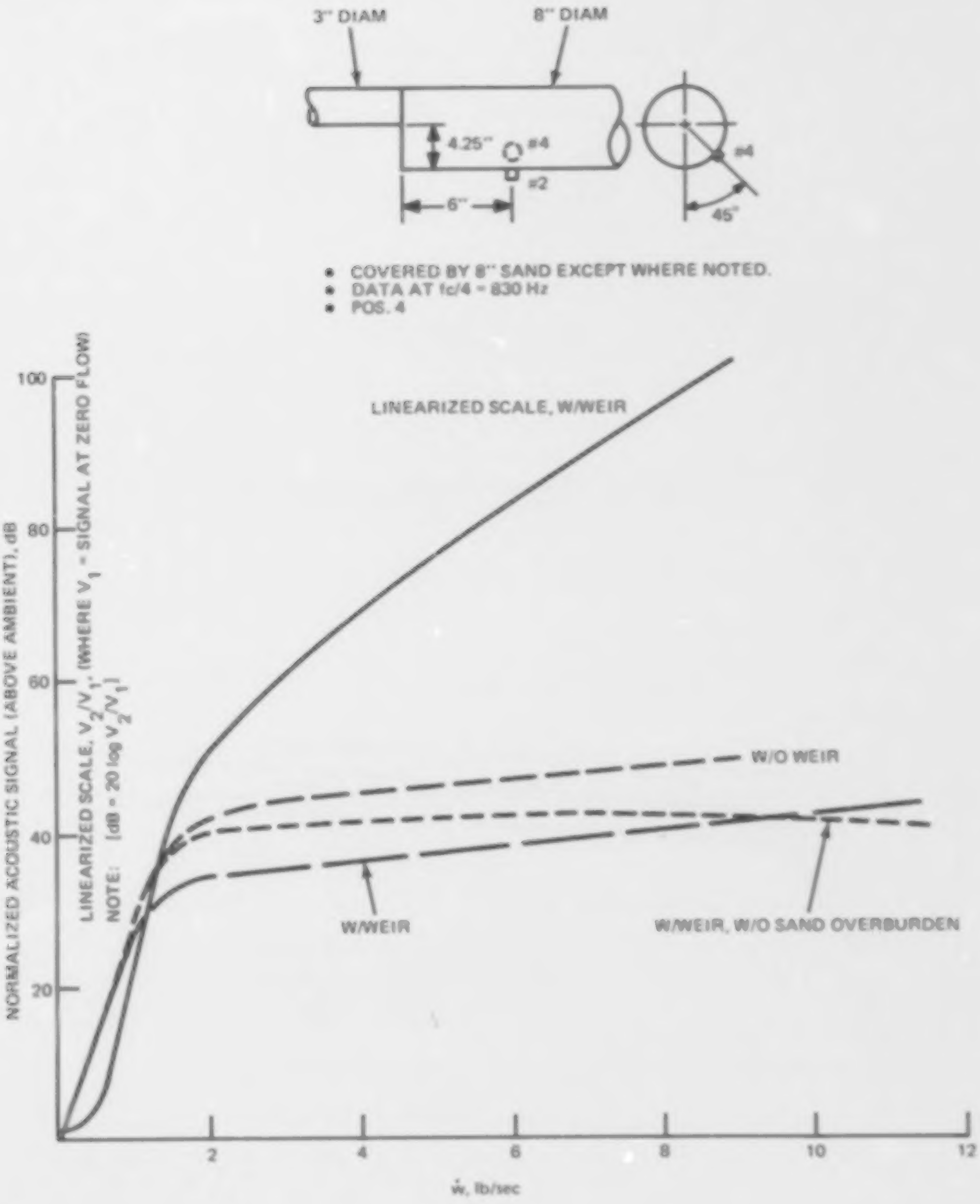

Fig. 43 Variation of normalized acoustic signal with flow rate for different test conditions (flush inlet, eccentric cylindrical pipe step)

level reduction of about 5 dB when the highest weir is placed at the pipe exit. This is measured at a sensor location slightly greater than one diameter downstream from the discontinuity plane.

The effect, at one sensor location, of the 8-in. (20.3 cm) deep overburden of sand on the normalized signal trend, at the characteristic frequency, is given by Fig. 43. At flows above 1.5 lb/sec (0.68 kg/sec) and no weir at the pipe exit, the sand covered installation has a greater signal for a flow rate than the unburied conduit. This trend also exists for the buried pipe with a weir. The acoustic signal trend assumes a large change in slope, for dB versus $\dot{w}$ axes, above $\dot{w} \approx 1.5$ lb/sec (0.68 kg/sec). This curve shape change does not mean greatly reduced resolution, however. If we convert the dB scale to a linear ratio scale, as depicted on Fig. 43, it is possible to resolve 0.025 lb/sec (0.011 kg/sec) in flow rate with working scale curves. In most practical system applications, a linear scale would be used for readout devices such as gauges and strip charts. The data of Fig. 44 presents absolute signal levels in dB, for three accelerometer locations.

4. Concentric Steel and Aluminum Pipes (Tests of October 29-30, November 11, 1974, and January 16-17, 22-23, March 21, 27, 31, and April 9, 1975)

The arrangements of flow conduits for these tests are similar to those described in the preceding Series 3 except that the 3-in. (7.6 cm) diameter steel pipe is attached concentric to the 8-in. (20.3 cm) aluminum pipe. Because of the actual physical dimensions of the pipes the waterfall height is 2.2-in. (5.6 cm) which corresponds to a characteristic

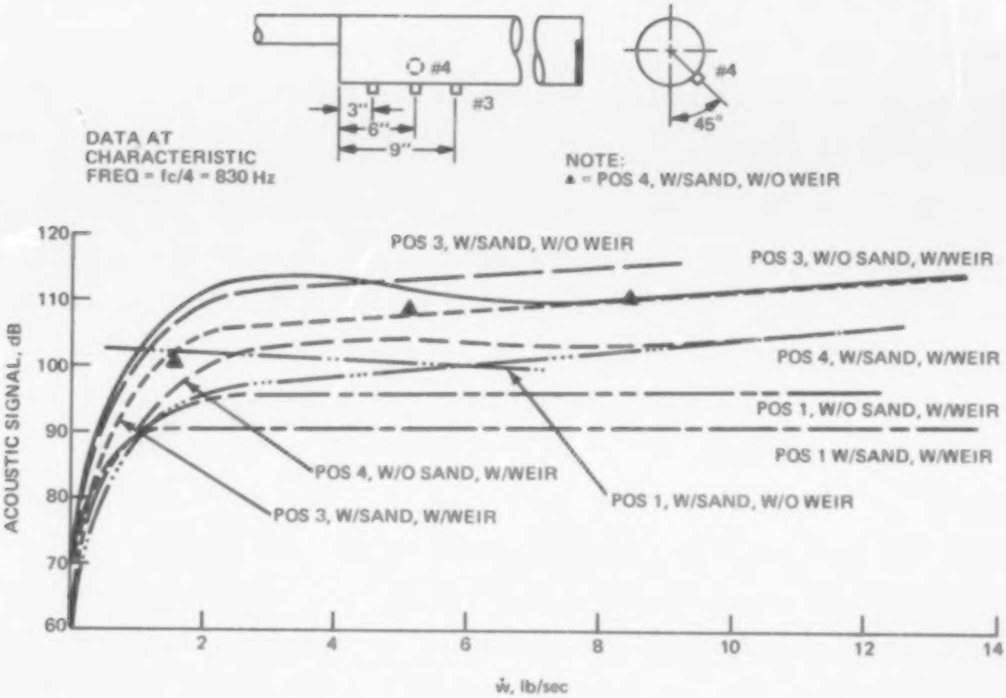

Fig. 44 Variation of acoustic signal with flow for 3 sensor locations and various test conditions

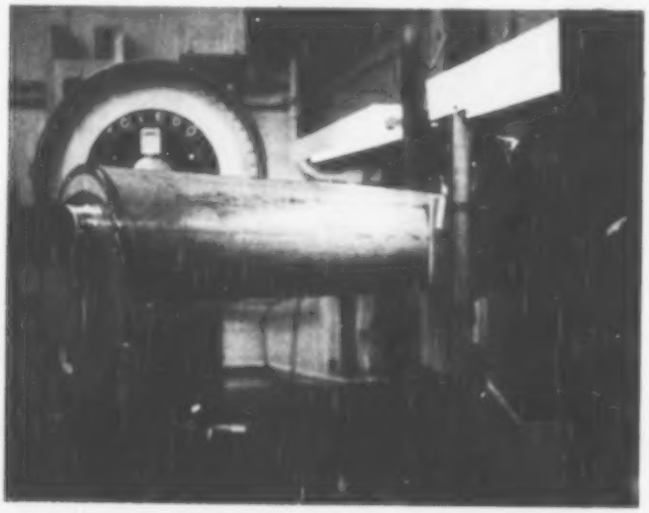

Fig. 45 Closeup of concentric discontinuity plane assembly of 3-inch steel water supply pipe to 8-inch diameter aluminum test pipe

frequency of 6700 Hz in water. The upstream end of the 8-in. (20.3 cm) pipe was closed by an aluminum plate and sealed with adhesive faced lead tape (see Fig. 45). The slope of the pipe assembly was minus 0.3% initially; this was altered in later tests to minus 3% to improve drainage. Flow rates to 15 lb/sec (6.8 kg/sec) were established at water supply pressures between 8 and 27 psi (0.56 and 1.90 kg/cm^2). Four different accelerometer models were used at four axial locations relative to the discontinuity plane, and at five circumferential positions at one axial position. As with the eccentric arrangement previously described, three weirs of differing heights were used at the exit plane of the conduit to force retention of water, of different depths, beneath the discontinuity plane. Also, tests were conducted with the pipes buried under one pipe diameter depth of coarse sand.

One additional test was made with this concentric array in which the bottom of the 8-in. (20.3 cm) diameter was filled with stone chips to a maximum depth of 1-in. (2.54 cm) along its entire 4 foot (1.22 m) length. This extreme pipe bed load condition was prevented from being washed away by the 4.24-in. (10.8 cm) weir plate at the exit plane. Views of this bed load, with the weir removed, are shown in Figs. 15 and 46 taken before water flows, and Figs. 16 and 47 taken after a series of tests with flow rates above 2-3 lb/sec (0.9 to 1.4 kg/sec), and 5 lb/sec (2.3 kg/sec), respectively. The purpose of these stone chips is threefold. First, it is used to indicate whether a diffuse solid material, which is not cemented to the conduit construction, could change the amplitude of acoustic

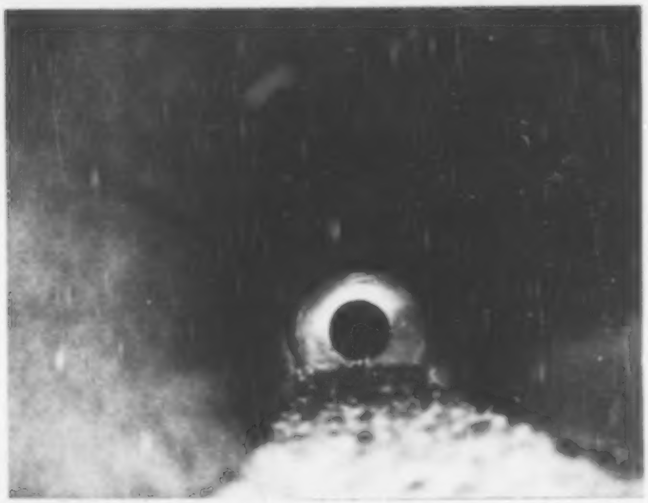

Fig. 46 Internal relation of 3-inch supply pipe to 8-inch test pipe with heavy bed load of stone chips. View taken before flow established

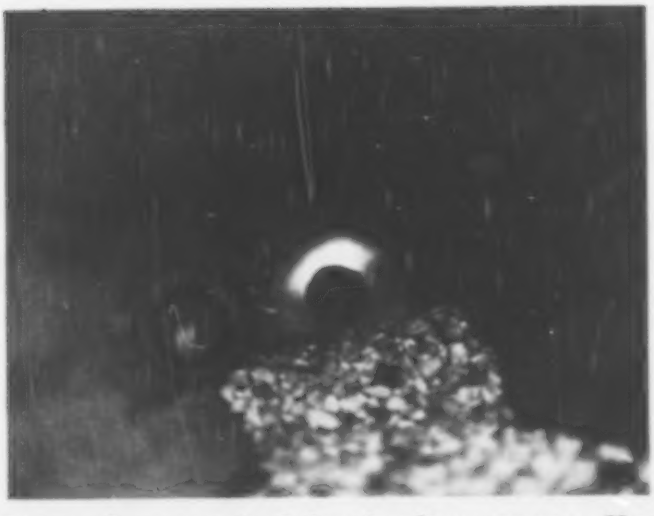

Fig. 47 View of upset bed load after water flow rate of 5 pounds per second

emission at the original characteristic frequency. Then, would the characteristic frequency be changed if the stones change the free fall height of the waterfall? Finally would the movement of the stones, under the influence of water flow, alter the amplitude of acoustic emission of the flow, or otherwise interfere with interpretation of the acoustic data? It was realized at the time that a bed load of stones (average specific gravity of 2.75) that reduced the flow cross section by almost 7.5 percent was likely to be an uncommon event. The test, however, was considered as potentially informative for more carefully designed future experiments. However, in recognition of the fact that the extremely heavy bed load conditions imposed by this test setup were unrealistic, a follow-up test was made in which the stone chips were uniformly distributed in as near a single layer of stones as possible, along the bottom inner surface of the entire length of 8-in. (20.3 cm) pipe.

Typical data for the concentric mounting with an extended inlet are presented in Figs. 48 and 49. The first gives the sensor signal component at a characteristic frequency of 6700 Hz for four sensor mounting locations. This signal has been normalized to the ambient noise level (zero flow) to compensate for the differences in sensitivity and installation for the two accelerometers. At a good sensor location, 3-in. (7.6 cm) downstream from the discontinuity plane, the normalized signals for several frequencies are shown by Fig. 49. It is evident from this figure that the trend at the characteristic frequency is uniquely unambiguous and useful for relating signal amplitude to flow rate. The other frequencies shown correspond to other peak amplitudes in

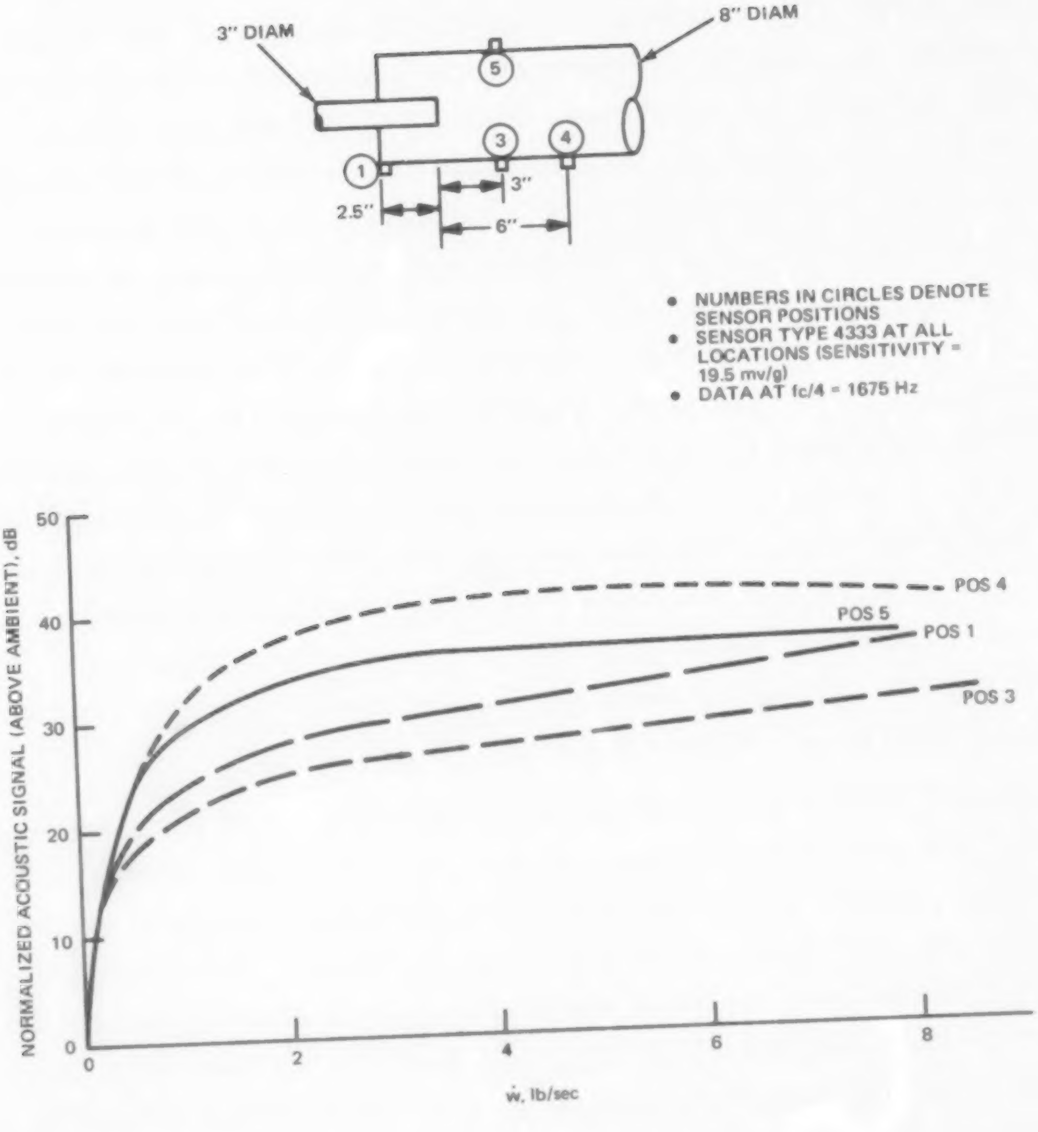

- NUMBERS IN CIRCLES DENOTE SENSOR POSITIONS
- SENSOR TYPE 4333 AT ALL LOCATIONS (SENSITIVITY = 19.5 mv/g)
- DATA AT fc/4 = 1675 Hz

Fig. 48 Variation of normalized acoustic signal with flow rate at various sensor locations and characteristic frequency (concentric cylindrical pipe array with extended inlet)

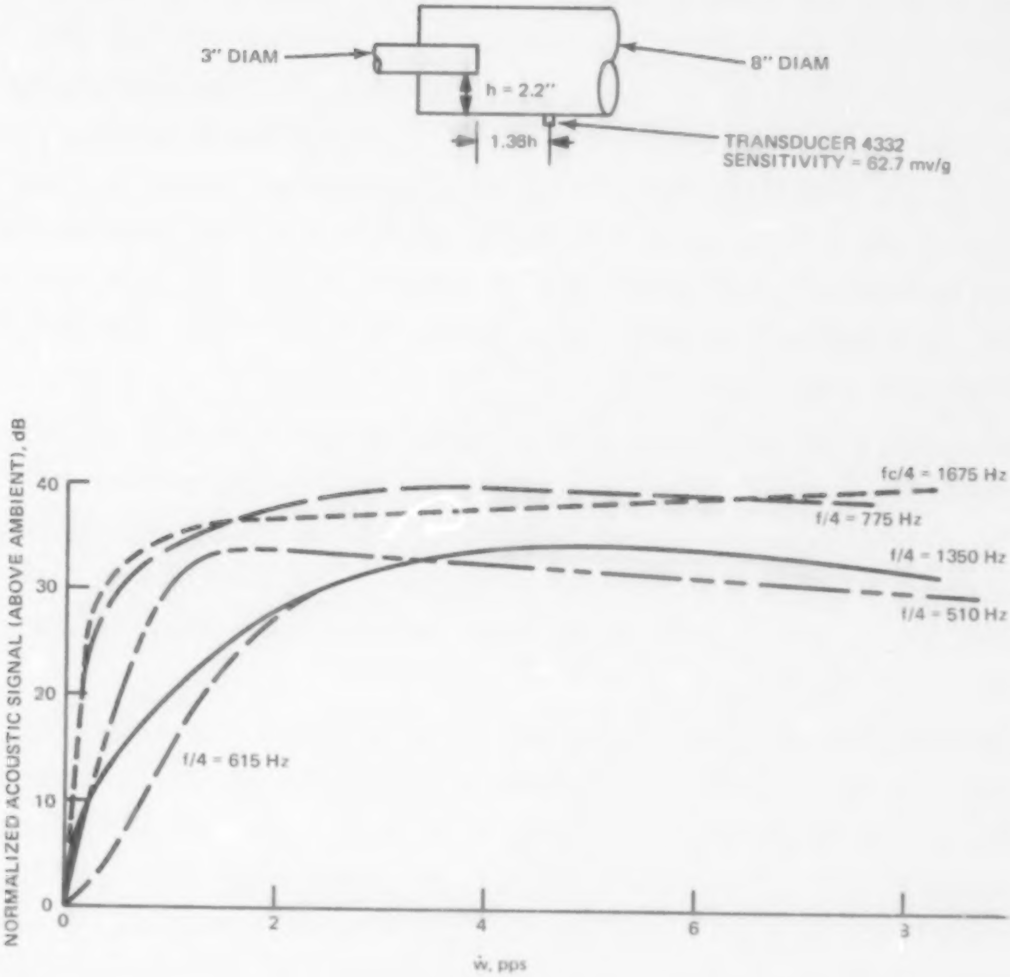

Fig. 49 Variation of normalized acoustic signal with flow rate for different frequencies (concentric cylindrical pipe array with extended inlet)

the spectral distribution resulting from Fourier processing of the recorded data.

The normalized data shown in Fig. 50 are results of the investigation into signal improvement by varying the circumferential location of the sensor attachment. The concentric cylindrical pipe array has a flush inlet in these tests. While all locations yield a generally similar result at low flows, the trends indicate that a position of 45 degrees to the bottom centerline appears to yield greater signals, at the intermediate to high flow rates, than at other circumferential positions.

The effect of different weir heights on the acoustic signal monitored at two positions, along the bottom centerline of the larger pipe, is shown by Fig. 51 for the characteristic frequency. Data obtained at position 2 are somewhat better than for position 1 at flow rates greater than about 8 lb/sec (3.6 kg/sec).

Comparative data for component frequencies of the sound other than the characteristic frequency, are given in Figs. 52 and 53 for the highest weir-equipped conduit. The overall signal strength for the entire recorded frequency range of 40 to 22,000 Hz is also given in Fig. 53. Data at position 3 always is of the highest amplitude because the sensitivity of the transducer used at this mounting location is about five times greater than for the other accelerometers. If the sources of acoustic signals were equally strong at each mounting stud location the accelerometer with enhanced sensitivity would produce a 14 dB greater signal than the less sensitive transducers.

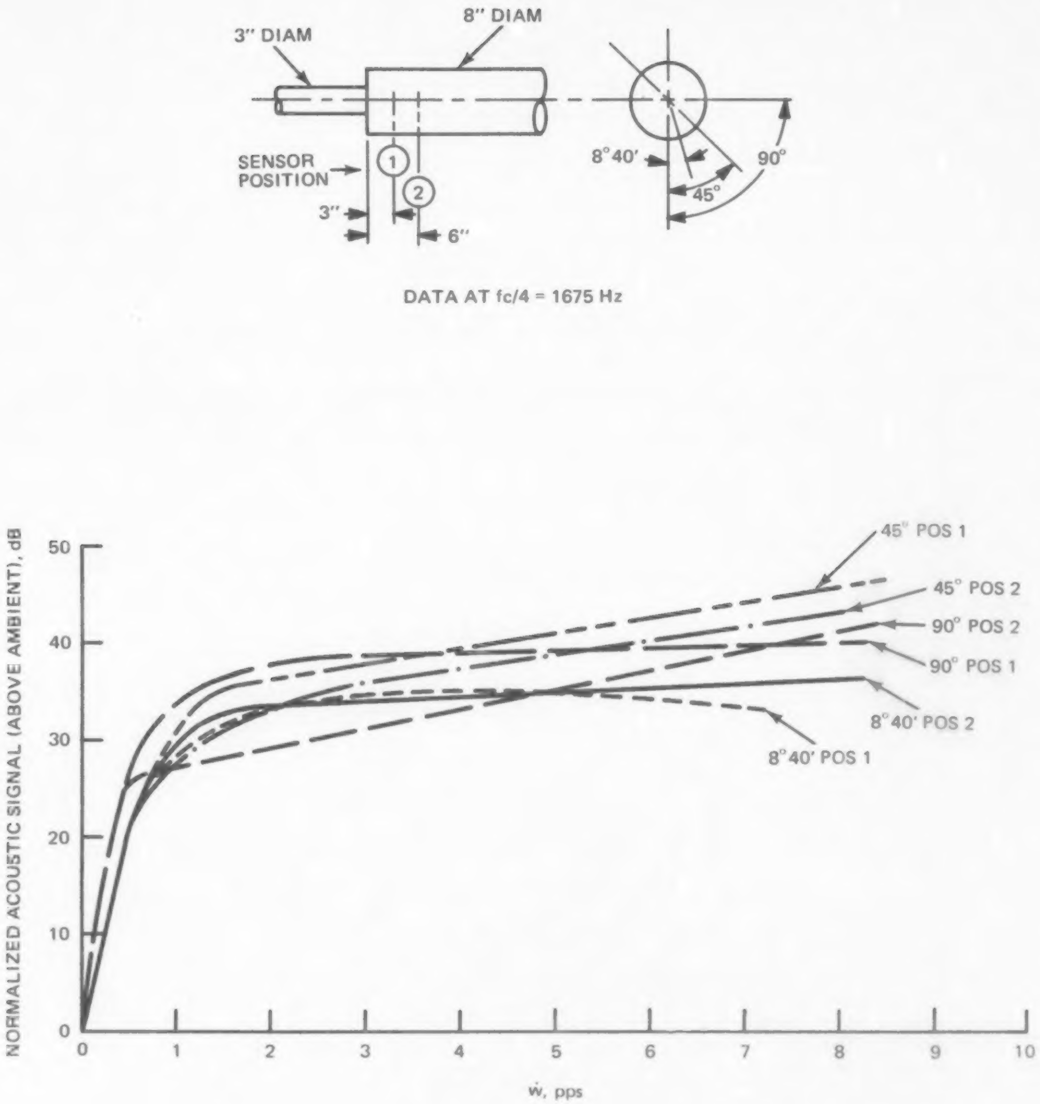

Fig. 50 Effect of sensor circumferential and axial location on useful signal (concentric cylindrical pipe array with flush inlet)

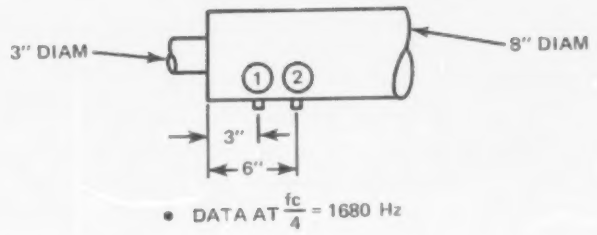
3" DIAM
8" DIAM
①
②
3"
6"
• DATA AT $\frac{fc}{4}$ = 1680 Hz

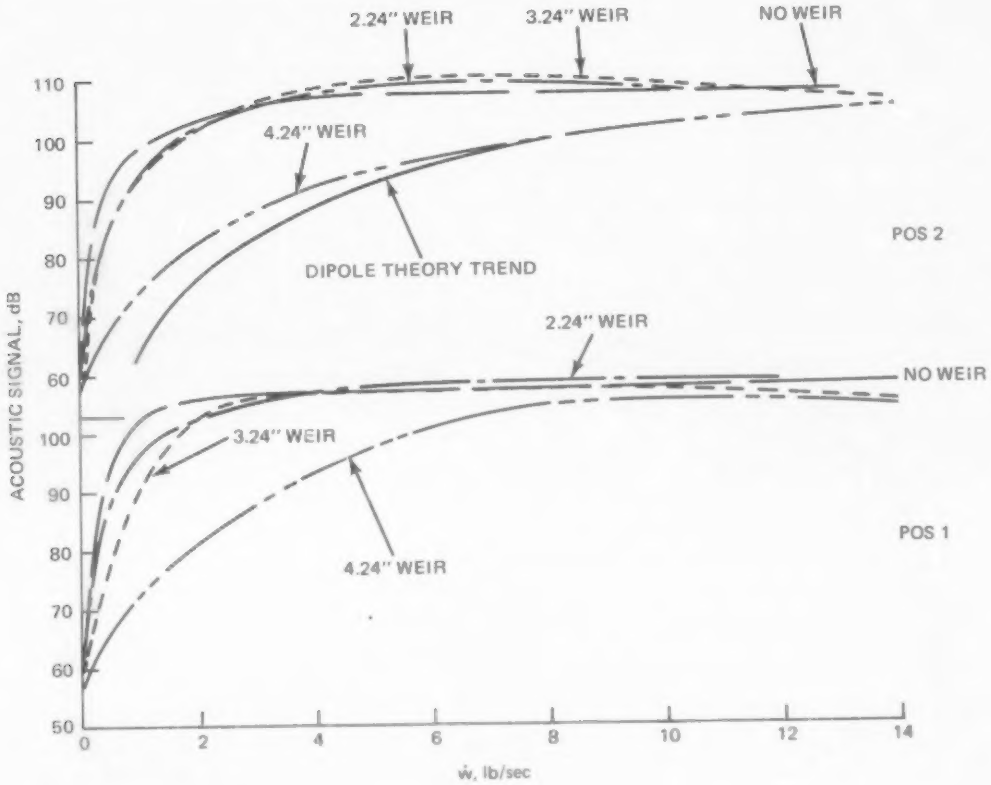

Fig. 51 Variation of acoustic signal with flow at two sensor locations for different test conditions (flush inlet, concentric cylindrical pipes)

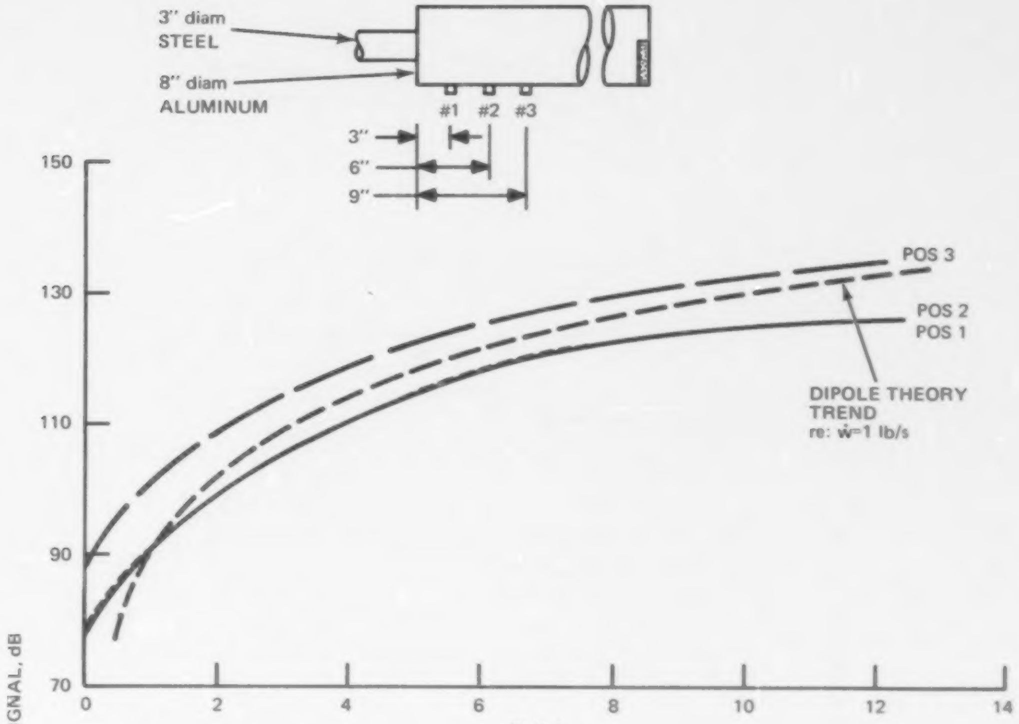

a) DATA AT f/4 ≃ 200 Hz

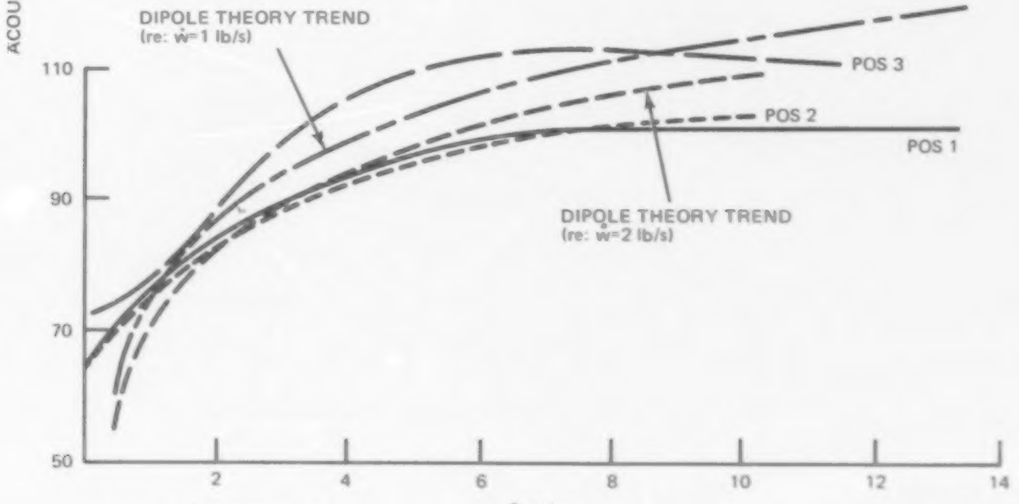

b) DATA AT fc/4 = 1680 Hz

Fig. 52 Variation of acoustic signal with flow at three sensor locations and for two frequencies - with 4.24" weir at pipe exit plane - (concentric cylindrical pipe elements)

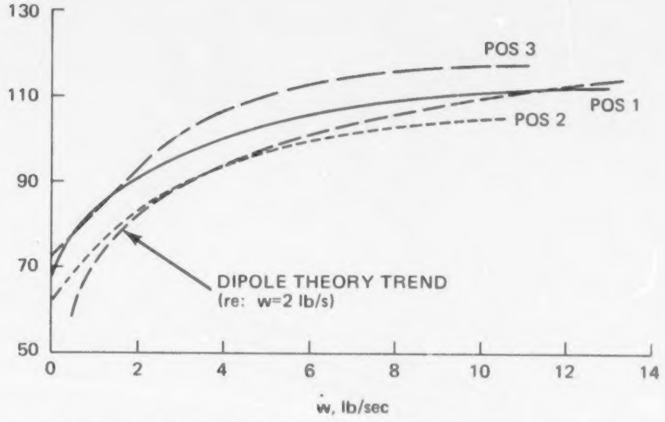

a) DATA AT f/4 = 1400 Hz

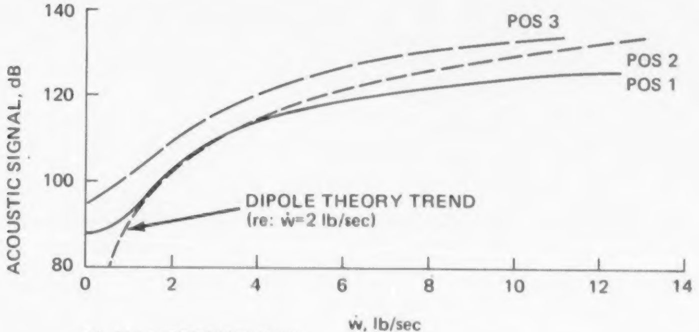

b) (ALL FREQUENCIES BETWEEN 40 AND 22,000 Hz)

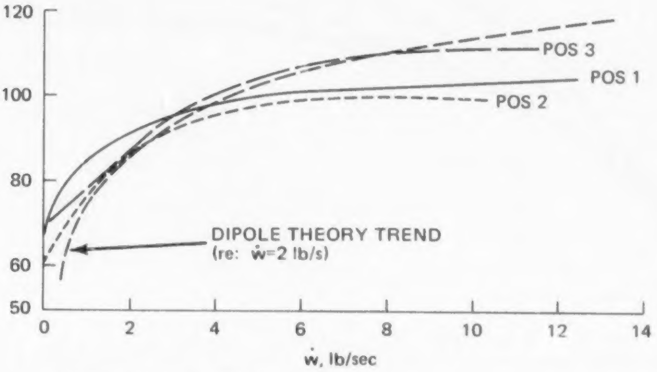

c) DATA AT f/4 = 2700 Hz

Fig. 53 Variation of acoustic signal with flow at three sensor locations and three frequency bands - with 4.24 inch weir at pipe exit plane - (concentric cylindrical pipe elements). See Fig. 52 for sensor position location on pipe.

Typical acoustic signal data where the section of joined pipes near the discontinuity plane is buried into a minimum of 8-in. (20.3 cm) of sand is given in Figs. 54 and 55. These curves are for three accelerometer locations and present the normalized acoustic signal component at four frequencies as well as the absolute overall signal. The normalized dipole theory trend is close to the signal trend at sensor positions 2 and 3 for the characteristic frequency (6720 ± 80 Hz).

The effect of the very heavy bed of stones, placed at the bottom of the 8-in. (20.3 cm) pipe, is indicated from the data plots of Fig. 56. At the characteristic frequency, the signals at both sensor positions are within 2 dB of each other, whereas for the overall range of frequencies about a 7 dB difference exists. It appears from the data shown in Fig. 56 that the weir's use results in a more gradual and resolvable signal trend, especially at the low flow rates up to about 8 lb/sec (3.6 kg/sec).

The acoustic signal obtainable for a bare conduit is compared to that with both heavy and light bed loads of stones, in Fig. 57. These data are for the characteristic frequency component as well as the integrated value over the entire frequency spectrum.

An appreciation of the physical action of the waterfall in displacing even a heavy bed of stones can be obtained from the sketches of Fig. 58, and Figs. 15, 16, 46, and 47. The drawings are interpretations of the experimenter's observa-

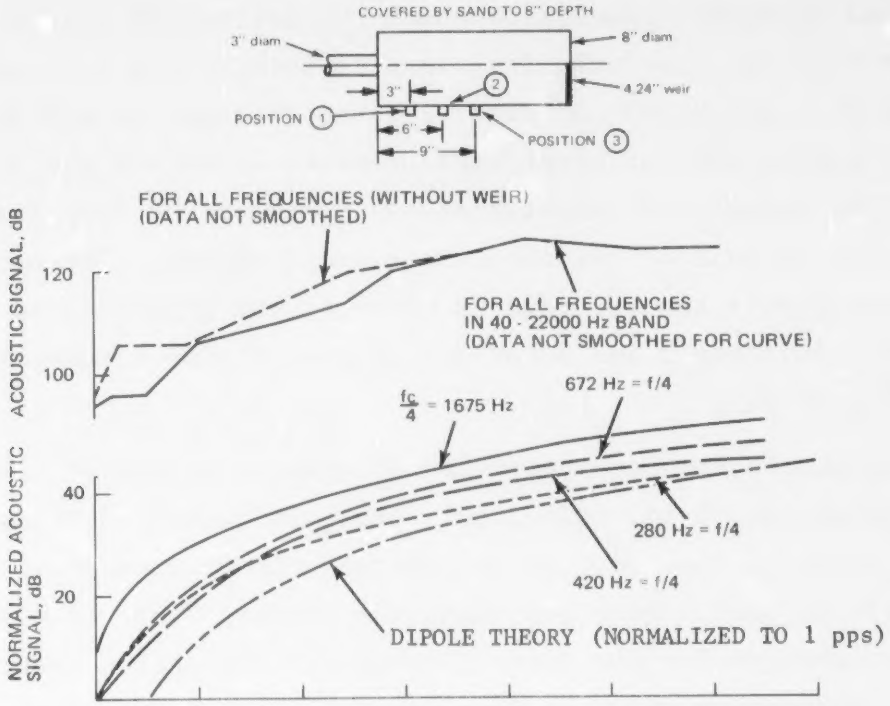

A) SENSOR POSITION 3

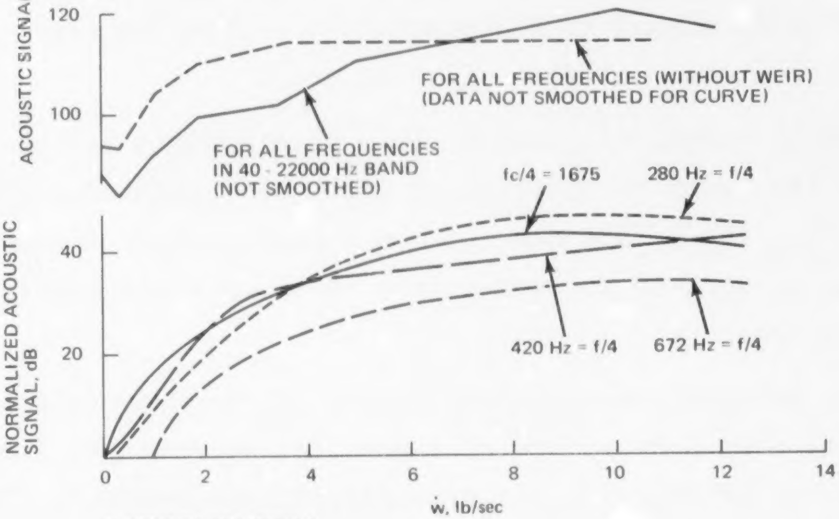

B) SENSOR POSITION 1

Fig. 54 Variation of acoustic signal with flow at two sensor locations and two frequency bands (concentric cylindrical pipe elements) - with 4.24" weir at pipe exit and 8" deep sand overburden, except where noted

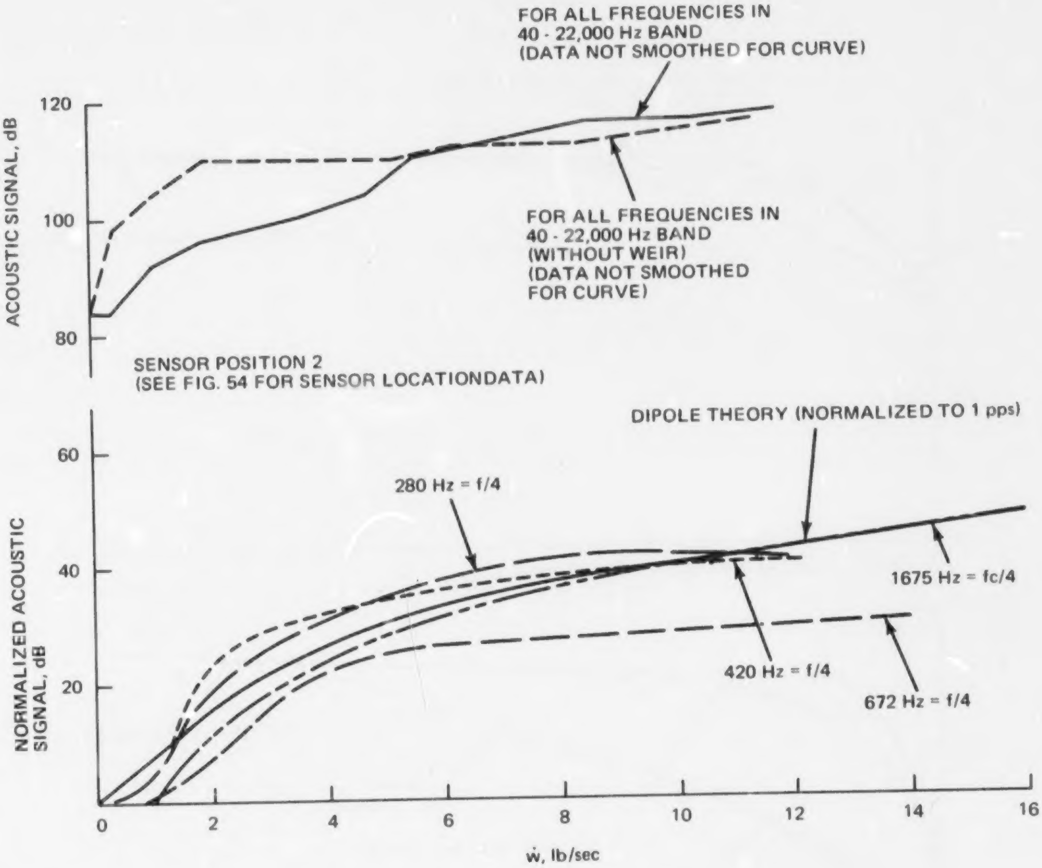

Fig. 55 Variation of acoustic signal with flow at five frequency bands and one sensor location (concentric cylindrical pipe elements) - with 4.24" weir at pipe exit and 8" deep sand over burden, except where noted

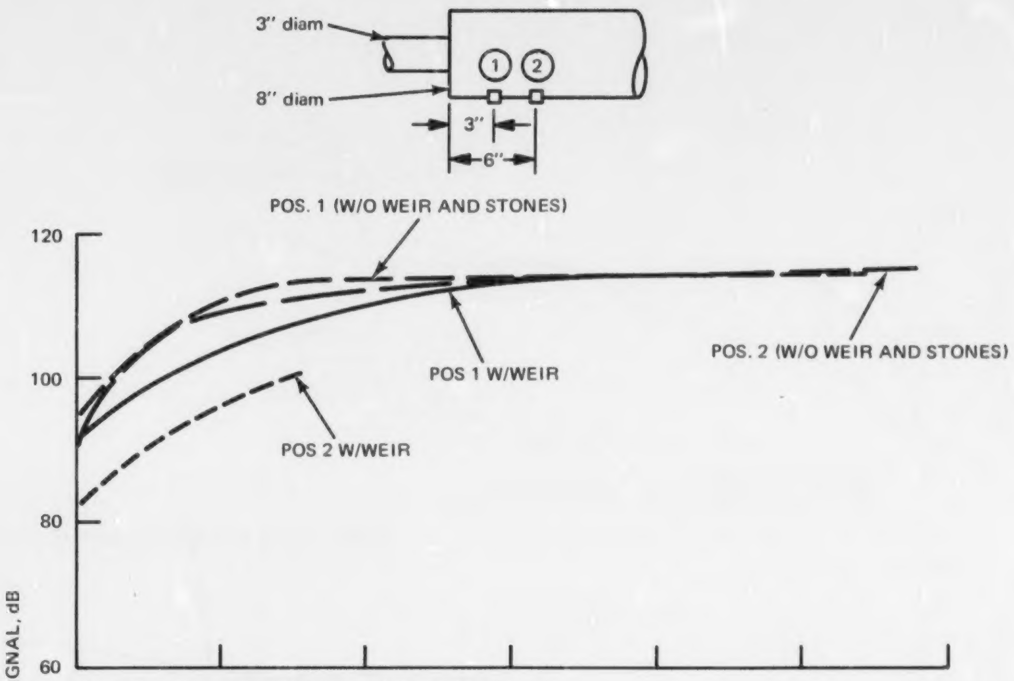

a) DATA AT ALL FREQUENCIES (40 - 22,000 Hz)

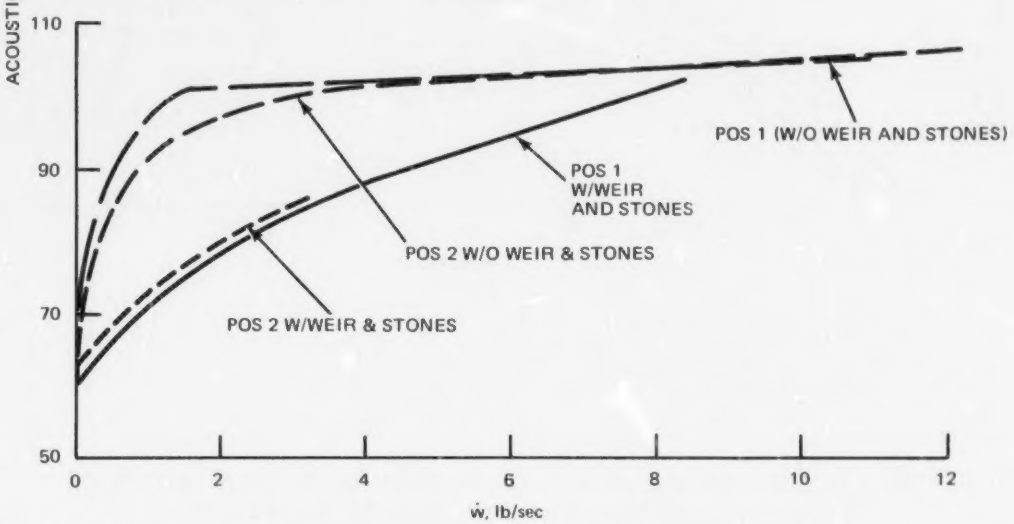

b) DATA AT fc = 6720 Hz

Fig. 56 Effect of heavy bed load of stones (1" deep) in 8" diam. pipe on acoustic signal variation with flow - sand covered array

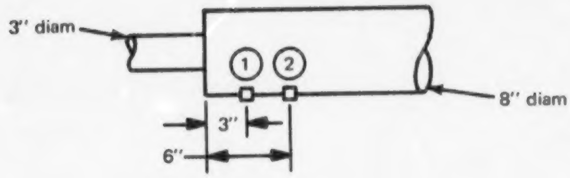

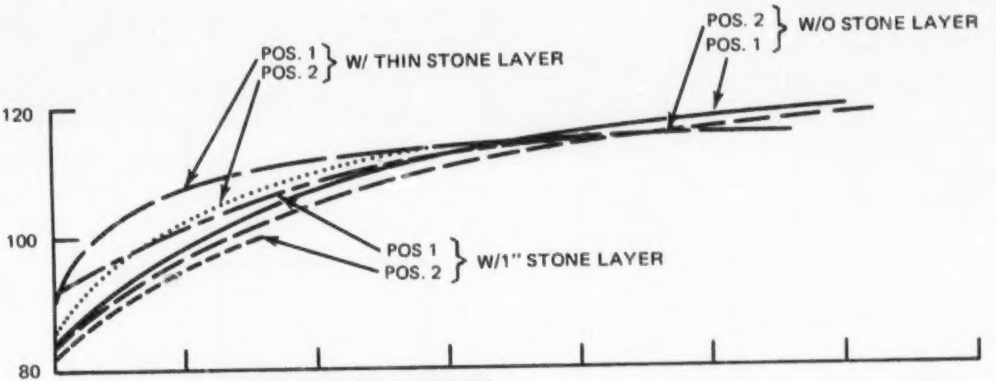

a) DATA AT ALL FREQUENCIES (40 - 22,000 Hz)

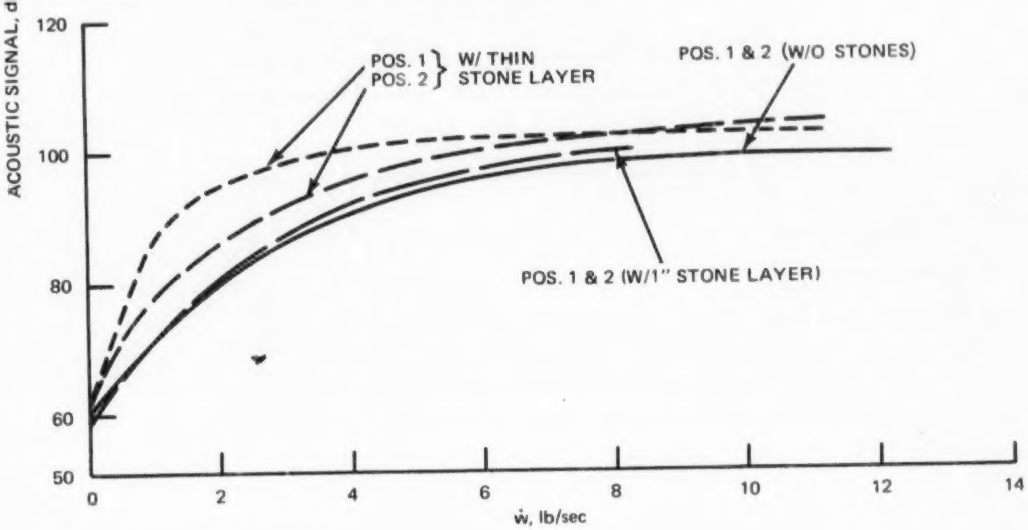

b) DATA AT fc/4 = 1680 Hz

Fig. 57 Effect of two bed loads of stones in 8 inch diameter pipe on acoustic signal variation with flow - sand covered array with 4.24 inch weir

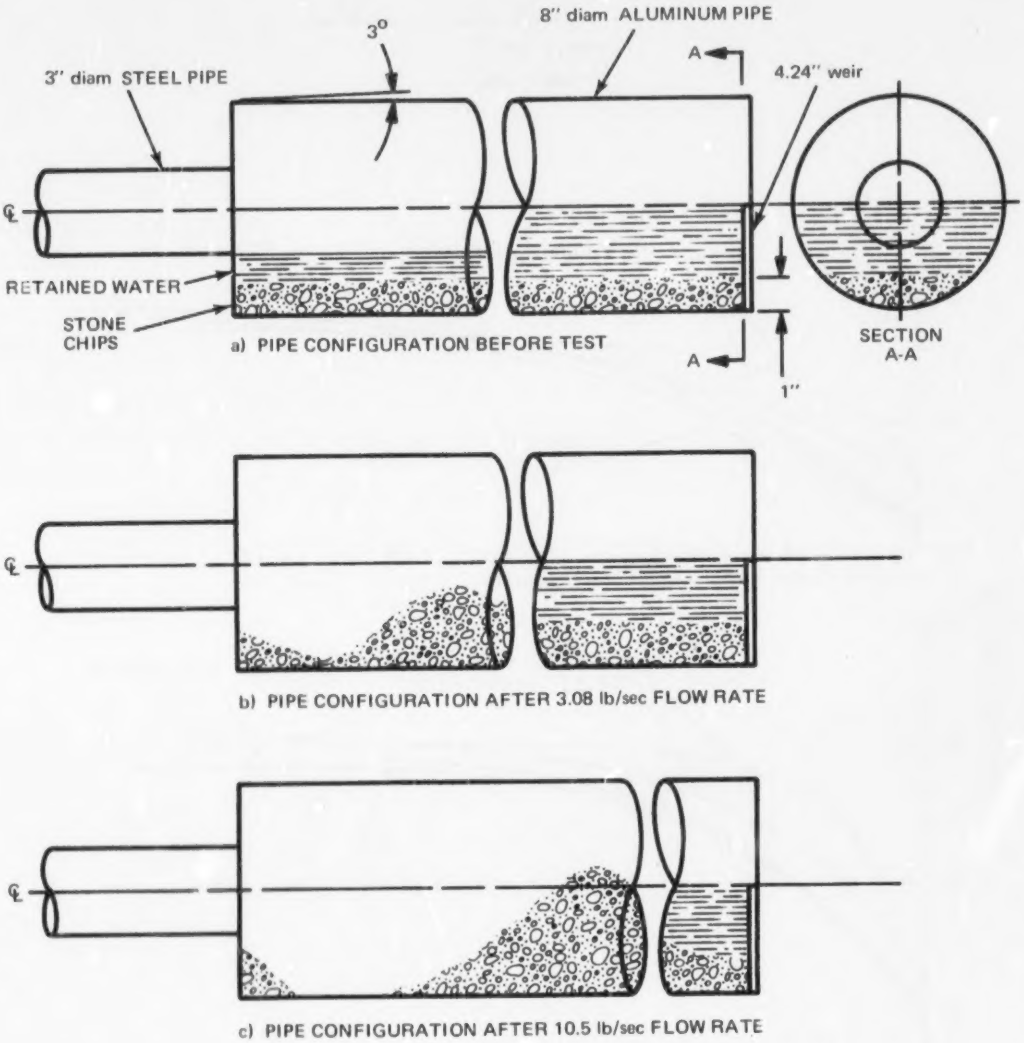
3°
8" diam ALUMINUM PIPE
3" diam STEEL PIPE
A
4.24" weir
℄
RETAINED WATER
STONE CHIPS
a) PIPE CONFIGURATION BEFORE TEST
A
1"
SECTION A-A
℄
b) PIPE CONFIGURATION AFTER 3.08 lb/sec FLOW RATE
℄
c) PIPE CONFIGURATION AFTER 10.5 lb/sec FLOW RATE

Fig. 58 Sketches of heavy bed load movement at different stages of water flow test conditions

tion after various stages of the tests. The observed local washout of the stone bed as the flow increases practically assures that the full discontinuity geometry will be maintained, and the characteristic frequency will be unaltered. Further tests where a bed load can be securely attached (e.g., by cement) to withstand such washout, could provide valuable extrapolation of the data already obtained. Figure 59 shows that absolute signal components at frequencies much above as well as much below the characteristic frequency (f_c) are of larger amplitude than f_c for the sensor location closest to the discontinuity plane (i.e., position 1). Note that since the zero flow (ambient) signal level is greatest for the lowest frequencies because of the mass distribution law, the signal-above-ambient at, for example, 800 Hz, actually is less than at the characteristic frequency for all flow rates. Position 3 is well downstream of the base of the waterfall but the acoustic data obtained there (see Fig. 59) are generally similar to that obtained at position 1.

5. Four Inch (10 cm) Diameter Transite Pipe (Tests of February 26-28, 1975)

A 4-in. (10 cm) ID Transite pipe, 44-in. (1.12 m) long, was installed at the end of the 3-in. (7.6 cm) ID facility water supply pipe (see Fig. 60). The main purpose of this test setup is to assess the transmission of flow acoustic emission through a nonhomogeneous, nonmetallic sewer pipe wall. Another objective is to examine a low sound loss technique for attaching transducers to the outer surface of the nonmetallic conduit. From physical properties data supplied

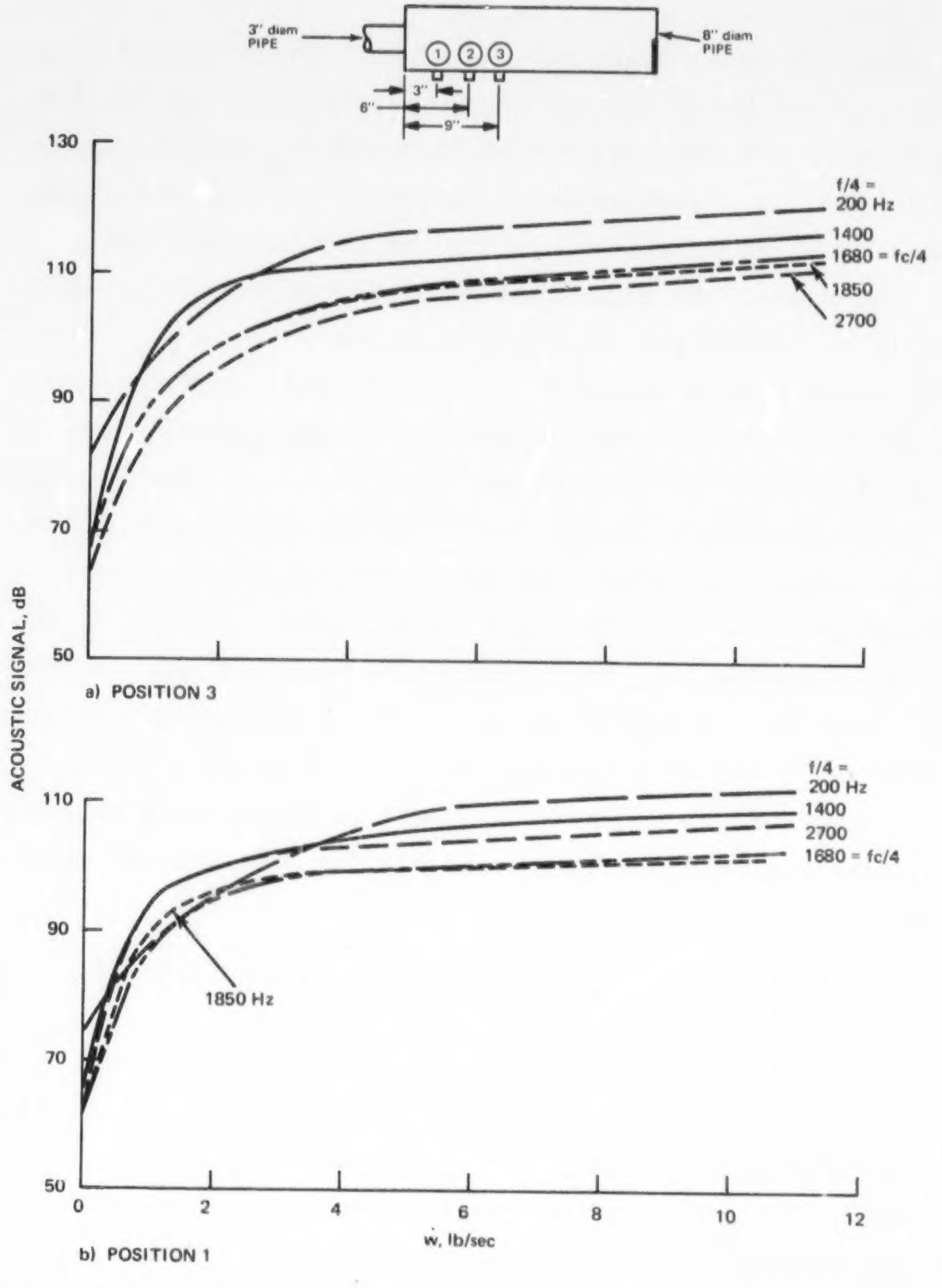

Fig. 59 Variation of acoustic signal with flow at four frequencies and two sensor positions (8" sand cover and monolayer of stone chips within 8" diam. pipe. 4.24" weir at exit of pipe)

by the manufacturer (Johns Manville[†]), it has been determined that the acoustic properties of Transite are comparable to concrete used in sewer pipe construction.

The discontinuity plane between the steel and Transite pipes is of the eccentric sudden enlargement type (flush entry) in which the roof line of the joined pipe sections is continuous. The eccentric, crescent-shaped gap between the pipes is filled by an aluminum plate and sealed by a Velmix (quick-setting) cement. The step discontinuity is 0.69-in. (1.75 cm) which corresponds to a characteristic frequency of 21,500 Hz. While the processed recorded data show acoustic spectral distributions generally similar to spectra obtained with metallic pipes, the characteristic frequency is found to be at or just above the upper threshhold of frequency response of the magnetic tape recorder used. Therefore, the reduced data could not be correlated reliably with mass flow and no graphic data presentations are to be made here. This temporary inconvenience was overcome by purchase of a 6-in. (15 cm) ID Transite pipe section as a replacement.

No difficulty was experienced in attaching the accelerometer mounting studs by Devcon "F" (80% aluminum) epoxy cement. However, it was noticed that the mounting studs were somewhat more easily sheared off the Transite pipe than the metallic pipe because of the tearing of a thin veneer of epoxy impregnated Transite from the parent material. If a sensor installed in this way were to remain undisturbed in a buried installation, we would not expect this kind of shear failure.

[†] Private communication from R. C. Elliott, Johns Manville Sales Corporation, Manville, New Jersey (January 1975).

6. Six Inch (15.2 cm) Diameter Transite Pipe (Tests of April 23, 24, 28, May 5, and June 26, 1975)

The second series of tests involving a nonmetallic nonhomogeneous conduit material used a 6-in. (15.2 cm) diameter Transite, 5 foot (1.52 m) long, sewer pipe section. The 3-in. (7.6 cm) diameter steel pipe of the facility water supply was attached to the Transite pipe by a machined plastic mounting collar and blanking plate (see Fig. 61) so that the roof line was continuous, and a sudden 3-in. (7.6 cm) step resulted at the discontinuity plane (see Fig. 11). This step size corresponds to a characteristic frequency of about 5570 Hz. The joint was sealed at the external surface by silicone-based caulking. Data were obtained with three accelerometer transducers at six mounting locations including one on the bottom centerline of the 3-in. (7.6 cm) steel pipe and 3-in. (7.6 cm) upstream of the discontinuity (position 7). Other sensor locations, not monitored during previous test series, were at the bottom centerline of the Transite pipe, 7-in. (17.8 cm) upstream of the exit plane (position 9) and 2.3-in. (5.9 cm) downstream of the discontinuity plane (position 1). The Transite pipe was set at a 3 degree downward slope and the bottom lip of the pipe was 19.25-in. (49.0 cm) above the floor of the diversion trough. Test conditions included simulated buried and unburied pipe installations, flow rates up to 15 lb/sec (6.8 kg/sec), and initial pressurization levels of 12 to 29 psi (0.84 to 2.04 kg/cm^2).

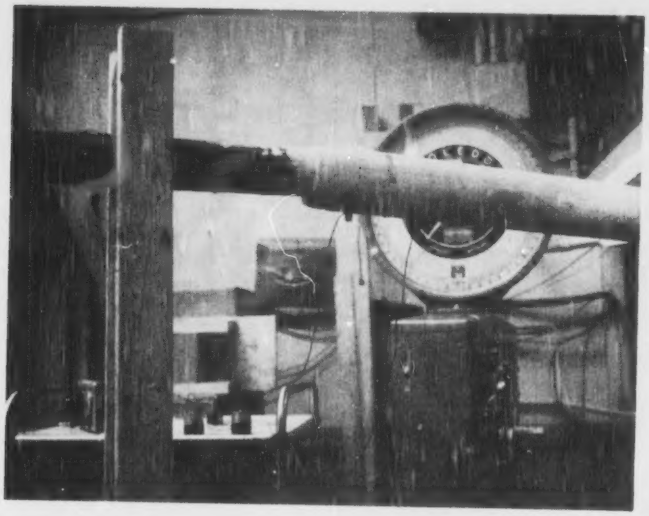

Fig. 60 Closeup of eccentric connection of 3-inch water supply pipe to 4-inch diameter transite test pipe

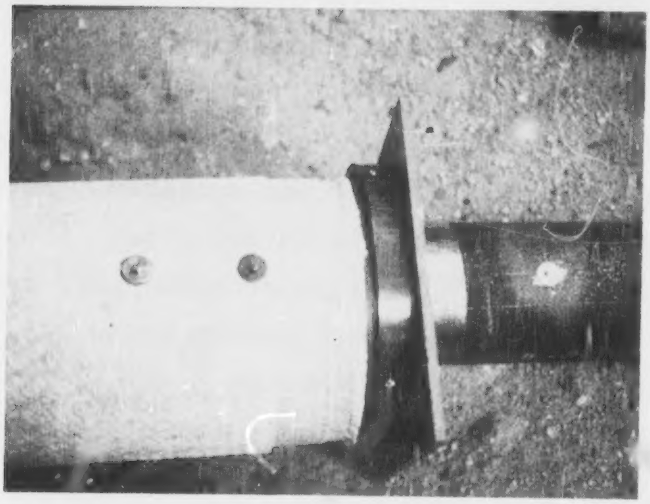

Fig. 61 Closeup of special assembly collar used for eccentric connection of 3-inch pipe to 6-inch diameter transite test pipe. Flow is from right to left. Two sensor mounting studs are shown cemented at top centerline surface of transite pipe

For a special set of runs using this pipe configuration, laboratory equipment was developed to introduce solid particles (screened sand) into the water supply at a point 18 feet (5.5 m) upstream from the test section; this equipment and technique has been described in detail in Section IIIB. Because of the slot in the 3-in. (7.6 cm) pipe line for feeding sand, flow rates above 6 lb/sec (2.7 kg/sec) could not be run without water spillage from the opening. Typical results of this test series are presented by Figs. 62 to 65.

7. Field Test Preview (Test of July 1, 1975)

The field test preview was conducted at the Grumman sewage treatment plant "A" adjacent to the corporation's building 12 in Bethpage, New York. The flow conduits monitored consist of 10-in. (25.4 cm) diameter steel pipes. Because of the preliminary nature of the tests and the need for flexibility, we decided to attach the accelerometer sensor to the outer surface of the pipe by a special magnetic mounting stud marketed by the transducer supplier. Unfortunately, this mounting technique had not been used in the previous laboratory tests so no rigorous basis of comparative sound transmission ability was possible. Testing took place between approximately 10 am and 1 pm. Acoustic measurements were recorded on instrumentation tape over a 30 second time period. The first test location was in an underground control valve vault shown by Figs. 20 and 21. Sanitary sewage from several Grumman buildings feed into a distant wet-well where collection continues until a pump-activation level is reached. The pump supplies an approximately constant average flow of 650 gpm (2460 l/m) through

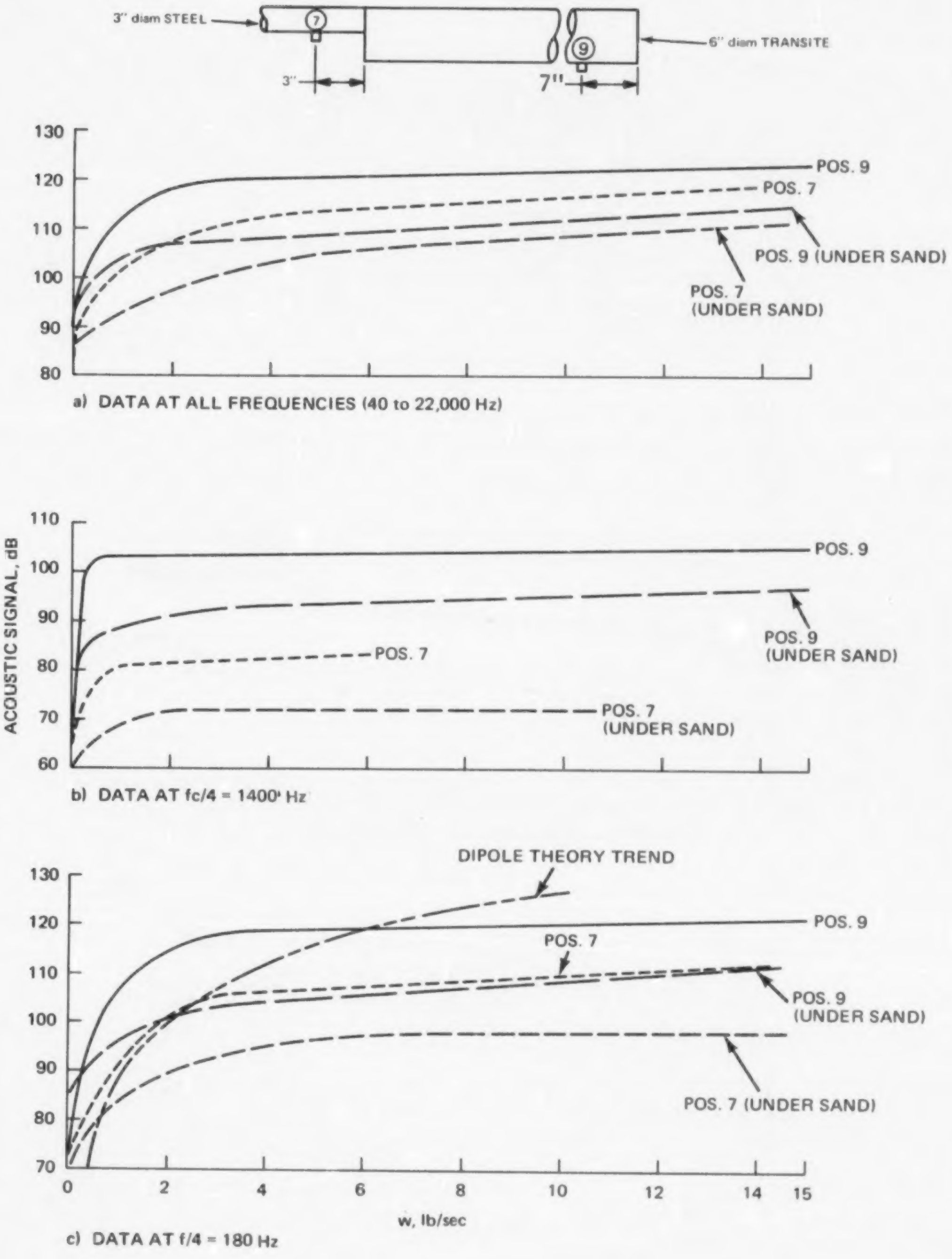

Fig. 62 Variation of acoustic signal with flow (eccentric cylindrical pipe array) - transite and steel pipe elements without sand overburden except where noted

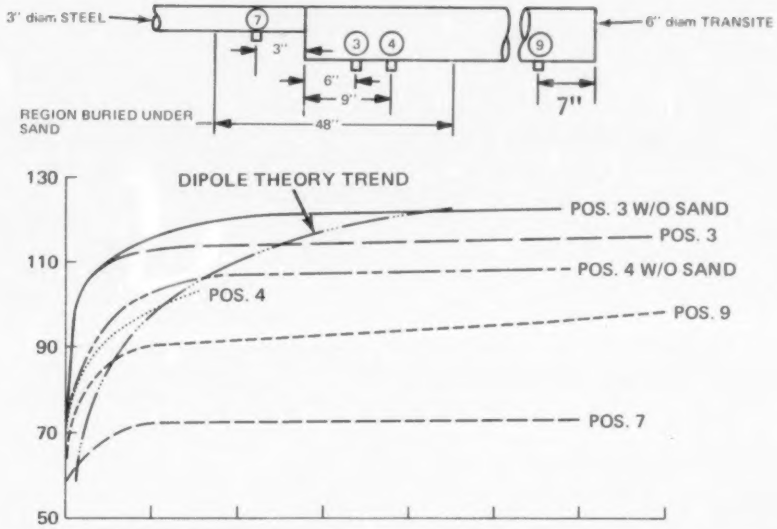

a) DATA AT fc/4 = 1400 Hz

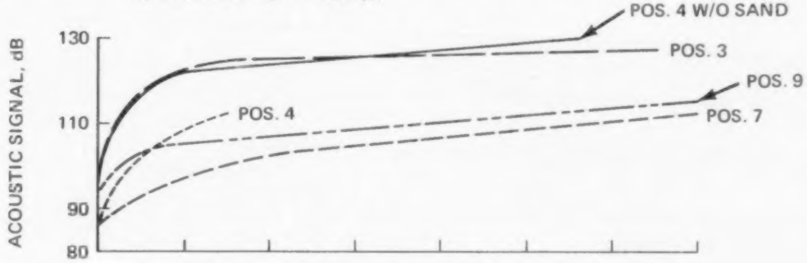

b) DATA AT ALL FREQUENCIES (40 to 22,000 Hz)

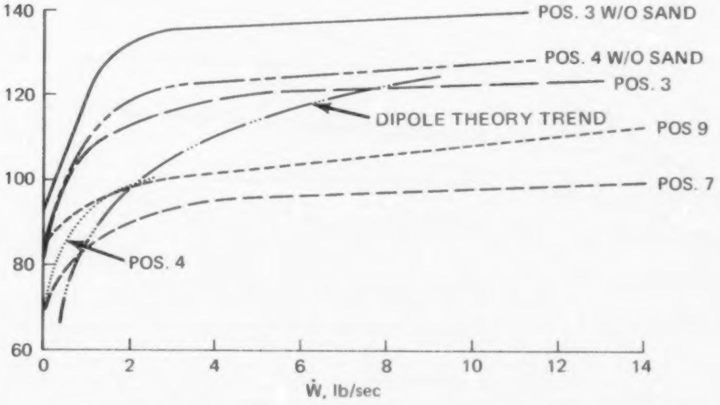

c) DATA AT f/4 = 180 Hz

Fig. 63 Variation of acoustic signal with flow (eccentric cylindrical pipe array) - transite and steel pipe elements buried under 8 in. (20.3 cm) of sand, except where noted

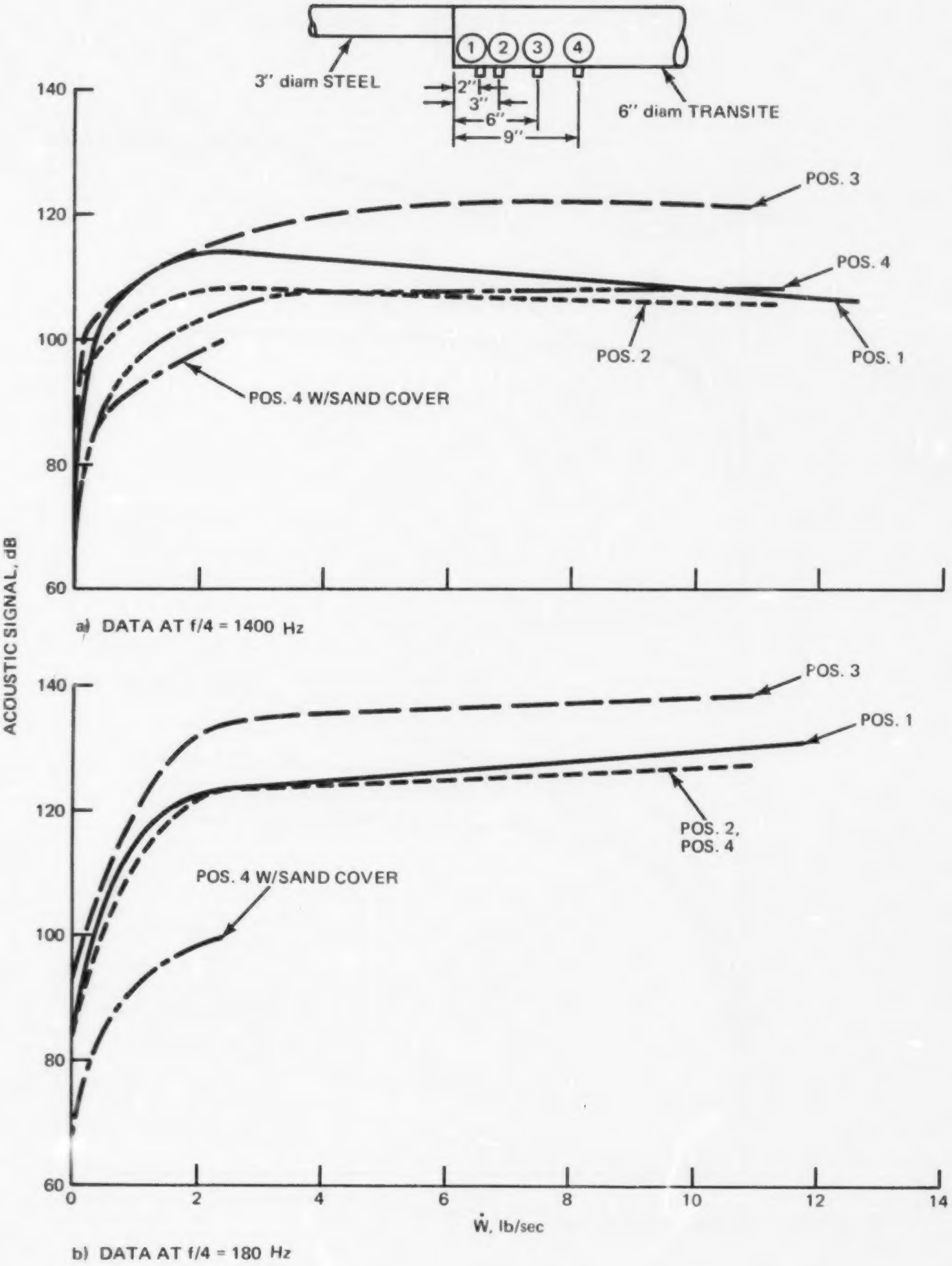

Fig. 64 Variation of acoustic signal with flow (eccentric cylindrical pipe array) - transite and steel pipe elements without sand overburden, except where noted

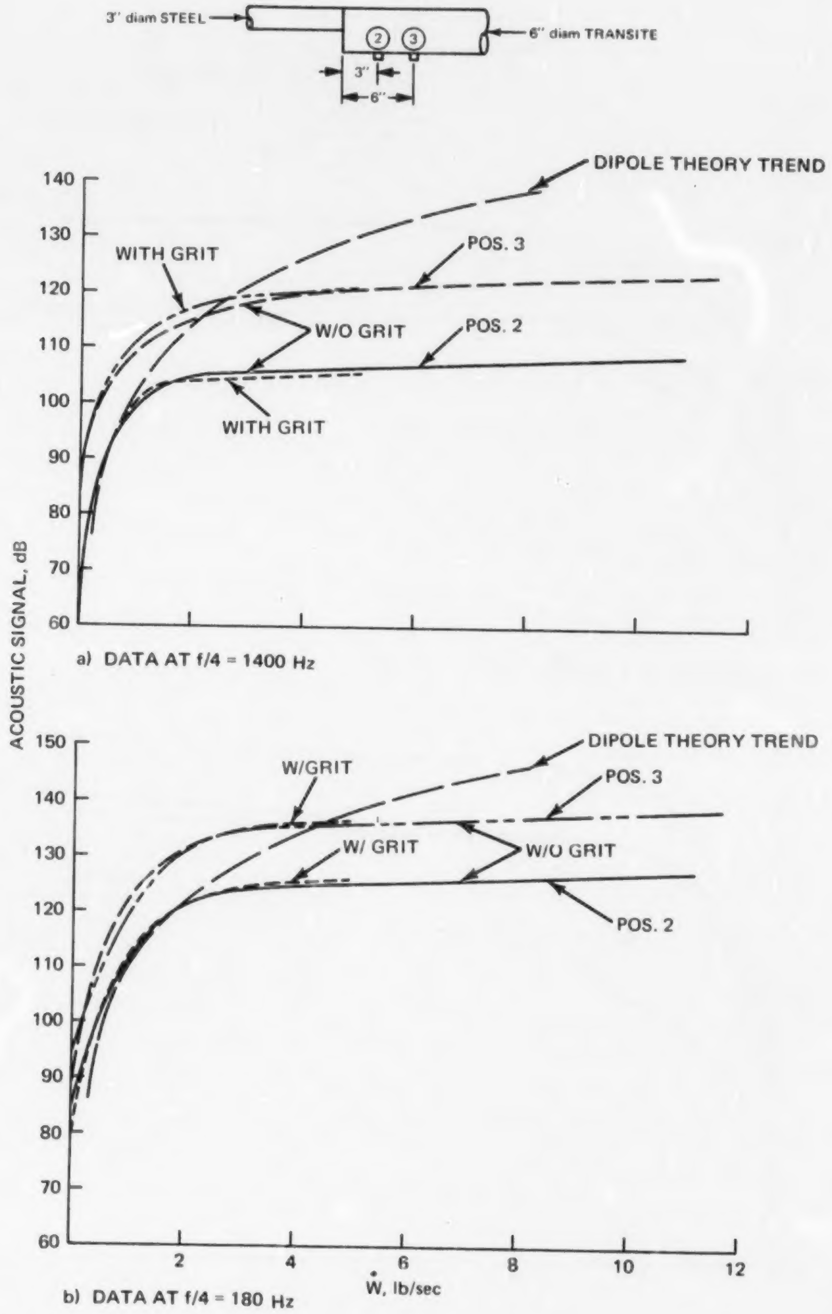

a) DATA AT f/4 = 1400 Hz

b) DATA AT f/4 = 180 Hz

Fig. 65 Effect of grit addition to water flow on the acoustic signal variation with flow - transite and steel pipe elements, without sand overburden, in eccentric assembly

the 10-in. (25.4 cm) pipe until the level in the wet-well drops to a cutoff point. The pipe discontinuity accessible for our measurements was an 8-in. (20.3 cm) plug valve connected by an 8 by 10 by 6-in. tee fitting to the 10-in. (25.4 cm) upstream supply pipe, and by an 8 by 10-in. reducer section to the downstream pipe. Several positions on the reducer, exit pipe, and upstream tee section were examined (see Fig. 66). Ambient noise measurements were recorded when no flow was evident; this fact was established by correlation of the observed level indicated by the tape recorder's monitoring meter and visual verification at the exit of the pipe, about 500 feet (152 m) away, at the aeration tank. The sources of ambient noises at the value include moderate road traffic about 500 feet (152 m) to the south and a railroad about 750 feet (228 m) to the east. One of the two ambient noise measurements coincided with passage of an eight-car passenger train.

The second field site where acoustic emission measurements were taken was at the point where the 10-in. (25.4 cm) pipe emerges from beneath the surface and discharges horizontally into an open, tortuous concrete channel feeding a comminuter (see Figs. 22 and 23). Close by, a 4-in. (10.2 cm) diameter steel pipe also discharges into the comminuter feed channel except the direction of flow is vertically downward. This smaller pipe conducts an additional 250 gpm (746 l/m), from a pump-equipped wet-well located in the Grumman factory building just north of the treatment plant.

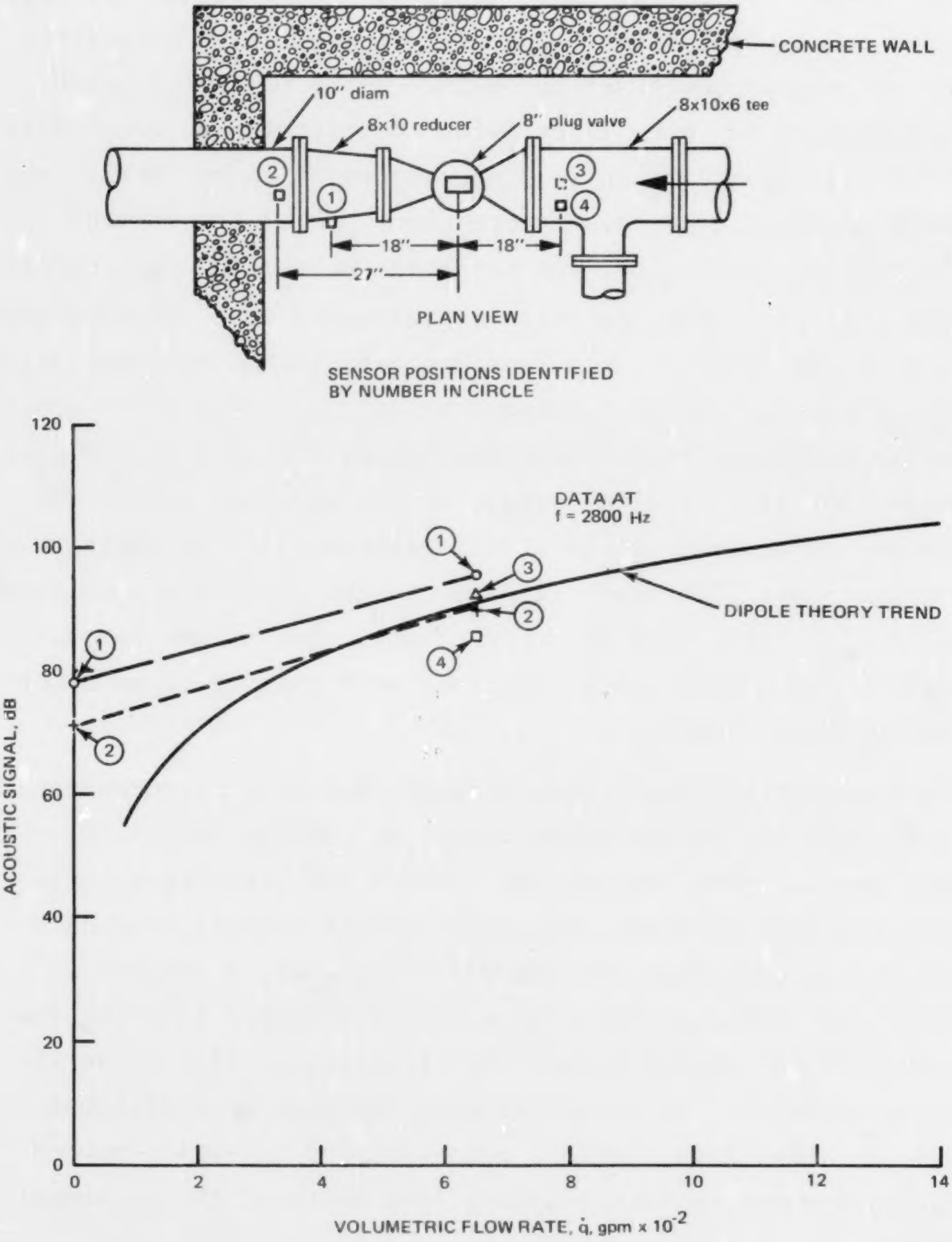

Fig. 66 Variation of acoustic signal with flow at Grumman waste treatment plant "A" valve vault for different sensor positions - first test series

Four locations on the horizontal leg of the 10-in. (25.4 cm) diameter steel pipe were monitored as shown by Fig. 67.

D. DISCUSSION

The results of this program can be summarized by the statement that no fundamental questions remain concerning the feasibility of Grumman's acoustic emission flow measurement technique applied to discontinuities at enlargements of conduit cross sections.

The test data have removed each of our initial reservations about the technique discussed in Section IIIA. The numerous tests established to demonstrate feasibility were, perhaps, influenced by the failures of so many more complex techniques when applied to sewer flow, and the contrasting relative simplicity of our passive nonintrusive method. But now, after extending the range of flow rate by a factor of 20, using four different pipe geometries or constructions, employing accelerometer sensors with four different sensitivities, and conducting a field test preview, the acoustic emission technique remains viable and appropriate for more exhaustive field testing leading to prototype systems.

To date, only laboratory equipment has been used to monitor flow acoustic emission and to process the raw data. This approach has had the advantages of minimizing equipment costs to the program, and of presenting greater measurement capability than the basic needs of tests to allow flexibility in conducting the exploratory research.

The assemblage of many high quality but multipurpose laboratory components to obtain acoustic recordings and to feed

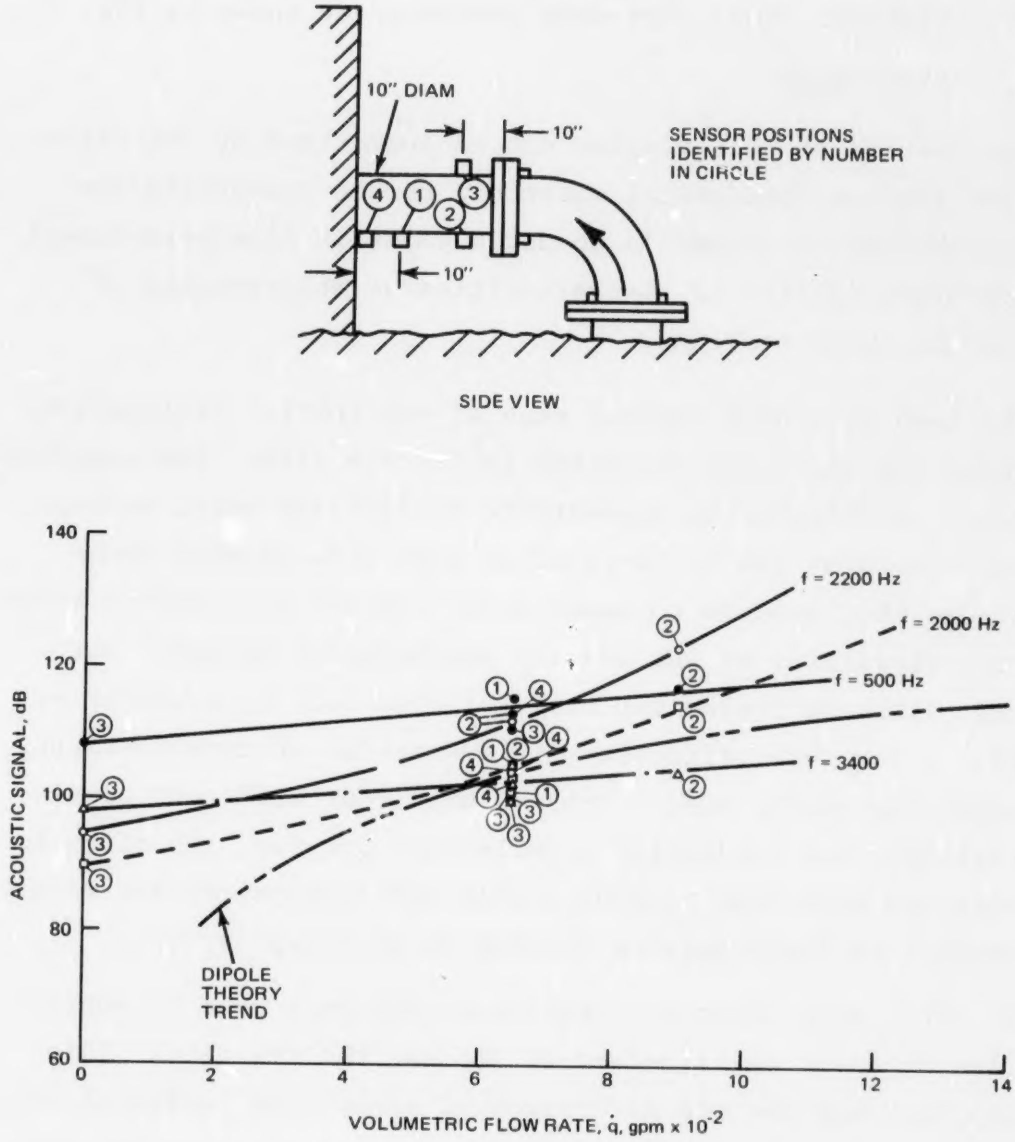

Fig. 67 Variation of signal with flow at Grumman waste treatment plant "A" aeration pond for different frequencies and sensor positions - second test series

these recordings through the Fourier analysis computer, introduces and compounds the inaccuracies and mismatches of each component in the system. The result of these unwanted signal distortions, or noise, is that the reproducibility of the processed signal components in narrow 10 Hz frequency bands is no better than ± 2 dB over the frequency response of the tape recorders. A 2 dB change is equivalent to a ratio of sensor signal levels of 1.26; while this seems small, at high flow rates this change can represent large absolute quantities of flow. The prospects for improving this situation are extremely good if less versatile, well-integrated electronic circuits and special purpose data processors are used. Now that most of the feasibility questions have been answered, prototype hardware need only consist of a simple accelerometer, for attachment to the sewer pipe, and a communications link to a simple, cheap, dedicated minicomputer.

While we have not determined the accuracy limits for the acoustic data because of the equipment involved, we have estimated the accuracy of the test facility's flow rate measurement equipment as from ± 7% for low flow, short sampling time (e.g., 10 seconds) conditions to ± 4% for high flow, long sampling time (e.g., 30 seconds or more) situations. These values compare favorably to commercial flow meters for sewage that often have accuracies worse than ± 10%.

The research facility has demonstrated sufficient versatility for the program, and accommodated various changes of pipe test configurations with relative ease. The only limitation we have experienced is an inability to sustain steady flow at high flow rates because of the limited plant water supply to the pressurization tank. Uniform as well as nonuniform flow conditions were established during the program although the latter profile was limited to flow rates less than 6 lb/sec (2.7 kg/sec). The maximum flow rate of about 15 lb/sec (6.8 kg/sec) is imposed by the present flow collection and measurement method. This capability could be doubled by facility modifications if justified by the scope of future test programs.

The superior acoustic data resulting from use of a high weir at the pipe exit and with simulated buried installations demonstrate that special precautions against acoustic reflections should be taken in laboratory investigations involving passive acoustic monitoring. Anechoic chambers typify such special measures. However, our simple inexpensive measures proved effective in accomplishing almost complete sound isolation. In most field measurements for sewer pipes, this problem does not exist. At outfalls, except if there are reflecting surfaces surrounding the exit, there should not be significant reflected sound to distort the acoustic emission characteristics of the flow.

The test results summarized in Fig. 68 indicate that the characteristic frequency component of acoustic emission of flow into an open trapedzoidal channel increases with flow. No undue precautions have been taken against sound reflections, but the open channel apparently produces diffuse radiation that does not reflect back efficiently to the channel. Although the dipole theory trend is approximated only at low flows, the signal component is unambiguous and therefore useful for flow measurement. For flows above 2.2 lb/sec (1.0 kg/sec) the 3 dB higher acoustic signature for

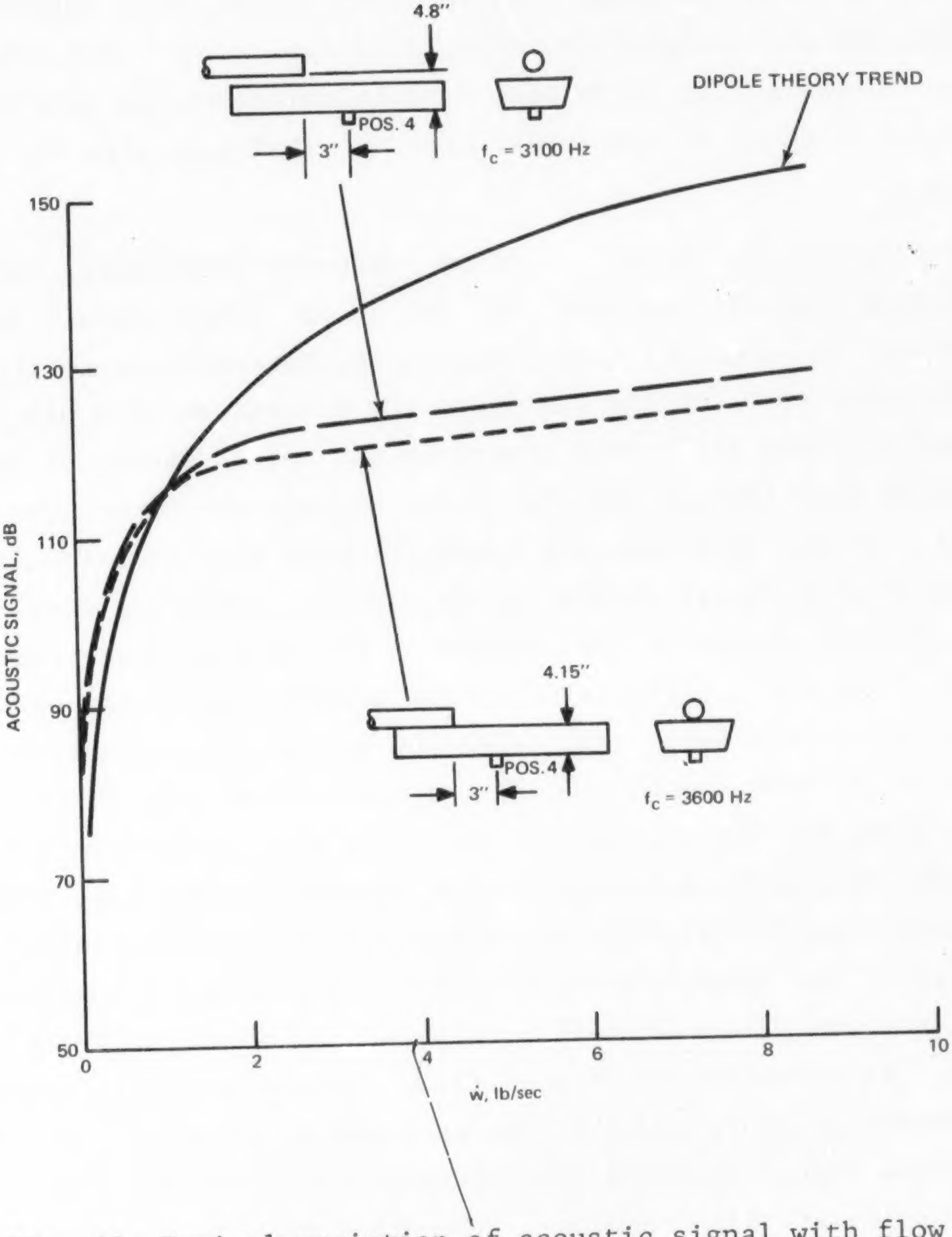

Fig. 68 Typical variation of acoustic signal with flow for two conduit configurations (cylindrical to trapezoidal cross-sectional discontinuity)

the higher waterfall is not considered trend-setting at this time, and is more likely peculiar to the test equipment setups at the two different test periods. Since these results confirmed and extended Grumman's 1972 exploratory data, further investigations with this conduit configuration were suspended in favor of completely closed cylindrical pipe elements.

The data for the 3-in. (7.6 cm) diameter steel water supply pipe (see Fig. 28) has 20 to 30 dB lower overall (all recorded frequencies) sound emission at intermediate to high flow rates than for the test conduits downstream of a discontinuity. This difference cannot be the result merely of transmission loss through the pipe walls because all pipes used (i.e., steel, aluminum, and Transite) have theoretical wall transmission losses within ±3 dB. It is concluded, then, that the greater output of the sensors on the various downstream test pipes are the result of strong acoustic radiation by pseudosound, dipole type, sources caused by the discontinuity. At zero flow, peak signal component amplitudes on the 3-in. (7.6 cm) pipe are observed at 80 and 2160 Hz, excited by presently unidentified sources in the laboratory (see Fig. 29b). Clearly, the latter frequency duplicates a major excitation source of the laboratory environment and although the signal amplitude increases with flow to about 5 lb/sec (2.27 kg/sec), it decreases for higher flows. Therefore, this signal component is ambiguous for flow measurement purposes because the same signal strength can represent more than one flow rate value at this frequency. The other peak in the spectral distribution, at the lower (880 Hz) frequency, increases in amplitude with flow rate at a somewhat slower rate than would be predicted by dipole theory (i.e., $\sim \dot{w}^4$)[1,2] at low to intermediate flow rates, but becomes more compatible toward the higher flow rates tested. On the other hand, this frequency component exhibits poor adherence to the theoretical near-field boundary layer variation ($\sim \dot{w}^3$).[6] The 880 Hz frequency is close to that which would be calculated as characteristic on the basis of the 17-in. (43.2 cm) drop from the pipe to the wooden diversion trough, so it is tempting to hypothesize the source of this peak signal component as the flow interaction with the solid surface of the trough. The monitored signal would be the sound reflected back through the open end of the 3-in. (7.6 cm) pipe. In any event, the slight 0.25-in. (0.64 cm) discontinuity caused by the pipe coupling produces no dipole sound signal within the 22,000 Hz frequency response limit of our recording equipment and no useful signal for flow measurement.

Figures 37 and 69 summarize the effect of an extended inlet on acoustic emission signal at characteristic frequency, for eccentric and concentric cylindrical pipe element assemblies. While Fig. 37 data show higher dB levels for the extended inlet, the useful signal above ambient is almost equal for both inlets because the zero flow (ambient) signal level is lower for the flush inlet. On the other hand, this does not hold true for concentric installations as shown by Fig. 69, where all signals are normalized to the zero flow level. For the extended inlet shown in Fig. 69, the sensor position atop the downstream pipe (5), measures 5 to 7.5 dB greater levels than at the bottom centerline, (3), but at the same axial distance from the pipe discontinuity. We interpret

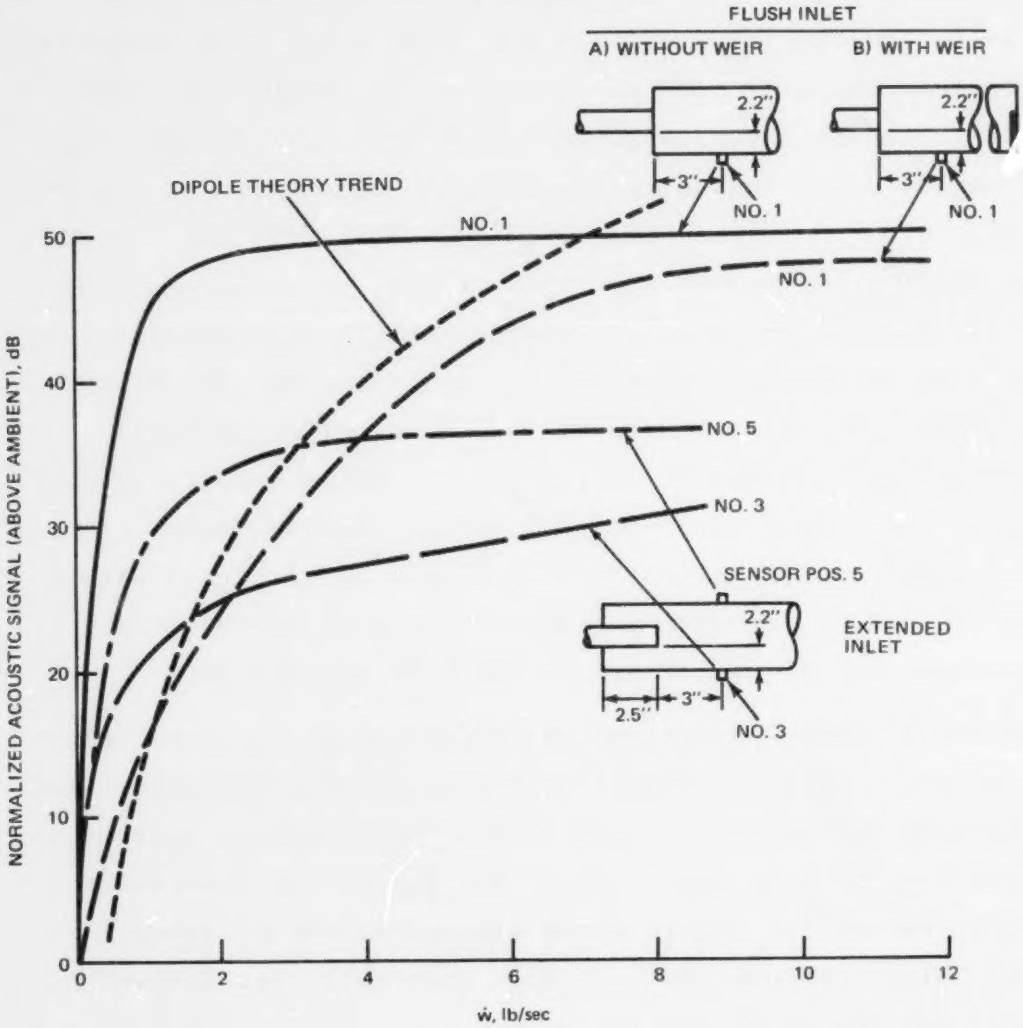

Fig. 69 Effect of extended inlet on acoustic signal variation with flow rate (concentric cylindrical pipe elements)

this as showing greater susceptibility of position 5 to reflected sound. As flow increases, the trend is for signals at both positions to converge. The flush inlet with a 4.24-in. (10.8 cm) weir produces lower signals than the open pipe exit at the same sensor position but its trend follows more closely that of dipole theory, to about 6 lb/sec (2.7 kg/sec) flow. At higher flow rates, the open and weir-equipped pipes display signal components approaching equality. Figures 43 and 44 effectively summarize the influence of laboratory sound reflections on signals obtained with the eccentric cylindrical pipe array.

With an end-positioned weir and sand burial, a constant 7.5 dB lower signal is monitored at position 4 (see Fig. 43) 6-in. (15.2 cm) from the discontinuity. At position 1 (see Fig. 44) the nearly constant difference of 5 dB for weir-equipped pipes with and without sand overburden is equivalent to the exposed installation having a sound source that is 1.8 times greater than the buried pipes, for flows greater than 1.5 lb/sec (0.68 kg/sec). At position 4 this signal difference because of sand overburden also is about 5 dB but only at flows between 2 and 9 lb/sec (0.9 and 4.09 kg/sec). When the only difference between test conditions is the presence or absence of the end weir, the signal level with the open ended pipe is 9 db greater than with the weir, for sensors at both positions 1 and 4. This difference is equivalent to an apparent ratio of sound source strengths of about 2.8. Similarly, at position 3 reductions in signal are caused by overburden or weir attachment (see Fig. 44) but of somewhat smaller magnitude than the previous two positions analyzed. Presumably, sensor position 3 has different exposure susceptibility to reflected sound because of its downstream-most location. The curves for positions 3 and 4 show that the effectiveness of the sand overburden in preventing sound reflection from affecting the sensor at each location becomes unimportant above 9 lb/sec (4.09 kg/sec) flows. This can be explained on the basis that the magnitude of externally reflected sound becomes 10 dB less than the internally produced flow interaction signal at flows of about 9.0 lb/sec (4.09 kg/sec) (e.g., two separate 100 dB acoustic signal sources produce 106 dB of combined acoustic signal, but if only one signal increases to 110 dB the combined signal is only 112 dB). Thus, we conclude that the exit plane weir and 8-in. (20.3 cm) deep sand cover screen the accelerometer pickups from being overpowered by flow sound and other external noises reflected back from the laboratory walls. When compensation is made for these reflected sounds, under laboratory conditions, completely unambiguous signals are obtained for the acoustic emission flow measurement technique in eccentric cylindrical pipe installations.

The results of Fig. 50 signify that acoustic signals are transmitted circumferentially with negligible loss at any particular axial pipe station. For unburied installations, the upper sector of the pipe surface probably is more vulnerable to externally produced noises. However, for typical buried pipe installations, acoustic pickups can be attached at any convenient circumferential position, which simplifies field instrumentation of existing sewer pipes.

Figures 51 through 55 indicate that the effect of an end weir plate and simulated buried installation is similar for the concentric arrangement of cylindrical pipe elements as it was for the eccentric pipe assembly. The highest weir prevents reflected sound, off the laboratory walls, from reentering the pipe and augmenting the acoustic signal of flow at the discontinuity. Because of the downward slope of the 8-in. (20.3 cm) conduit, the shorter weirs have no practical shadowing effect and result in data almost identical to the open ended pipe. When the acoustic reflection is minimized by pipeline burial and weirs, the data appear to follow closely the dipole theory prediction curve and are unambiguous with respect to flow rate.

Summary Fig. 70 shows how the pipe configuration changes the normalized acoustic emission signal at a fixed axial position downstream from the discontinuity plane. Both curves shown are for signal components at the characteristic frequency corresponding to the disturbance distance of the configuration. The influence of acoustic reflections is minimized here by burial under sand and attachment of an end weir. The monitoring position selected for data presentation always is downstream of the base of the waterfall but more so for the concentric pipes than the eccentric array because of the different discontinuity distances. Both data trends are unambiguous and useful for flow measurement although the concentric configuration data follows the dipole theory trend better than the eccentric configuration over a larger range of flows.

Figures 56 and 57 effectively show that stone bed loads do not thwart the acoustic emission technique. Further analysis of the spectral distributions resulting from the computer processed recorded sound reveals that a major part of

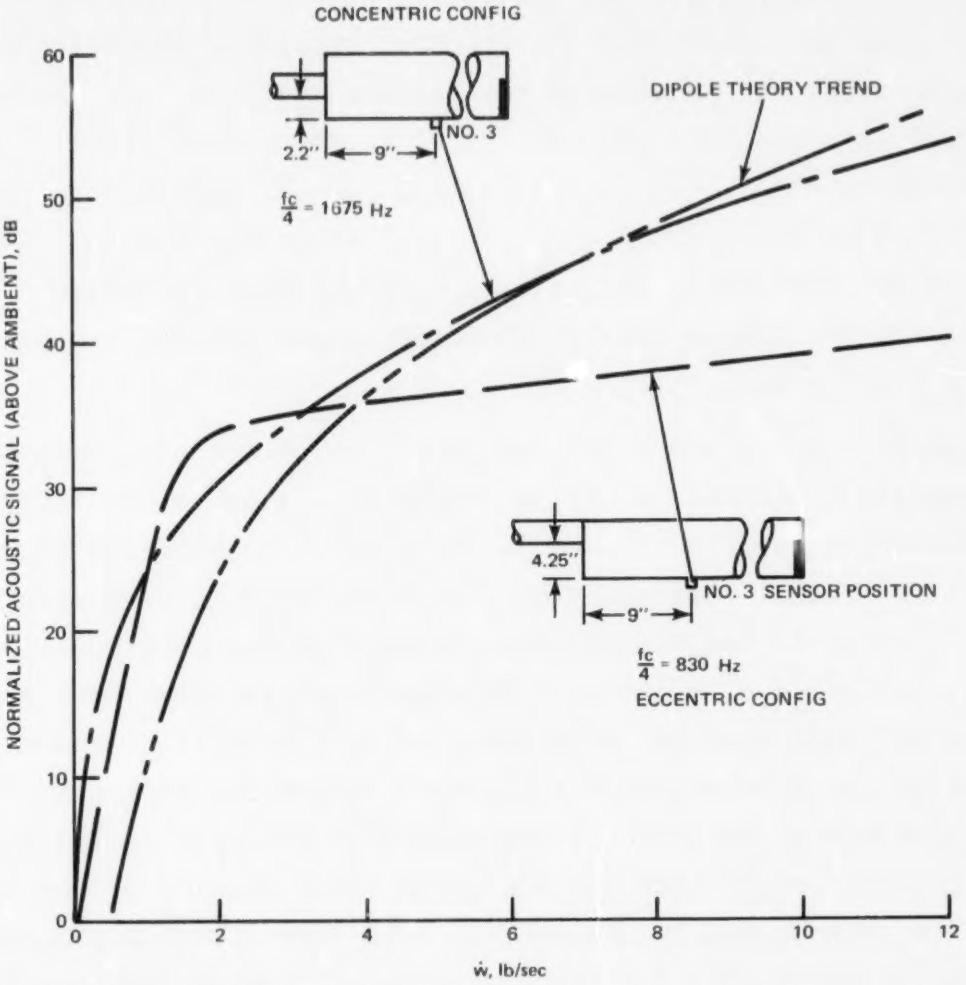

Fig. 70 Effect of pipe configuration on normalized acoustic signal variation with flow rate (cylindrical pipe elements) with 4.24 in. weir, 8 in. sand overburden, and flush inlet

the 7 dB difference in overall signal value between the two sensor positions, displayed in Fig. 56, is in the low frequency range, below 1200 Hz, rather than in the high range near the characteristic frequency of 6720 Hz. From Fig. 57 we see that when the tumbling stones of the heavy bed load are continuously being moved by the force of the water flow there results a greater sound level, integrated overall frequencies, than for the clean pipe, and a greater variation of the overall signal at different sensor positions. However, the spectral discrimination exercised to extract a signal relatable to flow (i.e., by obtaining signal components at characteristic frequencies) makes our technique effectively insensitive to the consequences of extreme saltation of the bed load; the bulk of the additional sound produced by rolling stones is in an unused part of the spectral distribution. While Fig. 57 indicates comparable trends for the thick layer of stones and the bare conduit, at the characteristic frequency, for a nearly monolayer bed load of stones the acoustic component is much larger than either of the other two test conditions at low flow rates. As the flows increase to intermediate and high rates the thin layer of stones is displaced just like the thicker, more mobile, bed load so that the persistent slightly higher acoustic signal measured must represent additional sound sources near the discontinuity. One explanation is that the turbulence produced by the sharp-edged stones scatters pseudosound and converts part of it into intense sound fields which are in a propagating mode.[1]

One of the pleasant features of passive acoustic monitoring of flow is that the overall sound quality is good enough to be listened to by humans. Further, the sound of processes as rolling stones are fully interpretable as such by experienced personnel listening to the sensor output. This type of information can be extremely helpful in remote operational monitoring of the condition of sewers to determine where maintenance is necessary.

If the thickness of the monolayer bed of stones were to be considered as reducing the discontinuity distance and acting like the solid wall of the conduit, the characteristic frequency would change to 7400 Hz from the 6720 Hz for the clean pipe. But the data of Fig. 59 at 7400 Hz coincides with that at the frequency for the bare conduit at all but the lowest flow ranges below 2.2 lb/sec (1.0 kg/sec). Where the very low flows do not move the stones, the signal at 7400 Hz is within 2 dB of the level at the original 6720 Hz. The data trend of Fig. 59 does not exactly match the 12 dB per doubling of flow rate predicted by dipole theory. However, the acoustic signals obtained are unambiguous for the range of flows tested, and are therefore useful for flow measurement in a geometrical setup similar to the laboratory arrangement.

Summary Fig. 71 shows that the acoustic emission flow measurement method can be used with metallic as well as inhomogeneous nonmetallic conduit materials of construction. Although the discontinuity distances of the Transite and aluminum pipes are different, we interpret the results of Fig. 71 at two sensor positions as indicating basically similar trends that are useful for flow measurement in both instances. The quality of sound transmission through the inhomogeneous

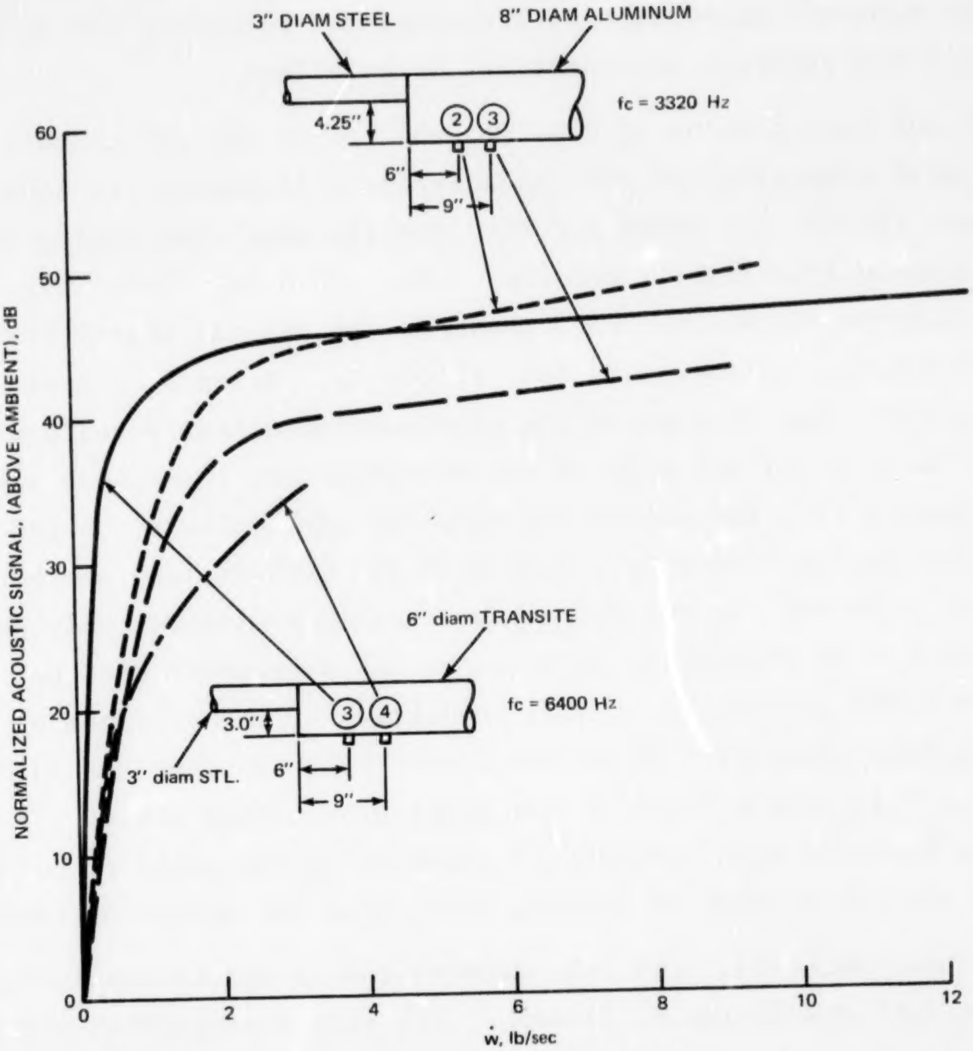

Fig. 71 Effect of pipe material on normalized acoustic signal variation with flow rate (eccentric cylindrical pipe elements and flush inlet) - 8 in. sand overburden

Transite material is very good and because concrete has similar acoustic properties to Transite, the prognosis for as yet untested concrete pipe sections is excellent.

In the data display of Fig. 62, the trends for the acoustic signal components at the characteristic frequency (~ 5600 Hz) and 720 Hz are shown for the Transite pipe exit monitoring location (position 9) and the 3-in. (7.6 cm) steel pipe monitoring location. Also shown is the overall signal for frequencies between 40 and 22,000 Hz. Since a 4 foot (1.2 m) long section of the pipe configuration, equally distributed on either side of the discontinuity plane, was supported within the wooden box made for simulation of buried installation, tests were made with and without sand overburden. However, of the two sensor locations plotted, only position 7 is physically affected by the overburden because the other position 9 is well downstream of the confines of the box. From Fig. 62 we see that the sound signal at position 9 is greater than on the steel pipe. This position on the Transite pipe has greater exposure to the sound produced by the interaction of falling water with the diversion trough.

If the 19.25-in. (49 cm) drop to the trough is considered the exit discontinuity distance, the exit characteristic frequency would be 720 Hz. The difference in signal amplitude between positions 9 and 7, at intermediate flow rates, is 11 dB at the assumed exit characteristic frequency, whereas it is 6 dB different for all recorded frequencies, and 18 dB different at the discontinuity characteristic frequency of 5600 Hz. A flow interaction mechanism to explain the higher acoustic signal at position 9 seems unsupported by the data. In addition, when the sound produced by the upstream pipe discontinuity is prevented from radiating normal to the pipeline axis into the laboratory (and reflecting back to the sensors) by an 8-in. (20.3 cm) layer of surrounding sand, the reduced signal amplitude is within 2 dB of being the same at both positions and all frequencies presented in Fig. 62.

Position 9 is in the far field of the pseudosound source near the discontinuity plane. It is known[1,2] that at these large distances from their source, pseudosound energy is converted into real sound which propagates throughout the flow. This is especially true where turbulence is added to the flow by sharp edges such as at the exit plane of the pipe or by a bed load of newly crushed stones (not weathered smooth) as noted earlier. From these considerations we then attribute the higher signal near the Transite pipe exit to sound reflected longitudinally back into the pipe by the nearby laboratory walls and diversion trough surfaces.

The higher magnitude of near field component signal levels, at positions closer to the pipe discontinuity plane (e.g., positions 3 and 4 compared to positions 7 and 9), is evident from Fig. 63. About 14 dB of the higher signal at position 3 is produced by the higher sensitivity of the accelerometer mounted there. The remaining 3-8 dB enhanced signal, depending on frequency, at positions 3 and 4 compared to position 9, undoubtedly is evidence of pseudosound production in the near field of the discontinuity plane. Furthermore, since position 4 is further downstream from the discontinuity, the signal obtained is about 4 dB less than that at position 3, for the characteristic frequency. Other data in Fig. 64 show that except in the low flow range, the acoustic signal obtained at position 3 is superior to signals at the other sensor locations examined, for the characteristic frequency component. This signal also is better or equal to that of the other positions at other frequencies. The sound insulation obtained with simulated buried installations is evident in both Figs. 62 and 63 at all sensor positions. The signal variation with flow at position 3 increases faster than the dipole trend at low flows, and varies slower than the dipole trend at intermediate to high flows. However, within the range of flows tested, an unambiguous signal is produced at the characteristic frequency and is usable for flow measurement.

Figure 65 shows the effect of adding solids to the flow. These sand particles, passing through mesh sizes between 0.85 and 2.36 mm, simulate sewage grit and were metered into the water supply well upstream so as to be well integrated into the flow passing the abrupt cross-sectional change in the pipe. However, although one can safely presume that each particle impacts the pipe wall many times, the aggregate effect of such collisions appears inconsequential relative to the near field acoustic emission of the flow. The acoustic signal at the characteristic frequency, as well as at a much lower frequency, is almost exactly the same for the flow containing grit as for the clean water flow. Also, despite a wide variation in grit concentration (between 86 and 1682 mg/liter of water) which was introduced for various test points, there is no discernible change in the result.

In the field test documented by Fig. 66, overall (all frequencies) sound levels of 80 to 84 dB were recorded for ambient noise, with the higher level occurring during the train movement. Overall sound levels of 96-104 dB were recorded with flow passing through the pipes. The lowest sound level was recorded at the top of the 10-in. (25.4 cm) pipe, some 27-in. (68.6 cm) downstream of the valve centerline. The highest overall sound level was measured at the bottom of the tee section, 18-in. (45.7 cm) upstream of the valve centerline. All four locations in the vicinity of the plug valve have peak amplitude components at a frequency of 2800 ± 80 Hz, as well as at several other frequencies which are not so universally present. This is an example of a situation where acoustic properties of the fluid and dimensional details are not accessible for direct measurement, and a characteristic frequency has to be determined by inspection of the spectral distribution. Compared to the ambient sound level at 2800 Hz (see Fig. 66) the sound level at three of the four locations in the vault are between 17 and 20 dB louder when flow is present. At the fourth location near the top centerline of the upstream tee section, the sound level at 2800 Hz is 14 dB louder when the flow is present than the ambient recorded near the top of the 10-in. (25.4 cm) downstream pipe [45-in. (1.14 m) away]. Comparison with a dipole theory trend drawn through the 650 gpm (2460 liter/min) data point shows reasonably good agreement with a linearized extrapolation of the trend through the ambient data point.

At the second field test site, the largest acoustic signal change with increasing flow (see Fig. 67) is for the component at a frequency of 2000 to 2200 Hz. Unfortunately, since the wet-well pumps produce constant volumetric flow rate, the acoustic data are at only two rates and full trends can only be estimated. It should be further noted that the signal at 900 gpm (3406 liter/min) is produced by flow discharged into the open channel from two pipe source sizes and with different flow orientations. At the characteristic frequency of 2200 Hz, selected by inspection of the spectral distribution, the increase in sound level is 11.5 dB between flows of 650 to 900 gpm (2460 to 3406 liter/min). The exponential law that follows these data for sound power, P_T, appears to be $P_T \sim Q^8$ rather than the $P_T \sim Q^4$ relation of dipole theory. At 2200 Hz, the vertical discharge of the 4-in. (10.2 cm) pipe and the reverberations by the walls of the open channel appear to be much greater sources of acoustic emission than the flow disturbance caused by the 90 degree bend in the 10-in. (25.4 cm) pipe. However, at another empirically selected frequency, 500 Hz, the increase in sound component amplitude agrees almost exactly with the 5 dB increment predicted by dipole theory for the ratio of flows for which data are available.

Perhaps the best explanation for these few data points is that dipole theory applies strictly to flow changes where the discontinuity geometry is of a singular nature and the conduit is extremely long in both directions. When two dissimilar discontinuities and sound reflections contribute to the overall sound being monitored, as is the case in the second of our field tests, the complex sound field is not properly described by simple dipole theory; further empirical investigation is needed for these situations.

SECTION IV

REFERENCES

1. Ffowcs-Williams, J., "Hydrodynamic Noise," in Annual Reviews of Fluid Mechanics, Vol. 1, Annual Reviews, Inc., Palo Alto, California, 1969.
2. Blokhintsev, D. I., "Acoustics of a Non-Homogeneous Moving Medium," NACA TM 1399, February 1956.
3. Olson, H., Acoustic Engineering, D. Van Nostrand Co., Princeton, 1957.
4. Beranek, L. L., ed., Interaction of Sound Waves with Solid Structures, Chapter 11, "Noise and Vibration Control," McGraw-Hill Book Co., New York, 1971.
5. Fair, G. M. and Geyer, J. C., Water Supply and Waste-Water Disposal, John Wiley and Sons, New York, 1954.
6. Haddle, G. and Skudrzyk, E., "The Physics of Flow Noise," Journal of the Acoustical Society of America, Vol. 46, No. 1 (Part 2), pp. 130-157, 1969.

SECTION V

GLOSSARY

Accelerometer - an electromechanical transducer that generates an electrical output when subjected to acceleration. Piezoelectric discs clamped between a mass and base develop a potential field when the acceleration of the mass exerts a force on the discs. The ratio of electrical output to mechanical input is called sensitivity.

Acoustic Emission - the radiation of sound generated by the interaction of fluid flow with a solid surface.

Acoustic Reflection - the change of direction of sound pressure waves impinging on a less than perfect sound absorbing surface.

Conduit Discontinuity - any change in a flow channel because of channel cross section or shape, or where flow direction is significantly changed.

Decibels (dB) - a measure of the ratio of two amounts of sound power. The range of sound pressure or intensity is so large that it is more convenient to use the logarithm to the base ten to express this ratio (bel). Decibel equals one tenth of a bel. When other quantities (e.g., voltage) are related to the square root of power, the number, n, of dB are: $n = 20 \log_{10}(v/v_o)$, where v_o is the referenced quantity.

Dipole - the type of sound source created when a fluid interacts with a solid surface to produce unsteady forces.

Because of its oscillating nature, this source is analogous to two point-sources equal in strength but opposite in phase and separated by a very small distance. The radiated power is proportional to the fourth power of flow speed. Because of the pressure cancellation in the plane normal to the dipole axis, the directionality of radiation is strongest along the dipole axis which is normal to the flow direction.

Hertz (Hz) - an international unit of frequency equal to the number of cycles per second.

Nonintrusive - not penetrating the fluid flow boundary.

Normalized Acoustic Signal - when transducers of different sensitivities measure the same sound source, their dB sound signals are different by the ratio of sensitivities. Similarly, when a constant sound source signal is measured against different background noise levels, the total signals are different by the relative difference in backgrounds. When using decibel units for sound level, the irrelevant variables of measurement such as background noise or sensor sensitivity can be eliminated by subtracting their dB contribution from the total signal. The resulting dB level then is the normalized signal, and is a more valid measure of the sound source alone.

Overburden - the soil or backfill covering a buried sewer pipe or flow conduit.

Passive Flow Measurement - a method of determining the mass or volumetric rate of flow by using energy normally radiated by the fluid flow as opposed to imposing external energy sources or flow energy dissipating devices.

Pseudosound - the pressure pulses produced in locally disturbed fluid flow that have characteristics of sound in the near field but do not propagate into the far field of the fluid. The radiation pattern of pseudosound is like a dipole sound source.

Sound Power (P_T) - the total amount of energy radiated by a sound source throughout a spherical envelope in a period of time (watts). In practice, the sound power level, L_w, is used to relate the ratio of sound power to a reference power. By international agreement, this reference power is 10^{-12} watts, and $L_w = 10 \log_{10}(P_T/10^{-12})$, dB.

Unambiguous Signal - a sensor output signal that can be interpreted as relating to only one flow quantity. Over a continuous range of signal output there are no intermediate minima or maxima with regard to the dependent parameter.